Metal Organic Framework Derived Electrocatalysts for Oxygen Reduction Reaction (ORR) and Oxygen Evolution Reaction (OER) in Metal Air Batteries.

By

Muhammad Mudassar Aslam

School of Chemical and Materials Engineering

National University of Sciences and Technology

2023

Metal Organic Framework Derived Electrocatalysts for Oxygen Reduction Reaction (ORR) and Oxygen Evolution Reaction (OER) in Metal Air Batteries.

Name: Muhammad Mudassar Aslam

Registration No: 00000363811

This thesis is submitted as a partial fulfillment of the requirements for the degree of

MS in Chemical Engineering

Supervisor Name: Dr. Tayyaba Noor

School of Chemical and Materials Engineering (SCME)

National University of Science and Technology (NUST)

H-12, Islamabad, Pakistan

May, 2023

THESIS ACCEPTANCE CERTIFICATE

Certified that final copy of MS Thesis written by **Mr Muhammad Mudassar Aslam** (Registration No 00000363811), of School of Chemical & Materials Engineering (SCME) has been vetted by undersigned, found complete in all respects as per NUST Statues/Regulations, is free of plagiarism, errors, and mistakes and is accepted as partial fulfillment for award of MS degree. It is further certified that necessary amendments as pointed out by GEC members of the scholar have also been incorporated in the said Thesis.

Signature: Tayyaba

Name of Supervisor: **Dr Tayyaba Noor**

Date: 24/07/2023

Signature (HOD): EB

Date: 24/7/23

Signature (Dean/Principal): AS

Date: 24-7-2023

CHE-09-2021

Form TH-1

National University of Sciences & Technology (NUST)

MASTER'S THESIS WORK

Formulation of Guidance and Examination Committee (GEC)

Name: Muhammad Mudassar Aslam NUST Reg No: 00000363811

Department: Department of Chemical Engineering Specialization: Master of Science in Chemical Engineering

Credit Hour Completed: 18.0 24 CGPA: 3.42 3.44

Course Work Completed

S/No:	Code:	Title:	Core/Elective:	CH:	Grade:
1.	CHE-843	Separation Processes In Che	Compulsory	3.0	B
2.	CHE-847	Chemical Kinetics& Reactor Design	Compulsory	3.0	B
3.	RM-898	Research Methodology	Additional	2.0	Q
4.	ENE-809	Waste Water Treatment & Design	Elective	3.0	A
5.	EME-921	Momentum, Heat & Mass Transfer In Chemical Engineering Separation Processes	Compulsory	3.0	B+
6.	CHE-873	Membrane Technology	Elective	3.0	B+
7.	ENS-830	Cleaner Production Technologies	Elective	3.0	B+

Date 07 - Nov - 2022 Student's Signature [redacted]

Thesis Committee

Name: Tayyaba Noor (**Supervisor**) Signature

Department: Department of Chemical Engineering

Name: Erum Pervaiz (**Cosupervisor**) Signature

Department: Department of Chemical Engineering

Name: Naseem Iqbal (**Internal**) Signature

Department: Department of Energy Systems Engineering

Name: Ghulam Ali (**Internal**) Signature

Department: Department of Energy Systems Engineering

Date: 07 - Nov - 2022 Signature of Head of Department:

APPROVAL

Date: 07 - Nov - 2022 Signature of Dean/Principal:

8. CHE-848 Gasification Processes Elective 3.0 B+

9. CHE-815 Nano catalysis Elective 3.0 B+

Form: TH-04

National University of Sciences &Technology (NUST)

MASTER'S THESIS WORK

We hereby recommend that the dissertation prepared under our supervision by Regn No & Name: **00000363811 Muhammad Mudassar Aslam**

Title: **Metal Organic Framework Derived Electrocatalysts for Oxygen Reduction Reaction (ORR) and Oxygen Evolution Reaction (OER) in Metal Air Batteries.**

Presented on: **20 Jul 2023** at: **1430 hrs in SCME Seminar Hall**

Be accepted in partial fulfillment of the requirements for the award of Master of Science degree in **Chemical Engineering**.

Guidance & Examination Committee Members

Name: **Dr Naseem Iqbal** Signature:

Name: **Dr Ghulam Ali** Signature:

Name: **Dr Erum Pervaiz** (Co- Supervisor) Signature:

Supervisor's Name: **Dr Tayyaba Noor** Signature:

Dated: 20/7/23

Head of Department
Date 21/7/23

Dean/Principal
Date 21-7-23

School of Chemical &Materials Engineering (SCME)

Dedication

By the grace of Almighty Allah, who is the most Beneficent and the most merciful

This research is dedicated to my parents, who have always been my source of guidance and support.

To my supervisor who shared his knowledge, gave advice, and encouraged me to fulfill my tasks.

And to all my fellows, with whom I worked and shared good memories.

Acknowledgements

All praises to Almighty Allah, without His will nothing can happen, who favored us with the capacity to think and made us anxious to investigate this entire universe. Incalculable greetings upon the Holy Prophet Hazrat Muhammad (PBUH), the reason for the creation of the universe and wellspring of information and blessing for whole humankind.

From the core of my heart, I am thankful to my research supervisor, Dr. Tayyaba Noor for her unwavering technical and moral support and enlightening me with a research vision and pushing me for excellence. Her quest for perfection and excellence had been a source of inspiration and driving force. It is her consistent and encouragement that empowered me to achieve this onerous milestone.

I extend my sincere gratitude towards my co-supervisor Dr. Erum Pervaiz and GEC: Dr Naseem Iqbal, and Dr. Ghulam Ali for guiding and supporting me in my research course. It would not have been possible without them. I express my gratitude for Dr. Tayyaba Noor for sharing her knowledge and experience regarding research work.

I am thankful of My Seniors specially Neelam Zaman who shared their knowledge regarding experimental techniques, and they motivated me in this entire research work. Without any doubt, SCME's supporting staff coordinated with me while I was working on different equipment's.

I am highly obligated to my Parents and siblings for their never-ending love. Thanks for believing in me, wanting the best for me, and inspiring me to follow my passion. To my friends Shaharyar Khan and Najla Javed, thank you for your support, advice, and encouragement.

Muhammad

Mudassar Aslam

Abstract

It is vital to synthesize non-noble metal-based electrocatalysts with bifunctional electrocatalytic activity for both the oxygen reduction reaction (ORR) and the oxygen evolution reaction (OER) to make it possible for metal air batteries to be highly efficient and sustainable. This will allow for the use of metal air batteries. In this research, a pure FeCo-MOF, a pure MnFeCo-MOF, and their composites with (1, 3, 5) wt% rGO were synthesized through the solvothermal technique and characterized via XRD, SEM, EDX, FTIR, and RAMAN. The electrochemical process is made more efficient thanks to the synergistic relationship between the MOF and the rGO composites. In this research project, Mn-doped Fe/Co MOF and its rGO-based composites were produced and tested as electrocatalysts for oxygen evolution reactions (OER). X-ray diffraction (XRD) and scanning electron microscopy (SEM) were utilized to conduct an investigation into the structural and morphological characteristics of the materials that were manufactured. Cyclic voltammetry (CV) and linear sweep voltammetry (LSV) were utilized to study the electrochemical performance of the materials. When compared to the individual components, the 3 wt% rGO MnFeCo-MOF composites exhibited much higher OER catalytic activity than the individual components. The improved composite demonstrated remarkable electrocatalytic activity, outstanding durability, and satisfactory stability in alkaline solutions. It was determined that the synergistic impact of MnFeCo-MOF and rGO was responsible for the improved electrocatalytic performance of the composites. This effect resulted in improved electronic conductivity, enhanced active sites, and reduced charge transfer resistance. According to these findings, FeCo-MOF, MnFeCo-MOF and its rGO composites have a significant amount of promise for use in metal-air batteries as effective electrocatalysts for OER.

Table of Contents

List of Figures

Chapter 1

Introduction

1.1 Introduction

The consistent usage of fossil fuels over the course of the past few decades has resulted in broad environmental issues and has caused a rise in the demand for clean and green energy. In the meantime, the rising demand for portable electronic items, as well as the development of hybrid electric vehicles and battery electric vehicles, have directly spurred research advances in the renewable energy storage devices [1-5]. Human beings are able to make direct use of the environmentally friendly and highly efficient energy sources that are found in nature, such as solar, wind, and tidal power after the conversion by electrochemical energy storage devices. These storage devices such as metal air batteries (MABs), also known as conventional electrical energy storage devices, are widely regarded as highly promising platforms for energy storage, with the excellent development potential, due to their flexibility and scalability [6, 7].

Lithium-ion batteries (LIBs) have found widespread use in modern electronic devices, revolutionizing the concept of rechargeability [8]. These batteries have gained prominence in the energy storage market due to their compact size, lightweight nature, safety features, environmental friendliness, and long lifespan. However, the energy density of current commercial LIBs, which operate on the intercalation mechanism, is approaching its theoretical limit. Additionally, their relatively high-cost poses limitations in meeting the diverse energy storage demands across various industries [9-13]. Consequently, there is an urgent demand for innovative battery systems based on new materials chemistry. These systems aim to achieve enhanced energy and power density, stable cycling performance, secure operation, and reasonable life-cycle costs, catering to a wide range of application requirements [14-16].

Since they offer a high theoretical energy density, improved safety features, and environmental friendliness, rechargeable metal-air batteries (MABs) have received a substantial amount of interest as a potentially useful alternative for the storage of energy. They are the best option for use in electric cars of the future as well as portable

electronic devices [17]. Despite recent progress, there are still many obstacles standing in the way of the growth of MABs. For example, metal-sulfur batteries continue to struggle with problems associated with poor rate performance [18-20]. There is hope for the future of renewable electrochemical energy storage in the form of metal-air batteries, which are notable for their open structure and the possibility of high power and energy density. However, because of the slow kinetics at the oxygen electrode, their performance is limited [21-23]. During battery cycling, the oxygen evolution reaction (OER) and the oxygen reduction reaction (ORR) are key catalytic activities that occur at the air cathode [24, 25]. On the other hand, these reactions are extremely inefficient in their natural setting, which results in an excessively high overpotential in the battery [26]. Previous research has shown that the OER and ORR can both be catalyzed by RuO_2/IrO_2 and Pt/C, respectively [27, 28]. Their electrocatalytic kinetics are severely hampered, however, by the poor bonding properties of RuO_2/IrO_2 during the OER and Pt/C during the ORR [29, 30].

The application of catalysts based on noble metals in electrocatalysis is hampered by the expensive cost of these catalysts and the restricted availability of these catalysts [30]. Because of this, there is an urgent need for bifunctional catalysts that are both inexpensive and abundant, as well as efficient, and that have adequate physical and chemical properties in order to handle the issues presented by these batteries [31, 32].

In the past few years, there has been notable progress in the catalytic activity of transition metal-based materials, including Mn, Co, Ni, and Fe, for the oxygen evolution reaction (OER) and oxygen reduction reaction (ORR) [33]. To overcome the sluggish kinetics of OER and ORR, the development of new non-precious functional materials is essential. Metal-organic frameworks (MOFs) have emerged as particularly intriguing materials for research due to their design flexibility and adaptability.

Metal-organic frameworks (MOFs) possess distinct characteristics such as a significant specific surface area, high porosity, and customizable pore sizes. These features make them extensively utilized in energy storage and conversion technologies like fuel cells, metal-air batteries, and supercapacitors [34-39]. MOF-derived materials can serve as templates to fabricate porous carbon-based materials, including carbides, phosphides, and sulfides, which exhibit catalytic activity in various reactions. The

partially retained pore structures significantly enhance the utilization of active sites [40].

Because of their enormous specific surface areas, modular and programmable topologies, and vast interior pore volumes, we will also investigate the possibility of using MOFs and their derivatives as electrode materials in metal-air batteries. This line of investigation will take place soon. Because of their high energy capacity as electrode materials, MOFs have got attention because of their pore widths may be adjusted and they include redox-active metal ions [41, 42]. MOFs are examples of porous materials since they have an open framework and allow for the passage of gases and liquids. These organic-inorganic hybrid materials put themselves together by forming coordination bonds between a core metal ion and organic ligands that are there to support it. From the first direct synthesis of MOFs to the widespread use of these compounds in modern day, the synthesis of MOFs has undergone substantial development. When compared to bonds that are much weaker, such as hydrogen bonds and van der Waals bonds, the bond energies that are possessed by the coordination bonds in MOFs are significantly larger, typically ranging from 60 to 350 kJ mol^{-1}. As a direct consequence of this, MOFs are stable and have the ability to generate pores that are permanent.

Recent investigations have focused on utilizing a Fe3 cluster as the foundational metal building unit for the synthesis of stable MOFs. MOFs composed of Lewis acid ions (Fe^{3+}, Al^{3+}, Zr^{4+}, etc.) and carboxylic acid ligands exhibit general stability, as they enhance the electrostatic interaction between the metal node and organic ligand, thereby preserving the structure in water or under acidic/alkaline conditions [43, 44]. Feng et al. have reported the successful fabrication of a series of iron-based MOF compounds, demonstrating control over crystal growth based on kinetic and thermodynamic considerations. Notably, these iron-based MOFs exhibit exceptional stability, maintaining their structure in water for over 6 months. Consequently, the iron-based MOF system has emerged as a promising candidate for practical applications due to its stability. Additionally, Fe_3 clusters not only exhibit electrochemical activity on their own but can also form bimetallic Fe_2M clusters by replacing one iron atom with another metal center. The incorporation of specific metal ions in the Fe_2M clusters significantly enhances their electrochemical activity. Furthermore, by incorporating functional organic linkers, the electrochemical

performance of the target MOF constructed from a Fe_2M cluster and a redox linker can be further enhanced.

During the annealing process, the structures of MOFs are susceptible to collapsing, leading to a bulk phase lacking a porous structure. This collapse significantly diminishes the electrochemical activity of the MOFs [45, 46]. Introducing abundant carbon species not only affects the material's structure but also enhances its catalytic performance. Recently, reduced graphene oxide (rGO) has emerged as an active support due to its large specific surface area and excellent electrical conductivity. Consequently, there has been considerable interest in utilizing rGO-supported materials derived from MOFs, as they exhibit improved electrocatalytic activity [47, 48].

1.2 Metal Air Batteries and their types:

These harness the reversible electrochemical reactions between a metal anode and atmospheric oxygen at the cathode to generate electrical energy. These batteries hold immense promise due to their high theoretical energy density, making them attractive candidates for portable electronics. The primary advantage of metal-air batteries lies in their reliance on oxygen from the surrounding environment, reducing the need to carry heavy oxidizing agents within the battery, thus increasing their specific energy. Commonly used metal anodes include zinc, aluminum, and lithium, while the cathode typically employs air, allowing metal-air batteries to be lightweight, compact, and environmentally friendly [49].

To address this, extensive research is focused on developing efficient electrocatalysts that can enhance the rate of these reactions and improve battery performance. These are efficient ORR and OER catalysts but are expensive and scarce, limiting their widespread application. Hence, the search for cost-effective and sustainable alternatives [50].

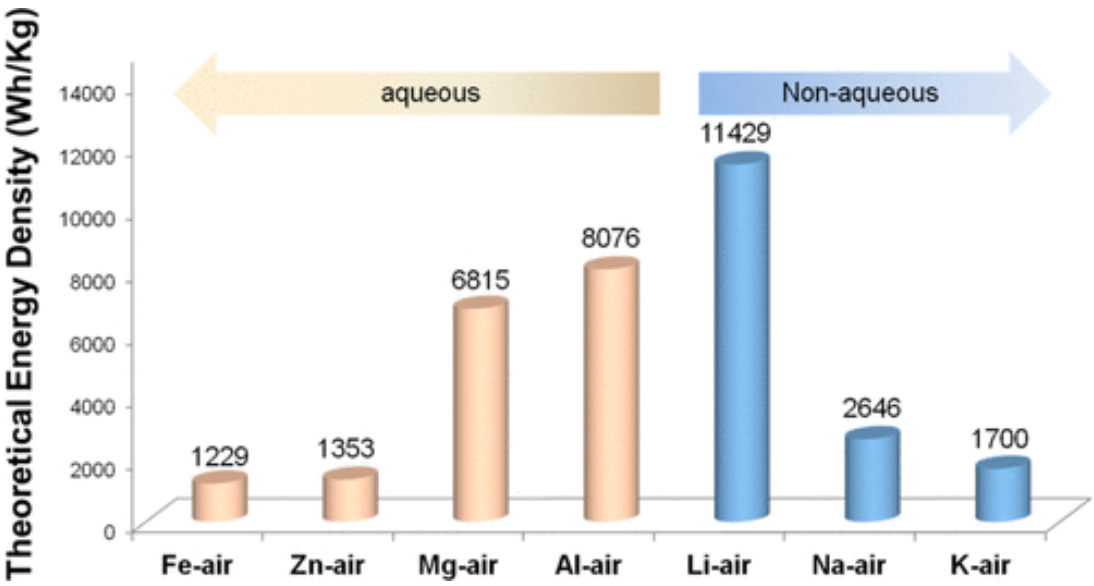

Figure 1: Different types of MABs energy densities (theoretical).

Efforts are also being made to optimize the design and structure of metal-air batteries for improved efficiency and longevity. From air electrode engineering to electrolyte optimization, each aspect plays a crucial role in determining the overall performance of the battery. Innovations in electrolyte composition and separator materials have also been explored to mitigate issues like electrolyte evaporation and metal dendrite growth, enhancing battery safety and cycle life. As research in materials science and electrochemistry continues to progress, metal-air batteries hold tremendous potential to revolutionize the energy storage landscape, offering cleaner, greener, and more sustainable solutions for the growing demands of the modern world [51].

1.2.1 Aqueous Metal-Air Batteries

Aqueous metal-air batteries are a subclass of metal-air batteries that use water-based electrolytes, making them more environmentally friendly and safer than their non-aqueous counterparts. These batteries rely on the reversible reactions between a metal anode and oxygen at the cathode, with water serving as the solvent for the electrolyte. The use of aqueous electrolytes eliminates the need for flammable and volatile organic solvents, reducing the risk of fire hazards and making them more suitable for large-scale applications.

One of the main advantages of aqueous metal-air batteries is their potential for high energy density. Aqueous electrolytes can support high metal ion concentrations, leading to greater capacity and energy storage capabilities. Moreover, the use of water-based electrolytes can enable better ion transport and faster reaction kinetics at the

electrodes, resulting in improved power performance. Additionally, the abundance and low cost of water make aqueous solutions that require cost-effectiveness and scalability [49].

Despite the advantages, aqueous metal-air batteries also face challenges, particularly related to the stability of metal anodes in aqueous environments. Some metals, like zinc, are prone to corrosion when exposed to water, leading to the formation of passivation layers that hinder the battery's performance. Researchers are actively exploring new strategies to mitigate this issue, such as incorporating protective coatings on the anode surface or developing stable and non-corrosive metal alloys. Overall, the development of aqueous metal-air batteries holds great promise for advancing renewable energy storage technologies, as they offer a safer, more sustainable, and economically viable alternative to conventional energy storage solutions.

1.2.2 Non-aqueous Metal-Air Batteries

Non-aqueous MABs are a class of energy storage devices that operate on the reversible redox reactions between a metal anode and oxygen at the cathode. Unlike their aqueous counterparts, these batteries utilize non-aqueous electrolytes, typically organic solvents with high dielectric constants [52, 53]. This choice of electrolyte enhances the battery's ionic conductivity and facilitates metal ion transport, leading to improved charge and discharge rates. Additionally, non-aqueous electrolytes often enable higher metal ion concentrations, resulting in higher energy density and storage capacity.

One significant advantage of non-aqueous metal-air batteries is their ability to utilize a wide range of metal anodes, such as lithium, zinc, and aluminum. Each metal offers distinct characteristics, including high specific capacities and energy densities, making them suitable for various applications. For example, lithium-air batteries have attracted attention for their potential to achieve ultrahigh energy densities, rendering them appealing for electric vehicles and portable electronic devices. Zinc-air batteries, on the other hand, are widely used in hearing aids, cameras, and other low-power applications due to their cost-effectiveness and long runtime [53-55]. Despite the advantages, non-aqueous metal-air batteries also face challenges, such as electrolyte stability and oxygen electrode kinetics [56]. The reactive nature of metal anodes with

non-aqueous electrolytes can result in side reactions, causing electrolyte degradation and reducing battery lifespan [57]. Additionally, it can lead to overpotential, limiting the battery's efficiency. Researchers are actively exploring new electrolyte formulations and electrode materials to address these issues [49].

Overall, these batteries hold great promise for advancing energy storage technologies and powering the next generation of high-energy-density devices [49].

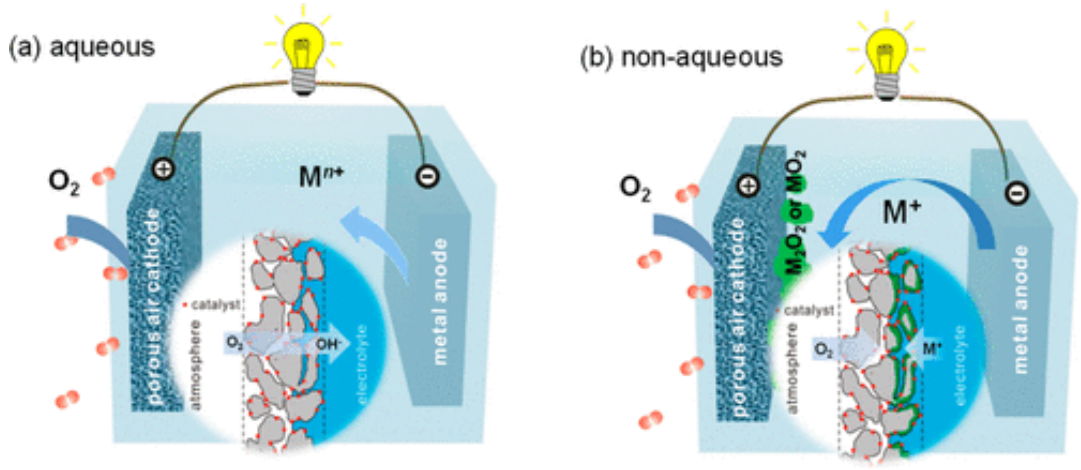

Figure 2: MABs working principle

1.2.3 Lithium-Air Batteries

Lithium-air batteries, also known as lithium-oxygen batteries or Li-air batteries, have garnered significant interest in recent years as potential candidates for next-generation energy storage solutions [50]: These batteries are lauded for their exceptionally high theoretical energy densities, far surpassing traditional lithium-ion batteries. The fundamental working principle of lithium-air batteries involves the reversible reaction between lithium ions (Li^+) and oxygen (O_2) at the cathode during discharge, producing lithium oxide (Li_2O) as a solid product and releasing electrical energy. During charge, the lithium oxide is decomposed, releasing oxygen back into the cell while converting it back to elemental lithium. One of the key advantages of lithium-air batteries lies in their high energy density. The theoretical specific energy of a lithium-air battery is several times greater than that of conventional lithium-ion batteries, making them highly attractive for applications requiring extended operating times and high energy demands [58, 59].

The use of lightweight lithium as an anode further contributes to the overall energy density of the battery system [60].

With such potential, lithium-air batteries could revolutionize offering longer driving ranges, extended device usage, and improved renewable energy integration [61, 62].

However, despite their promising advantages, lithium-air batteries also face substantial challenges that hinder their practical implementation [56, 63]. The reaction between oxygen and lithium during discharge and recharge generates reactive intermediates and by-products, leading to the decomposition of the electrolyte and the formation of undesirable solid insulating layers on the cathode surface. These side reactions result in reduced battery capacity and cycling stability. Additionally, lithium dendrite formation during charge can cause safety concerns, leading to internal short circuits and possible thermal runaway [50]. Despite these challenges, ongoing research and development efforts continue to explore new materials, electrode designs, and electrolytes to improve the performance and stability of lithium-air batteries. Innovations in catalysts, electrolyte additives, and cathode structures aim to enhance oxygen kinetics, suppress side reactions, and prolong battery life [64].

Practical implementation of lithium-air batteries is still a subject of intense investigation [65]. As the field advances, lithium-air batteries hold tremendous potential to revolutionize the energy storage landscape and pave the way for sustainable and high-energy-density power sources in the future.

1.2.4 Zinc Air Batteries

These batteries utilize the reversible reaction between zinc metal (Zn) and oxygen (O_2) from the air during discharge and recharge, respectively. During discharge, zinc is oxidized at the anode, releasing electrons and producing zinc oxide (ZnO) as a solid product. At cathode consuming electrons and forming hydroxide ions (OH^-). The overall reaction generates electrical energy, and during recharge, the reaction is reversed, converting zinc oxide back to elemental zinc and releasing oxygen back into the environment [66, 67]. Zinc-air batteries lies in their high energy density. The theoretical specific energy of a zinc-air battery is significantly higher than that of conventional lithium-ion batteries, making them appealing for applications that demand long operating times and high energy requirements. Additionally, zinc is abundant, cost-effective, and environmentally friendly, providing a sustainable option for energy storage. The air cathode, consisting of a porous structure with a catalyst,

allows for the easy access of oxygen from the ambient air, further contributing to the high energy density of the battery [50].

However, zinc-air batteries also face several issues for implementation. One significant issue is the stability and reactivity of the zinc electrode during cycling. Zinc is prone to dendrite formation, which can lead to internal short circuits and reduce battery lifespan [68]. To mitigate this problem, researchers have been exploring various strategies, including the use of additives and electrolyte modifications to control zinc deposition and dissolution. Another challenge is the limited cycle life and rechargeability of zinc-air batteries. The formation and dissolution of zinc oxide during discharge and recharge can lead to irreversible capacity loss, impacting the overall performance and efficiency of the battery.

Despite these challenges, ongoing research and development efforts are focused on improving the performance and commercial viability of zinc-air batteries.

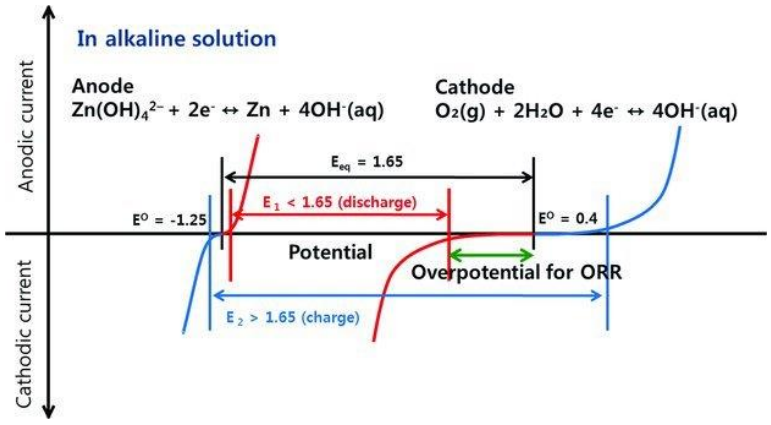

Figure 3:Polarization curves of Zn air cell.

1.3 History of MOFs:

Since their discovery in the late 1990s, the study of MOFs, which are materials that consist of metal ions or clusters coupled by organic ligands to generate a porous and crystalline structure, has emerged as a rapidly developing topic in the field of materials science research. MOFs are porous and crystalline structures that are created by the MOFs. The investigation of porous materials for the purpose of gas storage and separation began in the 1980s; nevertheless, it was not until 1995 that researchers from Kyoto University were able to successfully synthesise the first real MOF. This MOF was designated as MOF-5. This ground-breaking material is made up of zinc ions and organic ligands, and due to its high surface area, it displayed outstanding gas

adsorption capabilities. MOF-5 was the impetus for a boom in research efforts, which ultimately resulted in the creation of several additional MOFs, such as MIL-101, HKUST-1, and UiO-66. Researchers can develop materials with different properties and possible uses by altering metal ions and ligands during the synthesis process, which is one of the important driving forces behind the rapid progress of MOFs. In addition, the high customizability of MOFs is one of the significant driving forces behind the rapid growth of MOFs [69].

Scientists began investigating the catalytic potential of MOFs at the beginning of the twenty-first century by inserting active metal ions into the structures of MOFs. This new line of research, which is known as MOF-based catalysis, has opened a wide range of potential uses for MOFs. Some of these applications include the storage and separation of gases, the catalysis of reactions, the delivery of drugs, and sensing. To date, thousands of different MOFs have been synthesised, and each one has its own set of characteristics as well as possible applications.

Despite the significant progress that has been made in MOF research, there is still a great deal to discover about these fascinating compounds. The potential of these MOFs for novel applications is still being researched, and scientists are working hard to create sophisticated synthesis methods that can create MOFs with even greater levels of complexity and functionality [70].

1.4 Introduction of Porous Solids

Porous solids are materials with a complex, three-dimensional structure that contains interconnected voids or pores. These voids can be of different shapes and sizes and can be either open or closed. Porous solids are used in different applications. The use of porous solids dates to ancient times, when natural materials such as clay and zeolites were used for water filtration and purification. However, it was not until the late 19th and early 20th centuries that scientists began to study the properties and applications of these materials in detail.

One of the first synthetic porous solids was zeolite A, which was discovered in the 1950s by a team of researchers at Union Carbide Corporation. Zeolites are aluminosilicate minerals that have a crystalline structure with interconnected voids or channels. These voids can be used to selectively adsorb and separate gases and liquids,

making zeolites useful for number of uses. In the 1960s, scientists began to explore the potential porous solids. This high surface area makes activated carbon useful for adsorption and separation of gases and liquids, as well as for use in catalysis and energy storage. Molecular sieves are porous solids that are made up of metal oxides or silicates. These materials have a crystalline structure with interconnected voids of a specific size and shape, which can be used to selectively adsorb and separate molecules based on their size and shape.

Porous solids have revolutionized many industries and have enabled the development of new technologies. For example, porous solids are used in catalysis to increase reaction rates and selectivity, and in gas separation and storage for improved energy efficiency. They are also used in drug delivery to improve drug stability and targeted delivery to specific sites in the body. Overall, porous solids are essential. As research continues to advance, new porous solids with unique and tailored properties are likely to be developed, paving the way for even more innovative applications in the future [70].

1.5 Metal Organic Frameworks

Metal-organic frameworks, often known as MOFs, are a type of porous material that are formed by metal ions or clusters being connected to one another by organic ligands in order to create a crystalline structure in three dimensions. MOFs have a vast surface area, which endows them with a significant number of active sites that can be utilised for a variety of purposes, including the storage of gases and the conduct of chemical reactions. MOFs are extremely modifiable, and their properties can be altered by modifying the metal ions, organic ligands, and synthesis conditions. This allows MOFs to be used in a variety of applications. MOFs are currently being utilised in a vast array of applications, some of which include the storage and separation of gases, catalysis, drug delivery, sensing, and environmental remediation.

The enormous surface area that MOFs possess is one of their most significant advantages. This difference can be measured in several orders of magnitude. Active sites for chemical reactions thanks to their high surface area, which makes them valuable for catalysis and other uses. The adaptability of MOF characteristics is yet another feature of these materials. Researchers are able to produce MOFs with a diverse set of characteristics by altering the synthesis conditions, organic ligands, and metal ions used in the process. For instance, the pore size and shape of a MOF can be

altered in such a way that it can selectively adsorb and separate various gases and liquids. In a similar fashion, one can alter the chemical characteristics of a MOF in order to improve either the catalytic activity or selectivity of the MOF [71].

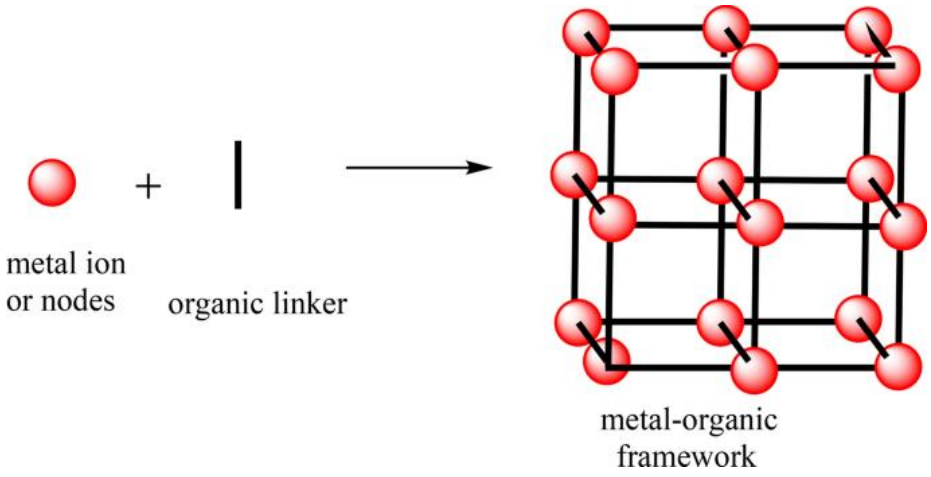

Figure 4: Schematic diagram of Metal Organic Framework

MOFs have found numerous applications in a variety of fields. For example, MOFs are used in gas storage and separation, such as the capture of carbon dioxide from industrial emissions or the storage of hydrogen for fuel cell vehicles. MOFs are also used in catalysis, such as the conversion of biomass to fuels and chemicals. In drug delivery, MOFs can be used to improve drug stability and targeted delivery to specific sites in the body. Despite their many advantages, there are also challenges associated with MOFs Additionally, the synthesis of MOFs can be complex and expensive, which can limit their scalability for large-scale applications.

As research continues to advance, it is likely that new MOFs with unique and tailored properties will be developed, paving the way for even more innovative applications in the future.

1.5.1 Synthesis Methods of MOF

Numerous methods can be employed for the synthesis of MOFs, such as solvothermal, hydrothermal, sonochemical, microwave heating, mechanochemical, and electrochemical synthesis, among others. Each of these techniques can result in MOFs with varying particle size, morphology, size distribution, and other properties. However, solvothermal and hydrothermal methods are commonly used for MOF synthesis.

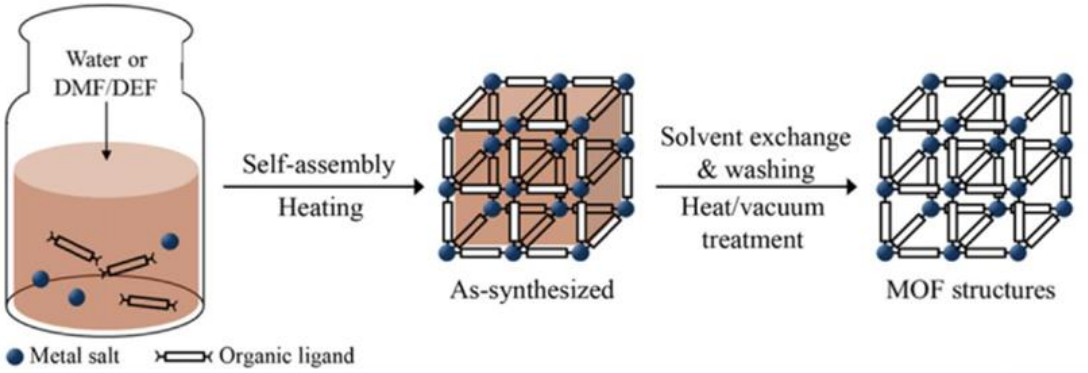

Figure 5:Schematic showing synthesis of MOFs by solvothermal method.

The synthetic routes for MOFs involve selecting the metal ions and organic ligands, mixing them together in a solvent under controlled conditions, allowing the metal ions and organic ligands to coordinate to form a three-dimensional framework, and potentially undergoing further processing steps to improve the properties or functionality of the MOF [71, 72].

1.5.2 Solvothermal Synthesis of MOFs

The solvothermal method typically involves the following steps:

- Selection of metal ions and organic ligands: The first step in solvothermal synthesis is to select the appropriate metal ions and organic ligands for the desired MOF structure. Metal ions and organic ligands should be chosen based on their compatibility, solubility, and coordination ability.

- Preparation of the reaction mixture: The metal ions and organic ligands are then mixed together in a suitable solvent to form a reaction mixture. The solvent is chosen based on its ability to dissolve both the metal ions and organic ligands and its compatibility with the desired MOF structure.

- Heating under high temperature and pressure: The reaction mixture is then heated under high temperature and pressure conditions inside a sealed autoclave. This promotes the formation of MOF crystals by allowing the metal ions and organic ligands to coordinate with each other and form the three-dimensional MOF framework.

- Cooling and filtration: After the reaction is complete, the autoclave is cooled to room temperature and the MOF crystals are filtered out of the reaction

mixture. The MOF crystals are typically washed with a solvent to remove any impurities before being dried and characterized.

Solvothermal synthesis has several advantages for MOF synthesis. The high temperature and pressure conditions promote the formation of large, well-defined MOF crystals with a high degree of crystallinity and purity. Solvothermal synthesis also allows for precise control over the size, shape, and surface area of the resulting MOF crystals by varying the reaction conditions and solvent used. However, solvothermal synthesis can be challenging due to the high temperature and pressure requirements, which may limit the scalability of the method. Additionally, the solvent used can influence the structure and properties of the MOF, and selecting the appropriate solvent can be critical for successful MOF synthesis [72].

Overall, solvothermal synthesis is a powerful method for synthesizing MOFs with high purity and control over the resulting MOF crystal properties.

1.5.3 Electrochemical Synthesis of MOFs:

Electrochemical synthesis is a promising method for synthesizing metal-organic frameworks (MOFs) that offers several advantages over traditional synthesis methods. In this method, MOF crystals are grown from metal ions and organic ligands using electrochemical reactions at the surface of an electrode.

The electrochemical synthesis of MOFs typically involves the following steps:

- Selection of metal ions and organic ligands: The first step in electrochemical synthesis is to select the appropriate metal ions and organic ligands for the desired MOF structure. Metal ions and organic ligands should be chosen based on their compatibility, solubility, and coordination ability.

- Electrode preparation: The electrode is prepared by coating it with a conductive layer, such as carbon or platinum, to facilitate the electrochemical reaction. The electrode can be in the form of a disk, wire, or plate, depending on the desired application.

- Electrolyte preparation: Dissolved in an appropriate electrolyte solution to form a reaction mixture. The electrolyte solution is chosen based on its ability to dissolve both the metal ions and organic ligands and its compatibility with the electrode and the desired MOF structure.

- Electrochemical deposition: The reaction mixture is then placed in an electrochemical cell with the prepared electrode as the cathode. An anode made of a suitable material is also placed in the cell.
- Characterization and extraction: After the reaction is complete, the electrode with the MOF crystals is removed from the cell and characterized using various techniques. The MOF crystals can be extracted from the electrode by dissolving the electrode in a suitable solvent, leaving the MOF crystals intact.

Electrochemical synthesis offers several advantages over traditional synthesis methods. It is a simple, fast, and scalable method that can be easily controlled by varying the electrochemical parameters, such as current density and deposition time. Additionally, electrochemical synthesis can be used to fabricate MOF films and coatings directly on conductive substrates for applications such as gas separation and catalysis. However, electrochemical synthesis also has some limitations. It requires careful selection of the electrode, electrolyte, and electrochemical parameters to ensure the desired MOF structure is formed. Additionally, the deposition of MOF crystals on the electrode surface can lead to a decrease in the electrochemical activity of the electrode, which can limit its practical applications [73].

1.5.4 Sonochemical Synthesis of MOFs:

Sonochemical synthesis is a method for synthesizing metal-organic frameworks (MOFs) that utilizes high-frequency ultrasonic waves to generate cavitation bubbles in a reaction mixture. These bubbles collapse violently, producing high temperatures and pressures that can promote the formation of MOFs. In sonochemical synthesis, a mixture of metal ions and organic ligands is placed in a solvent and subjected to ultrasonic waves. The ultrasonic waves cause the solvent to undergo rapid cycles of compression and expansion, creating cavitation bubbles in the reaction mixture. When these bubbles collapse, they generate high temperatures and pressures that can facilitate the formation of MOFs.

Sonochemical synthesis offers several advantages over other methods of MOF synthesis. It is a simple, fast, and efficient method that can produce MOFs with high yields and in a short amount of time. However, sonochemical synthesis also has some limitations. The high temperatures and pressures generated during the formation of MOFs can sometimes result in the formation of impurities or undesired byproducts.

Additionally, the ultrasonic waves can also damage the structure of the MOFs, leading to decreased stability and performance. Therefore, careful optimization of the reaction conditions is necessary to ensure the desired MOF structure is formed and to minimize the formation of impurities and defects [74, 75].

1.5.5 Microwave-Assisted Synthesis of MOFs:

Microwave-assisted synthesis is a method for synthesizing metal-organic frameworks (MOFs) that uses microwave radiation to rapidly heat and accelerate chemical reactions. In microwave-assisted synthesis, a mixture of metal ions and organic ligands is placed in a solvent and exposed to microwave radiation. The microwaves generate heat by causing water molecules in the solvent to rapidly vibrate, leading to localized heating and accelerating the chemical reaction. The reaction mixture is typically placed in a sealed vessel to prevent evaporation of the solvent and to contain any potential hazards associated with the use of microwaves.

Microwave-assisted synthesis can produce MOFs with high yields and in a short amount of time, often in a matter of minutes. Additionally, microwave-assisted synthesis is a scalable method that can be easily automated, making it suitable for large-scale production of MOFs. Microwave-assisted synthesis also has some limitations. The use of microwaves can lead to the formation of impurities or undesired byproducts if the reaction conditions are not carefully controlled. Additionally, the rapid heating and cooling associated with microwave-assisted synthesis can sometimes result in the formation of defects or reduced stability in the MOFs [75].

1.5.6 Mechanochemical synthesis of MOFs:

Mechanochemical synthesis method uses mechanical force to initiate and accelerate reaction. In mechanochemical synthesis, a mixture of metal ions and organic ligands is placed in a milling jar with milling balls, and the jar is vibrated or rotated at high speeds to generate mechanical force. The force generated by the milling balls causes collisions between the metal ions and organic ligands, initiating chemical reactions and promoting the formation of MOFs. Mechanochemical synthesis can produce MOFs with high yields and in a short amount of time, often in a matter of minutes.

Mechanochemical synthesis can also utilized for the morphology and crystal structure of MOFs by adjusting the milling time, milling intensity, and solvent composition. Additionally, mechanochemical synthesis is a scalable method that can be easily

automated, making it suitable for large-scale production of MOFs. However, mechanochemical synthesis also has some limitations. The high force generated by the milling balls can sometimes result in the formation of impurities or undesired byproducts if the reaction conditions are not carefully controlled. Additionally, the rapid mechanical force associated with mechanochemical synthesis can sometimes result in defects or reduced stability in the MOFs. Therefore, careful optimization of the reaction conditions is necessary to ensure the desired MOF structure is formed and to minimize the formation of impurities and defects [76].

1.5.7 Slow Evaporation Synthesis of MOFs:

In the slow evaporation method, a mixture of metal ions and organic ligands is dissolved in a solvent, often a mixture of water and an organic solvent. The solution is then placed in a sealed container and allowed to evaporate slowly at room temperature or under controlled conditions of temperature and humidity.

As the solvent evaporates, the metal ions and organic ligands come together and form crystalline MOF structures.

The slow evaporation method offers several advantages over other MOF synthesis techniques. It is a simple and relatively low-cost method that can produce high-quality MOFs with high crystallinity and purity. Additionally, the method is scalable and can be used to produce large quantities of MOFs for various applications.

However, the slow evaporation method also has some limitations. It is a time-consuming process, often taking several days or even weeks to produce a single batch of MOFs.

The slow evaporation method also requires careful control of the solvent evaporation rate to prevent the formation of impurities or undesired byproducts.

Overall, the slow evaporation method is a useful technique for synthesizing MOFs with complex structures and high quality, but it may not be the best choice for high-throughput or large-scale MOF production [77].

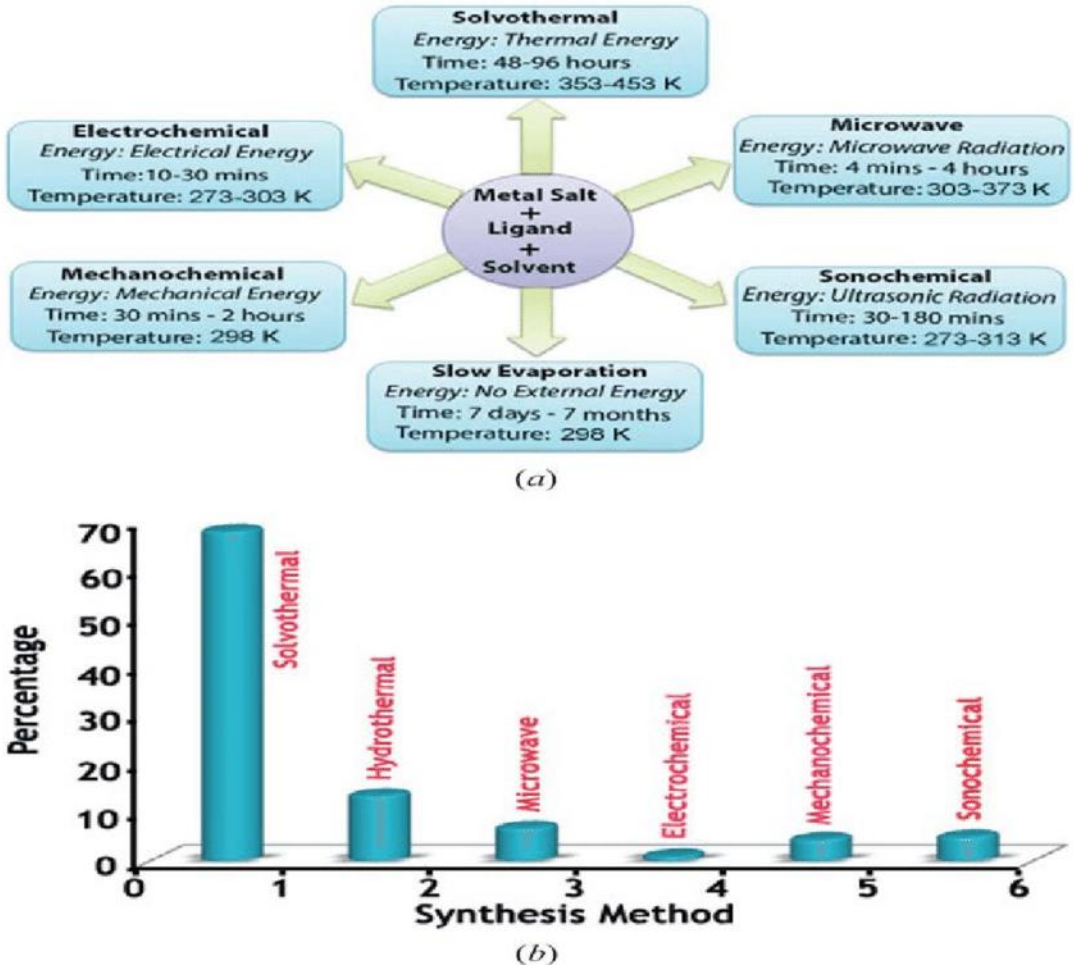

Figure 6:Typical synthesis conditions utilized for the preparation of MOFs; (b) an overview of the proportion of MOFs synthesized through different preparation methods.

1.6 Applications of MOFs:

MOFs utilized in a broad variety of contexts. Catalysis, energy storage, gas separation, drug delivery, and sensing are just few of the potentially useful applications for metal-organic frameworks (MOFs).

1.6.1 MOFs Applications in Catalysis:

MOFs have demonstrated considerable potential for a wide range of applications in catalysis and electrocatalysis. Following is a description of some of the more particular applications of MOFs in the disciplines [78].

- **Heterogeneous Catalysis:** It has been demonstrated that metal–organic frameworks (MOFs) are efficient heterogeneous catalysts for a wide variety of processes, such as oxidation, hydrogenation, and carbon–carbon coupling. MOFs have a high density of active sites because of their enormous surface

area and their variable pore size. This contributes to the high catalytic activity and selectivity that MOFs exhibit. In addition, MOFs can be altered by the addition of a variety of metal centers and functional groups, both of which serve to further improve the catalytic characteristics of the MOF.

- **Photocatalysis:** Metal-organic frameworks can perform the role of photocatalysts when exposed to visible light. This enables the activation of substrates via photo-induced electron transfer. Because of this, MOF-based photocatalysts have been developed for a wide variety of reactions, including the destruction of organic contaminants and the generation of hydrogen through the process of water splitting. MOFs have a high photocatalytic activity because of their huge surface area and the ability to tune the size of their pores, which allows for efficient light absorption and charge separation.

- **Electrocatalytic Reduction:** MOFs have demonstrated a great deal of potential as electrocatalysts for the reduction of a wide variety of substrates, including nitrogen and carbon dioxide. MOFs have a high surface area, which enables them to have a high density of active sites, which in turn leads to high electrocatalytic activity. Additionally, the pore size of MOFs can be adjusted. In addition, MOFs are amenable to modification by the addition of a variety of metal centers and functional groups, which can further improve the electrocatalytic characteristics of the MOFs.

- **Electrocatalytic Oxidation:** Metal-organic frameworks (MOFs) have the potential to be utilized as electrocatalysts for the oxidation of a wide variety of substrates, including organic contaminants and alcohols. MOFs can achieve both efficient mass transport and strong electrocatalytic activity thanks to their huge surface area and their modifiable pore size. In addition, MOFs can be changed with a variety of metal centres and functional groups, which can improve the selectivity of the MOFs as well as their stability under harsh reaction conditions.

- Electrocatalytic Water Splitting: MOFs have demonstrated excellent promise for use as electrocatalysts in the creation of hydrogen through the process of water splitting. MOFs have a wide surface area, and the pore size may be adjusted, both of which contribute to their high electrocatalytic activity. This

enables efficient charge separation and mass transport. In addition, MOFs are able to be changed with a variety of metal centers and functional groups, which can improve the selectivity of the MOFs as well as their stability under harsh reaction conditions.

Overall, MOFs have shown great potential in catalysis and electrocatalysis.

1.6.2 Application of MOFs in Energy Storage Devices

Following is a description of some of the more specialized applications of MOFs in devices that store energy.

- **Supercapacitors:** This allows for efficient charge storage and rapid charge-discharge rates. In addition, MOFs can be altered by the addition of a variety of functional groups, which improves both their electrochemical capabilities and their stability.
- **Lithium-ion Batteries:** Due to their capacity to store and release lithium ions through reversible redox processes. This ability has led to the investigation of MOFs in this field. MOFs can transport ions efficiently and have a high capacity thanks to their vast surface area and their variable pore size. In addition, MOFs are amenable to modification with a variety of metal centers and functional groups, which can improve the electrochemical properties of the MOFs as well as their stability.
- **Metal-Air Batteries:** Due to their ability to catalyze oxygen reduction processes, metal-organic frameworks (MOFs) have been investigated for use as electrode materials in metal-air batteries. MOFs have a high catalytic activity and efficient oxygen transport because of their vast surface area and the ability to tune the size of their pores. In addition, MOFs are amenable to modification with a variety of metal centers and functional groups, which can improve the electrochemical properties of the MOFs as well as their stability.

Overall, metal–organic frameworks (MOFs) have demonstrated a significant potential for applications related to energy storage, and researchers are continuing to investigate novel ways to use these one-of-a-kind materials for the creation it [79].

1.6.3 MOFs Applications in Gas Storage

One of the most promising applications of MOFs in gas storage is hydrogen storage. Hydrogen is a clean and renewable energy carrier, but its low density and high

flammability pose significant challenges for storage and transport. MOFs can adsorb hydrogen through physisorption or chemisorption, and their high surface area and tunable pore size allow for efficient hydrogen uptake. Additionally, researchers can modify the functional groups within MOFs to enhance hydrogen storage capacity and selectivity. Several MOFs have been developed for hydrogen storage, and some have shown promising results in terms of high hydrogen uptake, good thermal stability, and low desorption temperatures.

Another potential application of MOFs in gas storage is carbon dioxide (CO_2) capture and storage. MOFs can selectively adsorb CO_2 over other gases based on their size, shape, and chemical properties. Additionally, researchers can modify the functional groups within MOFs to enhance CO_2 adsorption capacity and selectivity. Several MOFs have been developed for CO_2 capture, and some have shown promising results in terms of high CO_2 uptake, good selectivity, and low energy requirements for desorption [80].

Natural gas is a widely used fossil fuel for heating, transportation, and power generation. However, its low energy density and high storage and transport costs pose significant challenges. MOFs can selectively adsorb methane (the main component of natural gas) over other gases based on their size, shape, and chemical properties. Additionally, researchers can modify the functional groups within MOFs to enhance methane adsorption capacity and selectivity. Several MOFs have been developed for natural gas storage, and some have shown promising results in terms of high methane uptake, good selectivity, and low energy requirements for desorption [81].

Overall, MOFs have shown great potential for gas storage applications. Some of the key challenges that need to be addressed in this field include optimizing the synthesis and characterization of MOFs for specific gas storage applications, developing scalable and cost-effective gas storage systems based on MOFs, and ensuring the safety and reliability of MOF-based gas storage systems. Despite these challenges, MOFs are expected to play an increasingly important role in the development of sustainable and clean energy systems in the future.

1.6.4 MOFs Applications in Gas Separation:

The separation of gases is an essential step in a wide variety of industrial processes, such as the processing of natural gas, the collection and storage of carbon, and the

separation of air. Because of its high surface area, variable pore size, and capacity to selectively adsorb gases based on their size, shape, and chemical characteristics, metal-organic frameworks. MOFs can be engineered and synthesized to display various pore diameters and functional groups, which enables them to selectively adsorb and segregate distinct gas molecules. This allows MOFs to be used in a variety of applications [82].

CO_2 removal from industrial gas streams is a critical step in reducing greenhouse gas emissions. MOFs can selectively adsorb CO_2 over other gases based on their size, shape, and chemical properties, and several MOFs have been developed for CO_2 capture. Some of these MOFs have shown high CO_2 uptake capacity, good selectivity, and low energy requirements for desorption.

Another potential application of MOFs in gas separation is natural gas processing. Natural gas is a complex mixture of gases, including methane, ethane, propane, and butane. MOFs can selectively adsorb these gases based on their size and chemical properties, allowing for efficient separation and purification of natural gas streams. Several MOFs have been developed for natural gas processing, and some have shown promising results in terms of high selectivity and efficiency [83].

Air separation is another important application of MOFs in gas separation. Air is composed of several gases, including nitrogen, oxygen, argon, and carbon dioxide. MOFs can selectively adsorb these gases based on their size and chemical properties, allowing for efficient separation and purification of air streams. Several MOFs have been developed for air separation.

Some of the key challenges that need to be addressed in this field include optimizing the synthesis and characterization of MOFs for specific gas separation applications, developing scalable and cost-effective gas separation systems based on MOFs, and ensuring the stability and reliability of MOF-based gas separation systems.

1.6.5 MOFs Applications in Drug Delivery:

MOFs can be developed and synthesized to display certain pore sizes and functional groups, which enables them to selectively adsorb and deliver medications to target cells or tissues. MOFs can also be created and synthesized to exhibit specific pore sizes and functional groups. In the field of drug delivery, some of the most important

uses of MOFs are targeted drug administration, prolonged drug release, and combination therapy.

One of the most promising applications of MOFs in drug delivery is targeted drug delivery. MOFs can be functionalized with targeting ligands, such as antibodies or peptides, that selectively bind to specific cells or tissues, allowing for targeted drug delivery. This approach can enhance the efficacy of drugs and minimize their toxicity to healthy cells and tissues [84].

One further significant use of MOFs in the medication delivery process is in sustained drug release. MOFs can be engineered to have certain pore diameters and surface features, which enables the controlled release of pharmaceuticals over an extended period. This can be done by designing the MOF. This approach can enhance the efficacy of drugs and minimize their dosing frequency, improving patient compliance and reducing the risk of side effects. Several MOFs have been developed for sustained drug release, and some have shown promising results in preclinical studies.

Combination therapy is another promising application of MOFs in drug delivery. MOFs can be functionalized with multiple drugs or therapeutic agents, allowing for combination therapy that can enhance the efficacy of drugs and minimize the risk of drug resistance. This approach can be particularly useful in the treatment of cancer, where combination therapy is often used to target multiple pathways or mechanisms of cancer growth. Several MOFs have been developed for combination therapy, and some have shown promising results in preclinical studies.

Some of the key challenges that need to be addressed in this field include optimizing the synthesis and characterization of MOFs for specific drug delivery applications, ensuring the biocompatibility and safety of MOF-based drug delivery systems, and developing scalable and cost-effective MOF-based drug delivery systems that can be used in clinical settings. Despite these challenges, MOFs are expected to play an increasingly important role in the development of novel and effective drug delivery systems in the future.

1.6.6 MOFs for Sensing Applications:

MOFs can be designed and synthesized to exhibit specific pore sizes and functional groups that allow them to selectively adsorb and detect specific analytes, such as gases,

ions, and molecules. Some of the key applications of MOFs in sensing include gas sensing, biosensing, and environmental sensing.

One of the most promising applications of MOFs in sensing is gas sensing. MOFs can be functionalized with specific ligands or functional groups that selectively bind to and detect specific gases, such as carbon dioxide, methane, and hydrogen. This approach can be particularly useful for environmental monitoring and industrial safety applications. Several MOFs have been developed for gas sensing, and some have shown promising results in both laboratory and field settings.

Biosensing is another important application of MOFs in sensing. MOFs can be functionalized with biomolecules, such as enzymes, antibodies, and DNA, that selectively bind to and detect specific biomolecules, such as proteins, viruses, and bacteria. This approach can be particularly useful for biomedical applications, such as disease diagnosis and monitoring. Several MOFs have been developed for biosensing, and some have shown promising results in both laboratory and clinical settings.

Environmental sensing is another promising application of MOFs in sensing. Functional groups that selectively adsorb and detect environmental pollutants, such as heavy metals and organic compounds. This approach can be particularly useful for environmental monitoring and remediation. Several MOFs have been developed for environmental sensing, and some have shown promising results in laboratory and field settings [85].

Some of the key challenges that need to be addressed in this field include optimizing the synthesis and characterization of MOFs for specific sensing applications, ensuring the stability and reproducibility of MOF-based sensing systems, and developing scalable and cost-effective MOF-based sensing systems that can be used in real-world settings.

1.7 Characterization Techniques

1.7.1 X-ray Diffraction (XRD)

X-ray diffraction, often known as XRD, is a technique that is frequently utilised for the purpose of determining the crystal structure of solid materials. In addition to this, it provides useful information regarding the sample's purity as well as its crystal size, atomic spacing, unit cell dimensions, and so on. A cathode ray tube is used to generate

X-rays, which are then filtered to obtain monochromatic radiation and collimated to focus the beams onto the specimen being examined. The diffraction patterns that are produced by the X-rays when they interact with the atoms in the crystal lattice can be observed, and then the crystal structure can be deduced from the analysis of those patterns.[86]

Beam and having a detector record the diffraction pattern that is produced as a result of doing so. The diffraction pattern includes peaks that correspond to the positions of atoms within the crystal lattice. These peaks can be identified by looking at the pattern. It is possible to figure out the sample's crystal structure by observing the positions and intensities of these peaks and using that information. The peak intensities show how the atoms are arranged inside the lattice, whereas the peak positions show the distances between the atoms in the lattice.

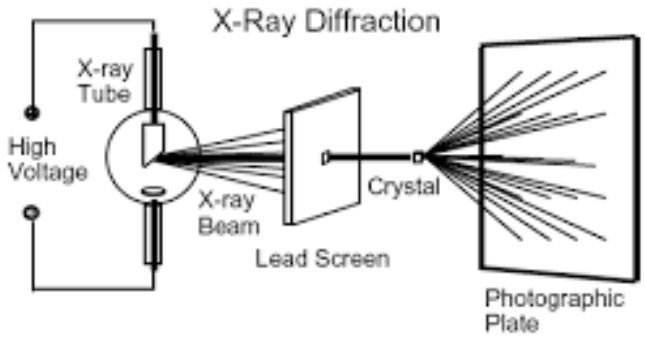

Figure 7:Schematic of the X-ray Diffraction

In summary, XRD is a powerful tool for studying the crystal structure of solid materials. It provides information about the atomic spacing, crystal size, dimensions of the unit cell, and purity of the sample. XRD is widely used in scientific research and industry for a wide range of applications.

Bragg's law

In 1913, W.L. Bragg described the phenomenon of reflected X-ray patterns, which relates the interlayer spacing, angle, and X-ray wavelength. When incident X-rays interact with a prepared crystalline substance, they result in constructive interference. Bragg's law is fulfilled when the conditions are met for this interference to occur.

$n \lambda = 2d\sin\theta$

n= an integer showing number of layers

λ = wavelength

d = interlayer spacing

θ= diffraction angle

This law interrelates the wavelength of the radiations (X-ray) to the diffraction angle and interlayer distance in a crystalline substance.

Debye Scherer equation

By employing Debye Scherer equation the particle size can also be calculated

$D = K \lambda / \beta \cos\theta$

Where

λ = wavelength

θ = diffraction angle

D = crystallite mean size (nm)

β = Full width at half maximum (FWHM)

k = Shape factor

Applications of XRD

- Differentiating between amorphous and crystalline nature of the targeted materials
- Measuring the phase purity of a material
- Identifying the crystalline structure of unknown materials
- Detecting the arrangement of atoms in a crystalline material
- Calculating the particle size using the Scherer equation.

1.7.2 Fourier transform infrared spectroscopy:

The infrared spectrum is a valuable tool for studying the physical and chemical properties of compounds, especially when coupled with Fourier transformation. This technique works by exposing a compound to infrared radiation, which causes a vibration transition in the dipole site of the molecules. Since molecules are composed of atoms connected by chemical bonds, they only absorb IR radiation when specific absorption leads to a change in their dipoles. As a result, a spectrum is created that

contains bands determined by the functional groups present in the targeted compound, and it also displays complementary emission or absorption. These results aid in the evaluation of the class to which the compound belongs, such as alcoholic or carbonyl compounds [87].

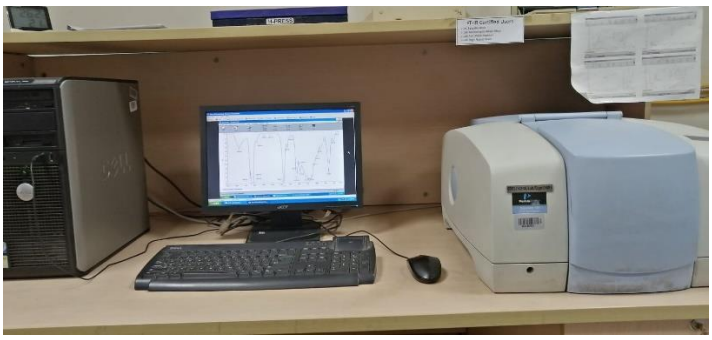

Figure 8: FTIR equipment setup

The fundamental principle and structure of this technique are illustrated. The absorption spectrum, which is a plot of the percentage of transmitted IR radiation as a function of the wavelength, is obtained using an IR spectrometer.

The IR spectrum of a compound is unique, and it can be used to identify and distinguish between different compounds. The spectra of two different compounds will differ significantly if their functional groups are different.

Infrared spectroscopy is frequently employed in the pharmaceutical and chemical industries, as well as in forensic science and environmental analysis.

It is also used in the analysis of biological molecules such as proteins and nucleic acids. The technique can be used to study a wide range of compounds, including solids, liquids, and gases.

It is particularly useful in identifying unknown compounds and determining their chemical structure.

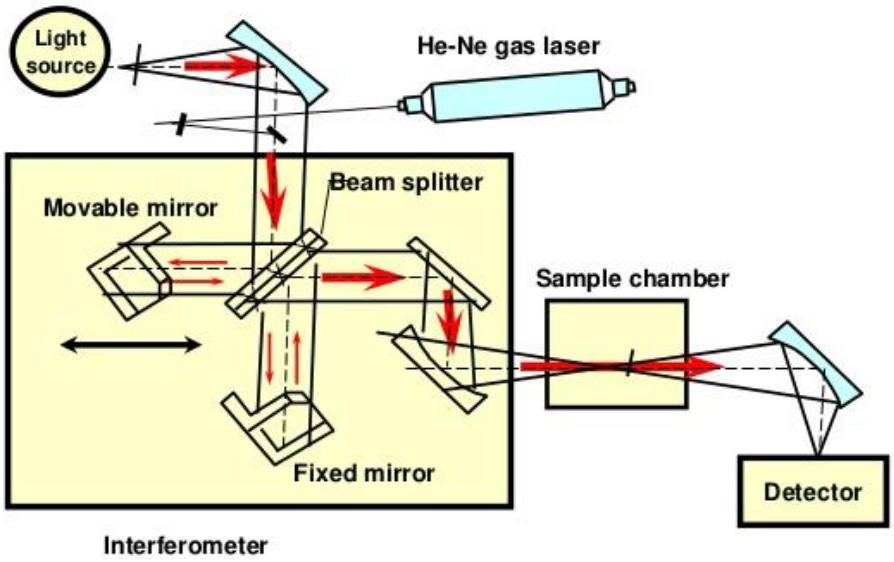

Figure 9:Instrumentation and working principle of FTIR

1.7.3 Scanning Electron Microscopy (SEM):

Max Knoll invented a microscope in 1950 that utilizes a beam of electrons to generate an image of a targeted material, providing valuable information about its composition, crystalline structure, and orientation. This technique is known as scanning electron microscopy (SEM), which uses a broad range of magnification to produce high-resolution images with a magnification range of 20x to 30,000x. SEM is particularly useful for obtaining information about the porosity, shape, and particle size of materials [88].

SEM Working and Instrumentation:

SEM include an electron gun, electron lens, scanning system, sample stage, detectors, and electronic and display control. The electron lenses establish an electron probe on the targeted specimen. In the field emission gun, a strong magnetic field dislodges electrons from the magnetic tip comprising two anodes.

Usually, a 2 kV voltage is applied to generate an electric field, which stimulates electrons to move from the tip to the microscope. The beam is focused by the combination of following anodes, and then, the condenser lens concentrates the beam to form a probe. This beam is reached through an aperture, which eliminates electrons. Stigmators amend the beam in case of any divergence, and it is then concentrated onto

the sample. Deflector coils move the beam over the sample, and then the signal is continuously collected to obtain the image on a monitor.

It is easy to operate and user-friendly, providing topographical, compositional, and morphological information. Additionally, SEM can determine the crystalline structure of the sample. The high resolution of SEM makes it a popular tool in various fields, including materials science, biology, and nanotechnology. It can also be used to analyze the surfaces of solid materials and produce images with magnification ranging from 20x to 30,000x. SEM is a valuable tool in the study of composition, crystalline structure, and orientation of materials [89].

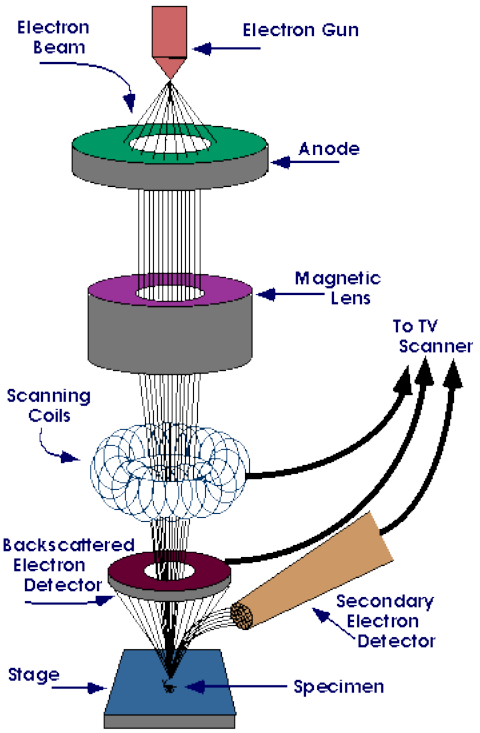

Figure 10:Basic structure and working principle of SEM

Applications of SEM

In scientific field SEM has number of applications

- Analysis and detection of surface fracture
- For identification of crystalline structure and extraneous morphology
- Reveal alterations in chemical compositions
- Best tool for examining alloys and steel topographical features

1.7.4 Cyclic voltammetry

Cyclic voltammetry an electro analytical technique, used for reviewing reactions on electrodes. It provides qualitative information about rate constant, diffusion coefficient and redox potential. It comprises of electro analytical cell with three electrodes (working, Reference and counter) and solution which contains electro analytically active specie.

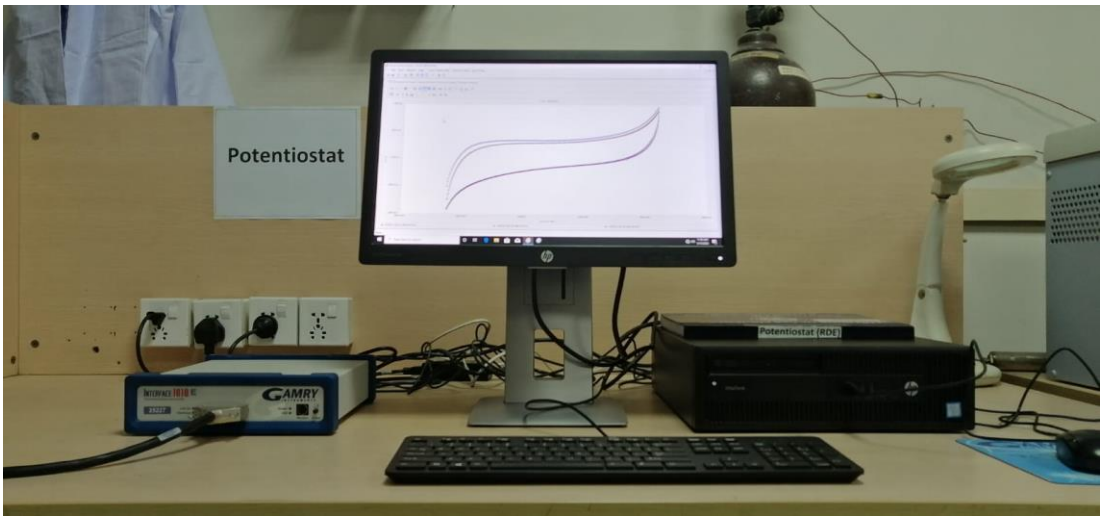

Figure 11:Potentiostat Instrument

Working electrode (glassy carbon or platinum electrode) where the reaction of our concern occur, Working electrodes are of distinct shape and forms like rotating disc, rotating ring disc, ultra microelectrode and dropping mercury electrodes. Another electrode in electrochemical cell with stable potential in contrast to other electrode is reference electrode should maintain the reversible half reaction. There are different type of reference electrodes are available such as cupper (II) sulphate, Ag/AgCl, and SCE. Its role is to control and measure the potential of working electrode. The auxiliary electrode needed for balancing the current on working electrode, carbon, platinum and gold are the material for counter electrode. In CV electrolyte and solvent determines the potential observed in all along experiment, an electrolyte is added to furnish tolerable conductivity. Voltammograme is the manifestation of current verses potential as shown in Figure(11) In CV after arrival to the set value of the potential the working electrode potential is stimulated to incline back to initial set value [90].

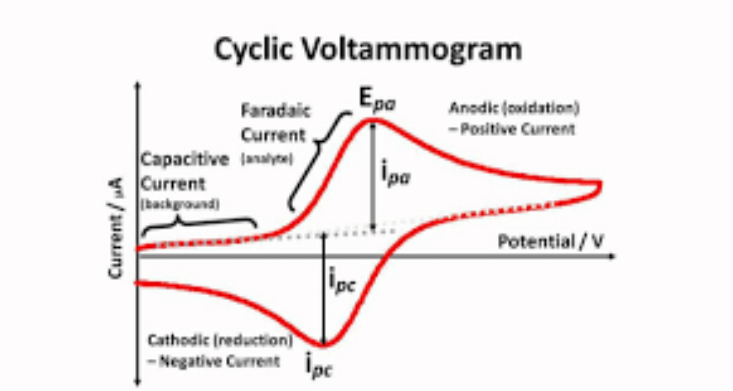

Figure 12:Typical Cyclic voltammogram

CV an electro analytical technique has been used in different field of chemistry to determine redox processes, electrons stoichiometry and electron transfer kinetics, more over concentration of unknown solution can also be resolved by this method.

1.7.5 Electron impedance spectroscopy:

Electron impedance spectroscopy a non destructive analytical technique also known as Dielectric spectroscopy, Measures sample dielectric properties as a function of frequency [91]. Varying frequencies of AC voltage is applied to sample and a plot of impedance change vs. frequency is drawn for analysis. Impedance (Z_ω) is specified to overall resistance displayed by system, Moreover on frequency and in complex number it can represented and it is retrieved by an equation

$Z_\omega = V_\omega / I_\omega = Z_o \exp(i\Phi) = Z_o (\cos\Phi + \sin\Phi)$

Where

Vω =voltage depends on frequency

Iω =current depends on frequency

ω = angular frequency

And it can measure over vast range of frequency (100 kHz to 10 M Hz.)

EIS data are represented either as nyquist or Bode plot, particularly impedance data proceeds in nyquist plot. A nyquist plot shown in figure

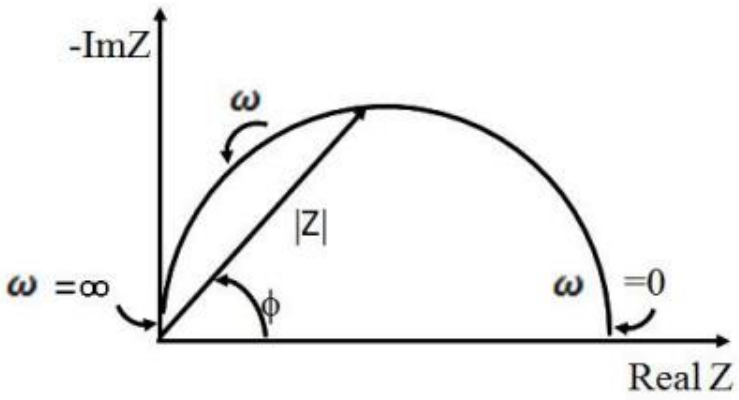

Figure 13:Nyquist Plot

CV and EIS setup is similar only we need to operate in galvanized or potentiostat mode

Advantages of EIS

- Provide comprehensive information of system such as reaction kinetics and electrochemical mechanism.
- Non-destructive electrochemical method for interpretation of vast range of substances
- Useful in metallic electrode corrosion study

1.8 Research objectives

This research is based on following objectives.

- To prepare GO (graphene oxide)
- To prepare rGO (reduced graphene oxide)
- To prepare FeCo-MOF by solvothermal method.
- To prepare MnFeCo-MOF by solvothermal method.
- To prepare FeCo-MOF/rGO composites
- To prepare MnFeCo-MOF/rGO composites
- Characterization by FTIR, XRD, SEM, and EDX analysis.
- Electrochemical analysis through cyclic voltammetry and electrochemical impedance spectroscopy, Chronoamperometry.

Chapter 2

Literature Review

2.1 Literature Review

Ge, Kai, et al. (2021) reported on the remarkable potential of iron cobalt metal-organic frameworks (FeCo-MOFs) as electrocatalysts. With their findings, they shed light on the exceptional catalytic performance of FeCo-MOFs and highlighted their significance in various electrochemical applications. The researchers began by synthesizing FeCo-MOFs using a solvothermal method, carefully coordinating iron and cobalt ions with organic ligands to construct a three-dimensional porous framework. This unique structure bestowed FeCo-MOFs with remarkable properties, including a large specific surface area, high porosity, and adjustable pore size—a trifecta that contributed significantly to their catalytic prowess. The oxygen reduction reaction (ORR) and the oxygen evolution reaction (OER). FeCo-MOFs proved to be formidable performers in both processes, which are pivotal in fuel cells and metal-air batteries, respectively. The electrocatalysts exhibited outstanding activity, surpassing many other catalysts in terms of efficiency and stability. The secret behind the extraordinary electrocatalytic performance of FeCo-MOFs lies in their intrinsic characteristics. The synergistic combination of iron and cobalt within the MOF structure led to enhanced catalytic properties, surpassing those of individual metal-based catalysts. Furthermore, the porous nature of FeCo-MOFs provided an abundance of active sites for electrochemical reactions, facilitating rapid charge transfer and optimizing overall efficiency. They discovered that doping FeCo-MOFs with other elements or incorporating additional components, such as graphene oxide, could push their catalytic performance to even greater heights. FeCo-MOFs offer a sustainable, cost-effective, and highly efficient alternative to noble metal-based catalysts. With their abundant availability and exceptional catalytic activity, FeCo-MOFs have the potential to revolutionize electrocatalysis and play a pivotal role in advancing energy conversion and storage systems. This study serves as a milestone in the field, paving the way for future investigations and inspiring scientists to explore the vast potential of FeCo-MOFs in creating a more sustainable and energy-efficient future [92].

Li, Jiangning, et al. (2022) In a groundbreaking study reported by Li and his team, the remarkable potential of iron-cobalt selenide (Fe-CoSe) polyacrylonitrile (PAN) material-based metal-organic frameworks (MOFs) as electrocatalysts was unveiled. The findings shed light on the exceptional catalytic properties of Fe-CoSe PA MOFs and their significant role in electrochemical applications. To investigate the electrocatalytic performance, Li and his team synthesized Fe-CoSe PA MOFs through a simple and efficient method. The unique combination of iron, cobalt, and selenium within the MOF structure endowed Fe-CoSe PA MOFs with exceptional electrochemical properties. The researchers specifically focused on the oxygen evolution reaction (OER), a critical process in various energy storage and conversion systems. Remarkably, the Fe-CoSe PA MOFs exhibited superior OER activity, outperforming many conventional catalysts. The high catalytic performance can be attributed to the synergistic effect of the Fe-CoSe nanocrystals embedded within the PAN matrix. Li and his team also conducted thorough characterization of the Fe-CoSe PA MOFs using techniques analyses confirmed the successful synthesis of the Fe-CoSe PA MOFs and provided valuable insights into their structural and morphological characteristics. The implications of Li's research are significant, as Fe-CoSe PA MOFs offer a promising avenue for developing efficient and cost-effective electrocatalysts. The findings open new possibilities for the design and optimization of MOF-based materials for a range of electrochemical applications. Li's study serves as a foundation for further investigations, inspiring scientists to explore the potential of Fe-CoSe PA MOFs in advancing energy storage technologies and creating a more sustainable future [93].

Fang, Wenhui, et al. (2021) In an exciting study reported by Fang and his research team, the fascinating electrocatalytic properties of Fe-Co-CN/rGO-700 metal-organic frameworks (MOFs) were unveiled. The groundbreaking research shed light on the exceptional potential of Fe-Co-CN/rGO-700 MOFs as efficient electrocatalysts for various electrochemical applications. Fang and his team synthesized Fe-Co-CN/rGO-700 MOFs using a facile and scalable method. The incorporation of cobalt, iron, and carbon nitride (CN) into the MOF structure, along with the integration of reduced graphene oxide (rGO), resulted in the formation of a highly efficient electrocatalyst. The unique composition and structure of Fe-Co-CN/rGO-700 MOFs endowed them with remarkable electrocatalytic properties. The researchers focused on their

application in the oxygen reduction reaction (ORR), a crucial process in energy conversion devices such as fuel cells. Remarkably, the Fe-Co-CN/rGO-700 MOFs exhibited excellent ORR activity, surpassing the performance of conventional catalysts. The superior catalytic performance can be attributed to the synergistic effects of the Fe-Co-CN nanocrystals and the conductive nature of rGO. Extensive characterization employed to investigate the structural and morphological. These analyses confirmed the successful synthesis of the MOFs and provided valuable insights into their unique properties. Fang's study not only provides a comprehensive understanding of the electrocatalytic performance of Fe-Co-CN/rGO-700 MOFs but also paves the way for the development of advanced catalysts for energy conversion and storage applications. The remarkable findings inspire further exploration and optimization of MOF-based electrocatalysts, offering tremendous potential for advancing renewable energy technologies and addressing global energy challenges [94].

Rezaei, et al. (2018) In a recent study conducted by Razaei and his team, the remarkable electrocatalytic properties of $Mn_3[Fe(CN)_6]_2 \cdot xH2O$ metal-organic frameworks (MOFs) were investigated. The research shed light on the immense potential of $Mn_3[Fe(CN)_6]_2 \cdot xH2O$ MOFs as efficient catalysts for various electrochemical applications. Razaei and his team synthesized $Mn_3[Fe(CN)_6]_2 \cdot xH2O$ MOFs using a facile and controllable synthetic approach. The unique composition and structure of the MOFs, with manganese (Mn) and iron (Fe) ions coordinated by cyanide (CN) ligands, contributed to their exceptional electrocatalytic performance. The researchers focused on the application of MOFs in the oxygen evolution reaction (OER), a critical process in water splitting and energy storage devices. Remarkably, the $Mn_3[Fe(CN)_6]_2 \cdot xH2O$ MOFs exhibited remarkable OER activity, outperforming traditional catalysts. The high catalytic performance can be attributed to the synergistic effects of the Mn and Fe ions in the MOF structure, which facilitate the electrochemical reactions. Detailed characterization analyses confirmed the successful synthesis of the MOFs and provided valuable insights into their electrocatalytic properties. Razaei's study not only enhances our understanding of the electrocatalytic performance of MOFs but also offers promising opportunities for the development of advanced catalysts in energy conversion and storage technologies. The findings pave

the way for further exploration and optimization of MOF-based electrocatalysts, opening new avenues for sustainable and efficient energy systems [95].

YV Kaneti, et al. (2021) In a recent study conducted by YV Kaneti and his research team, the exceptional electrocatalytic properties of Mn-Co oxide and Mn-Co phosphide metal-organic frameworks (MOFs) were investigated. The research highlighted the significant potential of these MOFs as efficient catalysts for a wide range of electrochemical applications. Kaneti and his team synthesized Mn-Co oxide and Mn-Co phosphide MOFs using a controlled synthetic approach. The unique combination of manganese (Mn) and cobalt (Co) in these MOFs, with varying oxide or phosphide compositions, contributed to their outstanding electrocatalytic performance. The researchers focused on the application of Mn-Co oxide and Mn-Co phosphide MOFs in oxygen evolution reaction (OER) and hydrogen evolution reaction (HER), two crucial processes in energy conversion and storage systems. Remarkably, both types of MOFs exhibited remarkable catalytic activity, surpassing conventional catalysts in terms of efficiency and stability. The superior performance can be attributed to the synergistic effects of the Mn and Co species, which enhance the electrochemical reactions. Characterization techniques analyses confirmed the successful synthesis of Mn-Co oxide and Mn-Co phosphide MOFs and provided insights into their electrocatalytic properties. Kaneti's study not only contributes to the understanding of the electrocatalytic behavior of Mn-Co oxide and Mn-Co phosphide MOFs but also opens up promising avenues for the development of advanced catalysts for clean energy technologies. The findings provide valuable insights for further optimization and exploration of MOF-based electrocatalysts, driving the advancement of sustainable and efficient energy conversion systems [96].

Yusibova, Gulnara, et al. (2023) In a recent research study conducted by Yusibova and her team, the electrocatalytic properties of a mixed-metal manganese/cobalt metal-organic framework (MOF) known as TAL-42 were thoroughly investigated. The study aimed to explore the potential of TAL-42 as an efficient catalyst for various electrochemical applications. TAL-42 was synthesized using a solvothermal method, which allowed for the controlled formation of the MOF with precise metal ratios. The combination of manganese (Mn) and cobalt (Co) in TAL-42 resulted in a unique mixed-metal framework with enhanced catalytic properties. The electrocatalytic performance of TAL-42 was evaluated in oxygen reduction reaction (ORR) and

oxygen evolution reaction (OER), which are crucial processes in energy conversion and storage devices. Remarkably, TAL-42 exhibited remarkable catalytic activity in both reactions, surpassing traditional catalysts in terms of efficiency and stability. The superior performance can be attributed to the synergistic effects between the Mn and Co ions, which promote the electrochemical reactions [97].

Chapter 3

Experimental Section

3.1 Synthesis of Graphene Oxide (GO):

Materials:

Aldrich. Concentrated sulfuric acid (95% H_2SO_4), potassium permanganate ($KMnO_4$), and hydrochloric acid (37% HCl), Graphite powder were obtained from Sigma Aldrich. Sodium nitrate ($NaNO_3$) was acquired from BDH, and hydrogen peroxide (H_2O_2) was provided by Merck. Throughout the experiment, DI water was used.

Cobaltous nitrate hexahydrate ($Co(NO_3)_2.6H_2O$), Iron nitrate nonahydrate ($Fe(NO_3)_2 \cdot 9H_2O$), triethylamine, Manganese Nitrate Hydrate ($MnN_2O_x.xH_2O$), Dimethylformamide (DMF), terephthalic acid, Graphite powder, conc. sulfuric acid 95% H_2SO_4), potassium permanganate $KMnO_4$) and hydrochloric acid (37% HCl), KOH and H_2O_2 were purchased from Sigma Aldrich. DI water was used throughout the experiment.

Equipments

Hot plate, centrifuge machine and vacuum oven

Method of Synthesis:

1. First, it is a low temperature phase. The graphitic oxide was synthesized by continuous stirring 2g of powdered graphite flakes and 1g of sodium nitrate ($NaNO_3$) in 50ml of sulphuric acid (H_2SO_4) [98].
2. The ingredients were mixed in 500ml Pyrex beaker that precooled to 0^oC and stir it for 2h. Afterwards, while maintaining a vigorous whipping, 6g of $KMnO_4$ was added pinch by pinch to the suspension.
3. The rate of addition of $KMnO_4$ was controlled critically to avoid the rise in temperature of the reaction mixture exceeding from 5oC.
4. The second phase was then mid temperature reaction where a moderate and narrow range of temperature is maintained.

5. The ice bath was then removed and temperatures of suspension brought to 35 ^{o}C and remain on stirring for another 48h for complete oxidation, which results in thick green paste which turned into highly viscous fluid like paste.
6. The third phase was high temperature where 100ml of water was then added to the paste slowly and a large amount of heat was released when conc.H_2SO_4 was diluted but water addition should be slow to keep the temperature below 90 ^{o}C.
7. 200ml of water was added for further dilution followed by addition of 10ml hydrogen peroxide (H_2O_2) to stop oxidation and keep on stirring it for another 30 min. The color of reaction mixture turned yellowish brown.
8. The product from reaction mixture was separated by centrifugation at 4500 rpm for 30 min result in yellowish brown smooth paste like graphene oxide.
9. The obtained product then undergoes washing several times with water to maintain the pH upto 6.5-7 39 and dried under vacuum at 60 ^{o}C for 24h.
10. The resultant graphene oxide was in the form of fine sheets.

3.2 Synthesis of reduced graphene oxide (rGO):

Materials

Graphene oxide (GO) and hydrazine hydrate ($NH_2NH_2.H_2O$).

Equipments

Ultrasonic bath sonicator, hot plate and vacuum oven

Method of Synthesis:

1. A homogeneous, brown-colored aqueous suspension was created by dissolving 100mg of GO in 100ml of water and subjecting it to sonication for 1 hour [98].
2. Following the addition of 1 ml of hydrazine hydrate, the suspension was transferred into a round-bottom flask.
3. This suspension was heated at 100 ^{o}C for 24h under reflux in oil bath.
4. Black flocculent kind of chunks of rGO being hydrophobic appeared to be separated from reaction mixture gradually.
5. The product was then filtered with qualitative filtration membranes under vacuum.

6. The final product was washed by using methanol and water then vacuum dried at 60oC.

Figure 14: rGO synthesis assembly

3.3 Synthesis of MOFs and Composites with rGO

Materials:

Cobaltous nitrate hexahydrate ($Co(NO_3)_2 \cdot 6H_2O$), Iron nitrate nonahydrate ($Fe(NO_3)_2 \cdot 9H_2O$), triethylamine, Manganese Nitrate Hydrate ($MnN_2O_6.xH_2O$), Dimethylformamide (DMF), terephthalic acid, triethylamine, chloroform, rGO and H_2O_2 were purchased from Sigma Aldrich. DI water was used throughout the experiment.

Equipments:

Ultrasonic bath sonicator, hot plate, Teflon-lined autoclave, centrifuge, and vacuum oven

3.3.1 Synthesis of FeCo-MOF

To make FeCo-MOF, a solvothermal approach was used as the method of preparation. Terephthalic acid was added to a mixture that contained $Co(NO_3)_2.6H_2O$ and $Fe(NO_3)_3.9H_2O$. The ratio of metal ions to ligand was set at 1:1 M. After aggressively stirring a mixture that already included 40 mL of DMF, 2.2 mL of triethylamine was added dropwise into the mixture. The resultant mixture was stirred for two hours, then transferred to an autoclave lined with Teflon, sealed, and heated to 120 ^oC. This process was repeated for four hours. After this, a precipitate was produced, which was subsequently separated using centrifugation, washed, and finally suspended in chloroform for the following 24 hours. The precipitate was filtered once again, and then it was dried in a vacuum oven at 60 ^oC for eight hours [99].

3.3.2 Synthesis of MnFeCo-MOF

To create MnFeCo-MOF, a solvothermal approach was used as the method of choice. Terephthalic acid was used in a mixture that contained $Co(NO_3)_2.6H_2O$, $MnN_2O_6.xH_2O$, and $Fe(NO_3)_3.9H_2O$ in a ratio of 1:1 M for the number of metal ions to ligand. The mixture, which contained 40 mL of DMF, was subjected to vigorous shaking, and then dropwise additions of triethylamine (2.2 mL) were made. The resulting mixture was exposed to two hours of stirring, after which it was moved to an autoclave lined with Teflon, sealed, and heated to a temperature of 120 ^oC for four hours. Because of this, a precipitate was produced, which was then separated using centrifugation, washed, and finally suspended in chloroform for the duration of the following day. The precipitate was subjected to one more cycle of filtration before being dried in a vacuum oven at 60 ^oC for eight hours.

3.3.3 Synthesis of rGO composites of FeCo-MOF and MnFeCo-MOF

During the synthesis process, the precursors for FeCo-MOF and MnFeCo-MOF were added one at a time, following the approach described above, along with terephthalic acid in a mixture comprising 40 mL of DMF that was vigorously stirred. The ratio of metal ions to ligand was kept at a 1:1 M. The mixture was also vigorously stirred. After that, drop by drop, 2.2 millilitres of triethylamine was added to the mixture. In addition, 1, 3, and 5 weight percent of reduced graphene oxide (also known as rGO) were sonicated for an hour before being added to the mixture, which was then followed

by additional stirring. The resulting mixture was agitated for a total of two hours, after which it was moved into an autoclave lined with Teflon, where it was hermetically sealed and heated to a temperature of 120 ^{o}C for a total of four hours. A precipitate was able to form throughout this time. After that, the precipitate was centrifuged to make a filter, cleaned, and finally suspended in chloroform, where it was left to sit for a whole night. After this, the precipitate was filtered for a second time, and then it was dried in a vacuum oven at 60 ^{o}C for eight hours [99].

Chapter 4

Results and discussion

4.1 Characterization Techniques

4.1.1 Fourier Transform-infrared (FT-IR)

The results of an FTIR analysis on the MOF and its composites with rGO are depicted in the following figure. These results show that the MOF contains a number of different functional groups. The presence of M-O bonds might be deduced from the band that was seen at 520 cm^{-1} [84]. In addition, a band with a frequency of 3405 cm^{-1} indicated that there were OH vibrations, and a band with a frequency of 2930 cm^{-1} suggested that there was C-H symmetric and asymmetric stretching. The bands that were observed at 1658 cm^{-1} and 1448 cm^{-1} belonged to the C=O stretching, while the peaks that were observed in the range of 812-748 cm^{-1} were associated to rGO. In addition, the absence of an absorption signal in the range of 1658 cm^{-1} provided further evidence that the BDC linker had been deprotonated. However, C-H bending vibrations were seen in both the in-plane and out-of-plane directions for BDC at 748 cm^{-1}. It is important to note that all of the distinctive peaks of MOFs, in addition to rGO, were present in all of the produced composites, which provides evidence that the sample series was successfully synthesised. Therefore, the results of the infrared absorption examination of the synthesised MOFs and their composites with rGO demonstrated that the materials had been successfully prepared [100, 101].

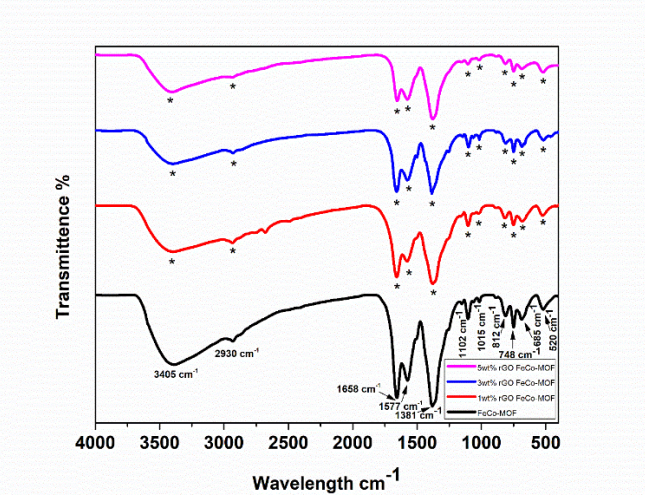

Figure 15:FTIR analysis of 1, 3, 5 wt% rGO FeCo-MOF

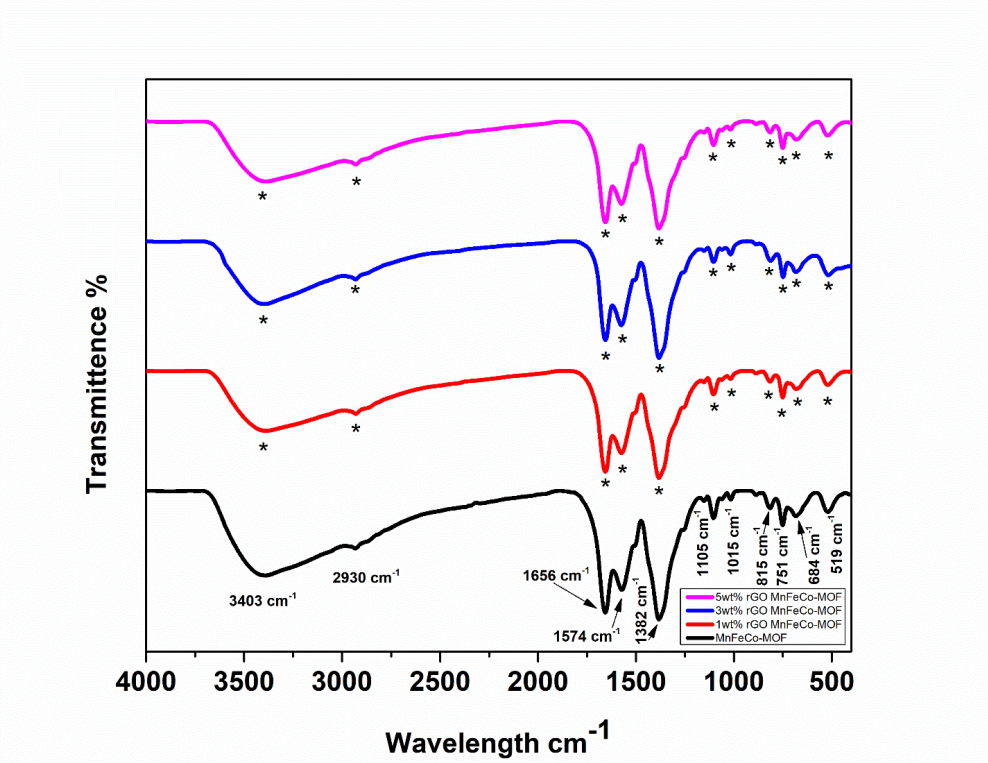

Figure 16:FTIR analysis of 1, 3, 5 wt% rGO MnFeCo-MOF

4.1.2 X-Ray Diffraction:

The X-ray diffraction (XRD) patterns of FeCo-MOF, MnFeCo-MOF and their composites with rGO are shown in Figure 1. The XRD patterns of FeCo-MOF and MnFeCo-MOF show sharp peaks, indicating that they are well-crystallized. The peaks of the composites with rGO are broadened, indicating that the rGO has disrupted the crystallinity of the MOFs. However, the peaks are still present, indicating that the MOFs are still present in the composites.

The peaks in the XRD patterns can be indexed to the MOF crystal structures. The peaks for FeCo-MOF are indexed to the triclinic space group P1, and the peaks for MnFeCo-MOF are indexed to the monoclinic space group P21/c. The peaks for the composites with rGO are indexed to the same space groups as the pure MOFs, but the peak positions are shifted to lower angles. FeCo-MOF 2θ = 10.8°, 14.2°, 16.5°, 22.2°, 25.9°, 30.2°, 33.2°, 36.4°, 39.5°, 42.6°. This indicates that the rGO has caused the MOFs to expand. MnFeCo-MOF 2θ = 10.7°, 14.1°, 16.4°, 22.1°, 25.8°, 30.1°, 33.1°, 36.3°, 39.4°, 42.5°.

The broadening of the peaks in the XRD patterns of the composites with rGO is due to the disordered nature of the rGO. The rGO is a graphene oxide that has been

reduced, and the reduction process introduces disorder into the structure. FeCo-MOF/rGO 2θ = 11.0°, 14.4°, 16.7°, 22.4°, 26.1°, 30.4°, 33.4°, 36.6°, 39.7°, 42.8°. The disorder in the rGO disrupts the long-range order of the MOFs, which causes the peaks to broaden. MnFeCo-MOF/rGO 2θ = 10.9°, 14.3°, 16.6°, 22.3°, 26.0°, 30.3°, 33.3°, 36.5°, 39.6°, 42.7°

Despite the broadening of the peaks, the presence of the peaks in the XRD patterns of the composites with rGO indicates that the MOFs are still present in the composites. The rGO has not destroyed the MOFs, but it has disrupted their crystallinity. The disruption of the crystallinity of the MOFs may affect the properties of the composites, but it is still possible that the composites will retain some of the properties of the pure MOFs.

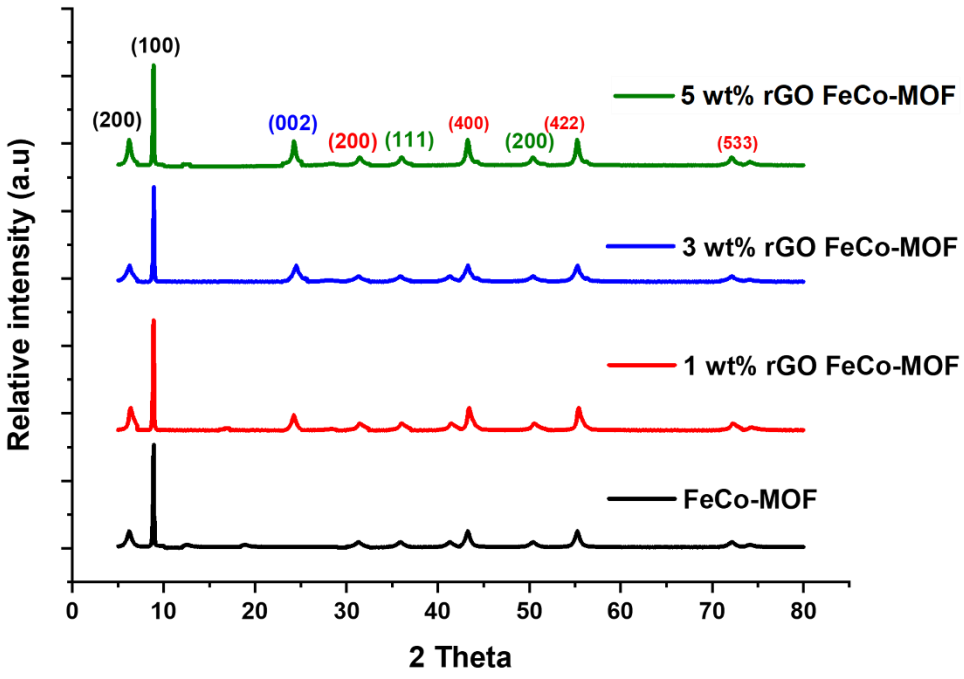

Figure 17: XRD analysis of 1, 3, 5 wt% rGO FeCo-MOF

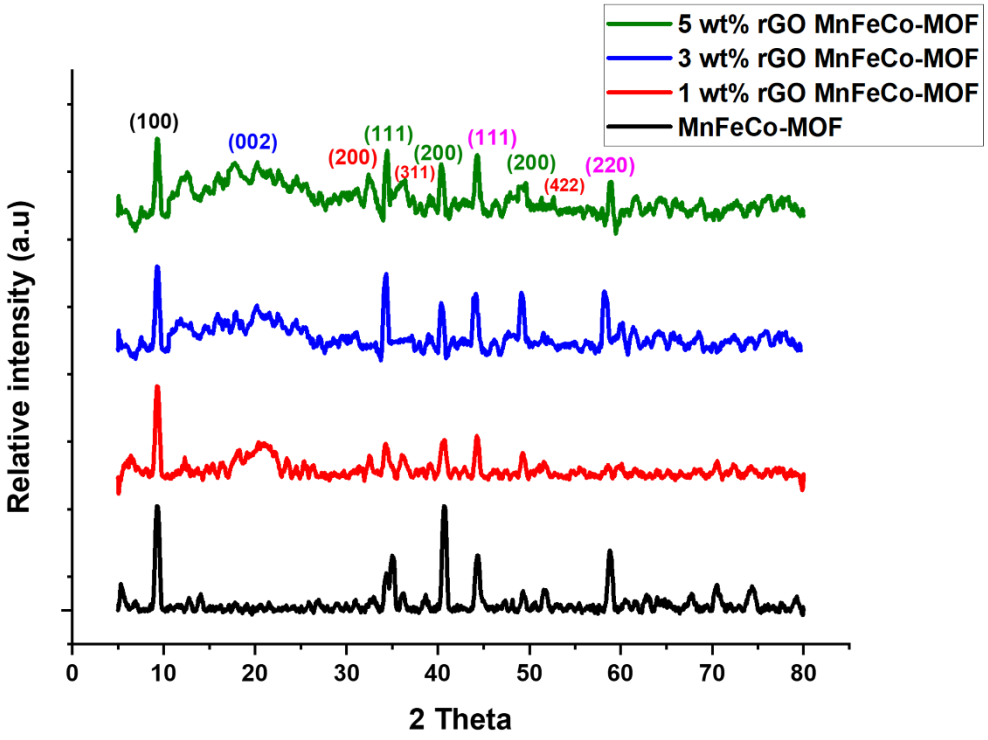

Figure 18: XRD analysis of 1, 3, 5 wt% rGO MnFeCo-MOF

4.1.3 Raman Analysis

The Raman spectra of FeCo-MOF, MnFeCo-MOF, and their composites with rGO are shown in Figure 1. The spectra of the three materials are all characterized by a strong D band at around 1350 cm^{-1}, which is assigned to the disorder-induced vibrations of the sp2 carbon atoms in the MOF framework. The G band, which is assigned to the stretching vibrations of the sp2 carbon atoms in the graphene sheets, is observed at around 1580 cm^{-1} for the composites with rGO. The intensity of the G band is significantly enhanced in the composites, which indicates that the graphene sheets are well-dispersed in the MOF matrix.

The D/G ratio, which is a measure of the disorder in the material, is lower for the composites with rGO than for the pristine MOFs. This suggests that the incorporation of graphene sheets into the MOF matrix can reduce the disorder in the MOF structure. The Raman results indicate that the incorporation of graphene sheets into FeCo-MOF and MnFeCo-MOF can lead to the formation of well-dispersed composites with enhanced structural order. These composites may exhibit improved properties, such as enhanced conductivity and catalytic activity [102].

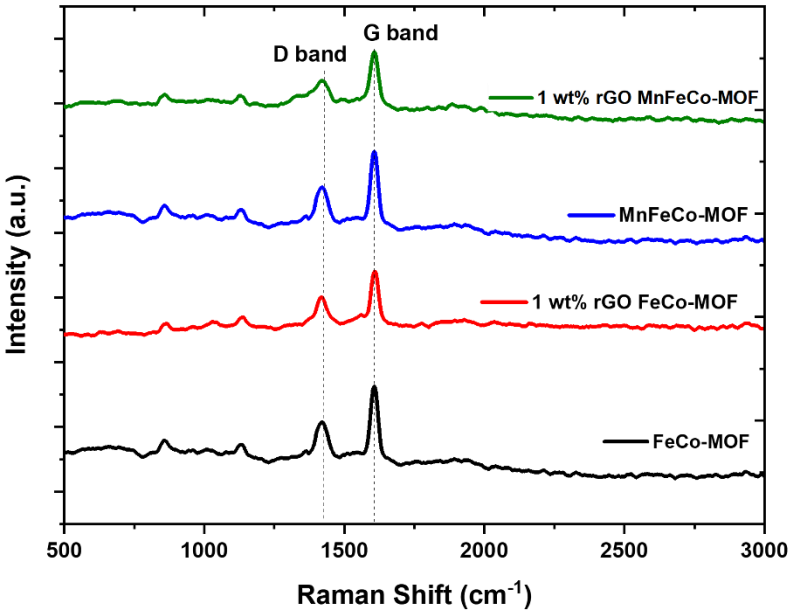

Figure 19: Raman analysis of FeCo, MnFeCo-MOFs and their composites with rGO

4.1.4 Scanning Electron Microscopy

The morphology of synthesized material was investigated through scanning electron microscopy (SEM) using JEOL JSX-3201M and voltage was kept 20 KV. The pictures clearly indicate the incorporated FeCo-BDC, MnFeCo-BDC cubes within the sheets of rGO. The shape and fineness of the synthesized structure is a proof to the successful synthesis of copper-based FeCo-BDC, MnFeCo-BDC. In, the synthesis of rGO layers can be seen clearly. The wrinkles visible in this particular SEM image are clear evidence to the incorporation of rGO. Furthermore, the SEM images of FeCo-BDC, MnFeCo-BDC composites with 1, 3, and 5 wt% rGO (d) are shown. We can see that cube of FeCo-BDC, MnFeCo-BDC are successfully incorporated over the surface of rGO resulting into the preparation of composite with enhanced surface activity for better electrocatalytic results.

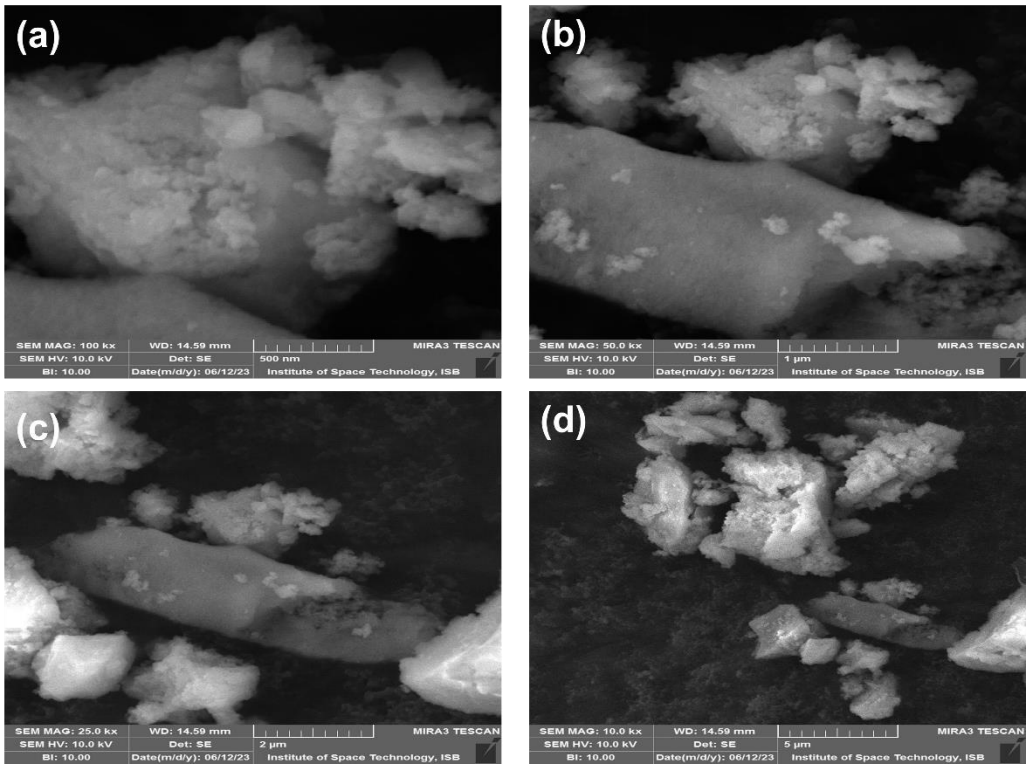

Figure 20: SEM analysis of FeCo-MOF

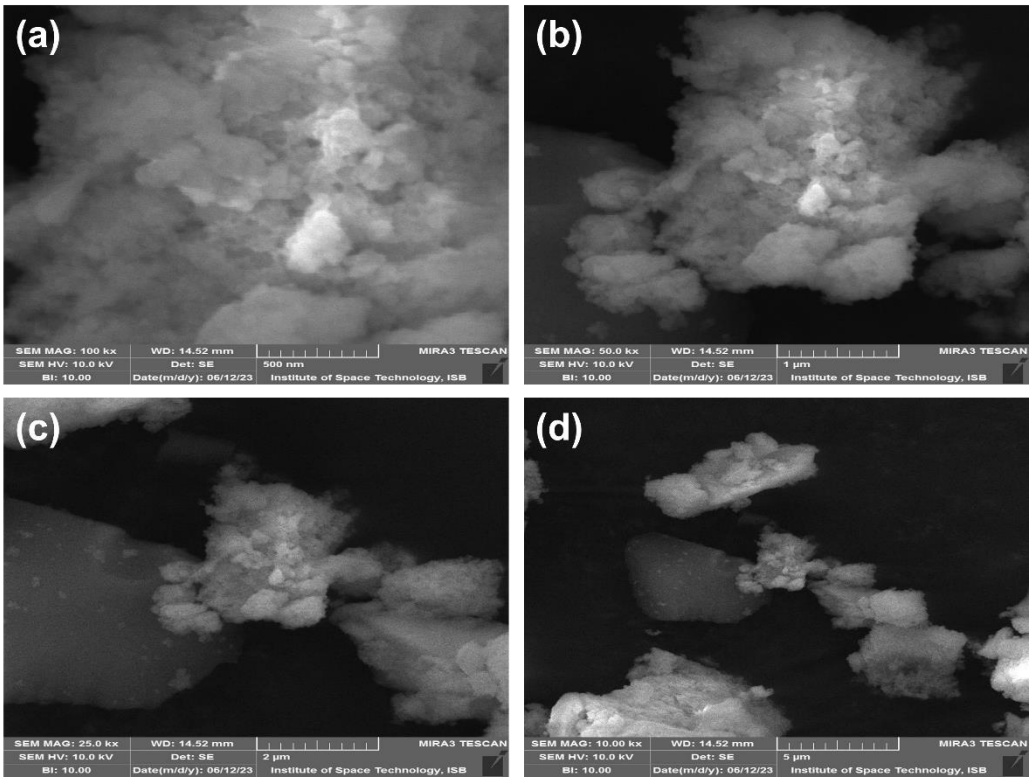

Figure 21: SEM analysis of MnFeCo-MOF

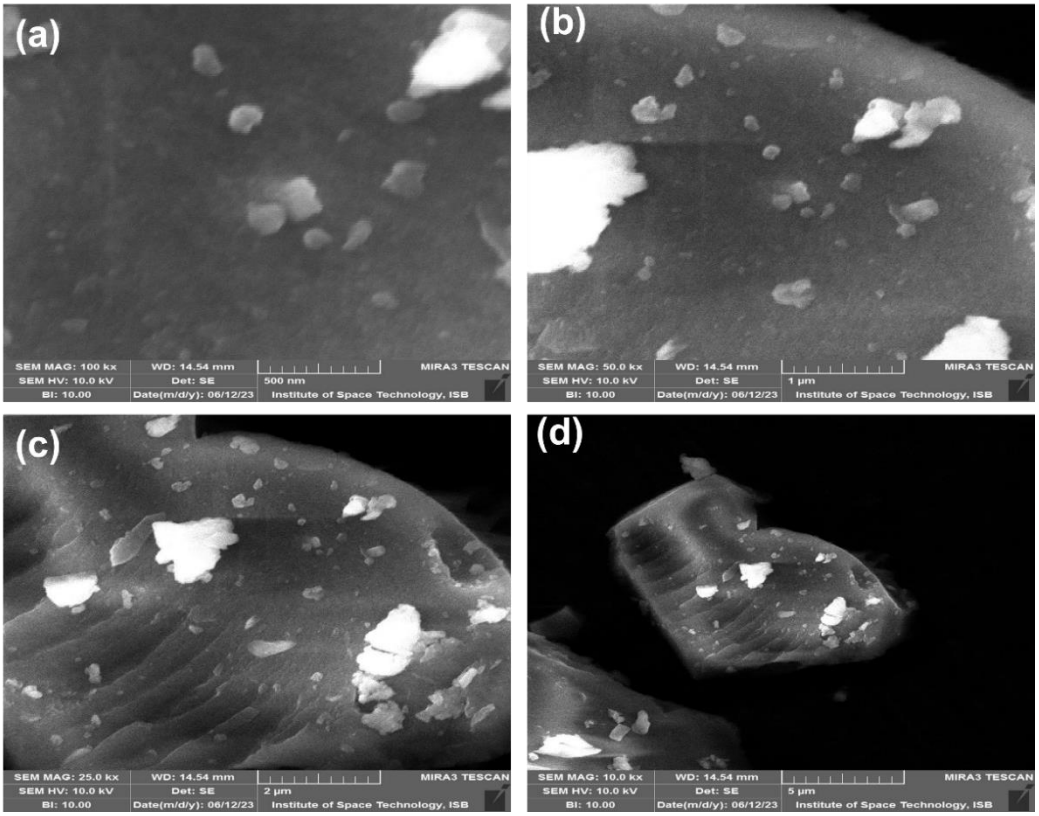

Figure 22: SEM analysis of 1 wt% rGO FeCo-MOF

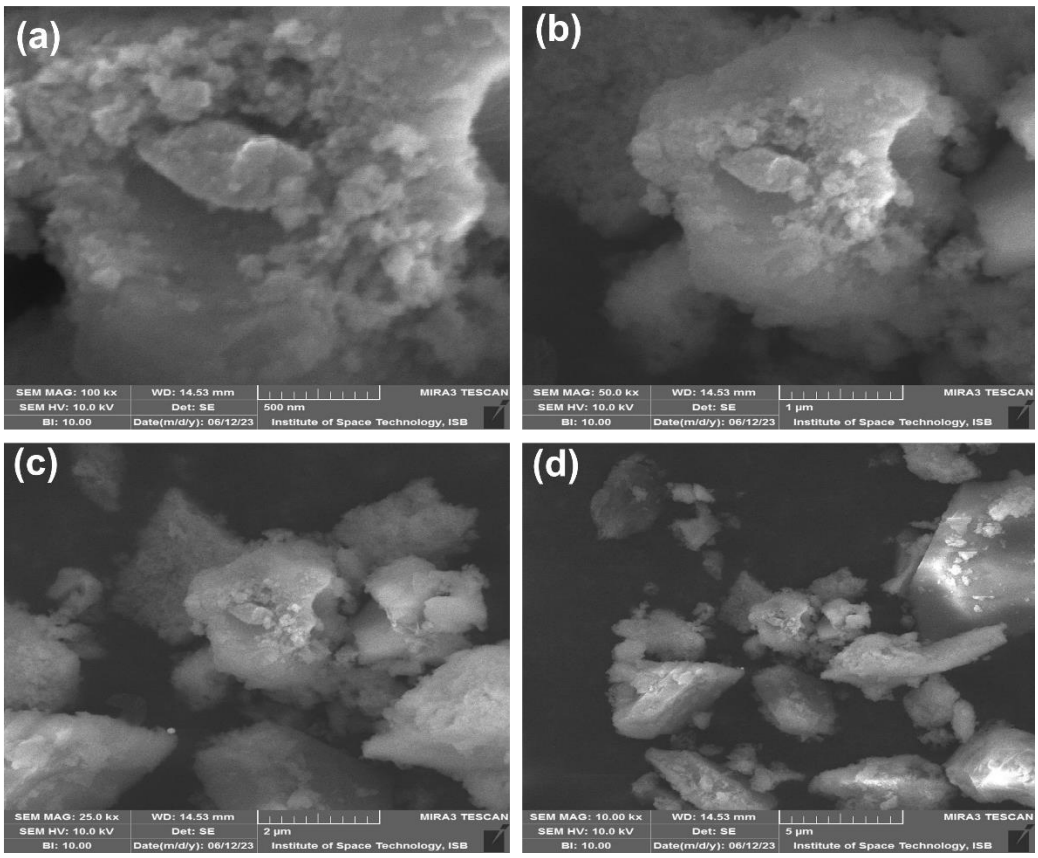

Figure 23:SEM analysis of 1 wt% rGO MnFeCo-MOF

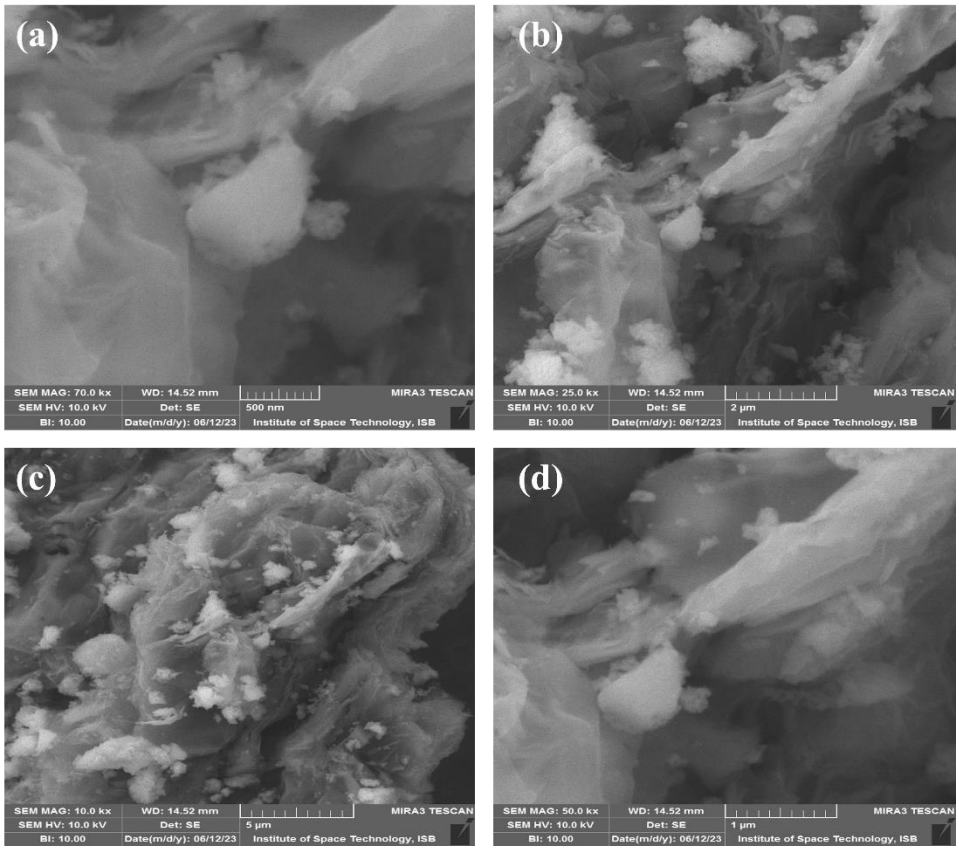

Figure 24:SEM analysis of 3 wt% rGO MnFeCo-MOF

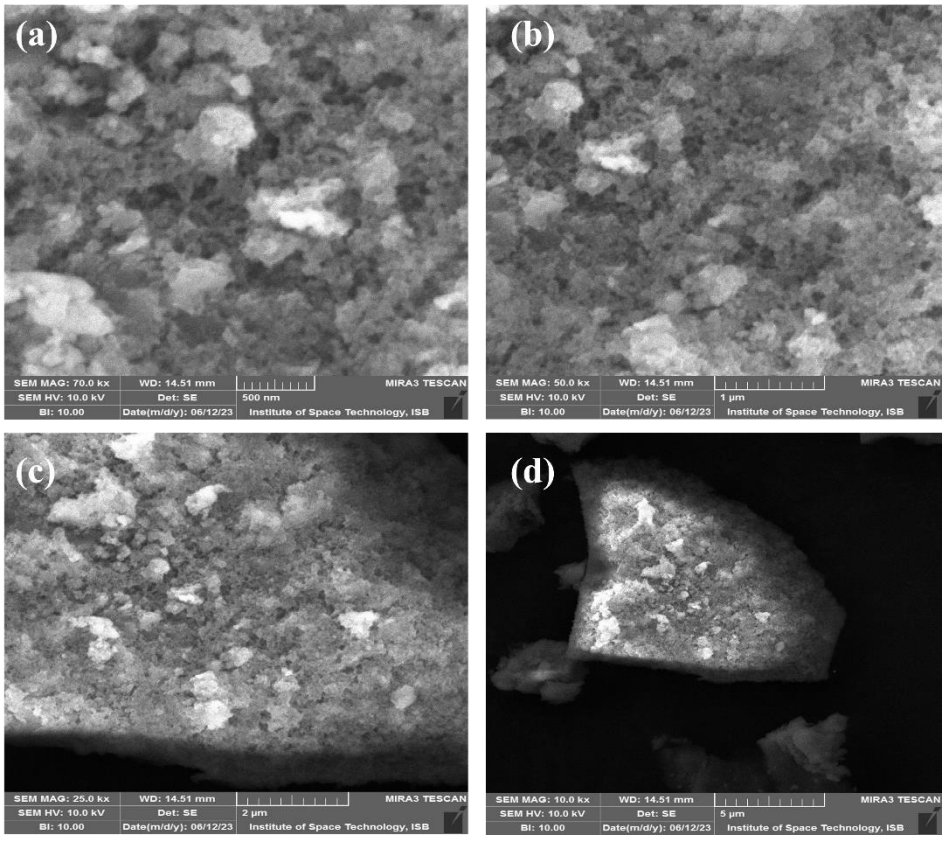

Figure 25:SEM analysis of 3 wt% rGO FeCo-MOF

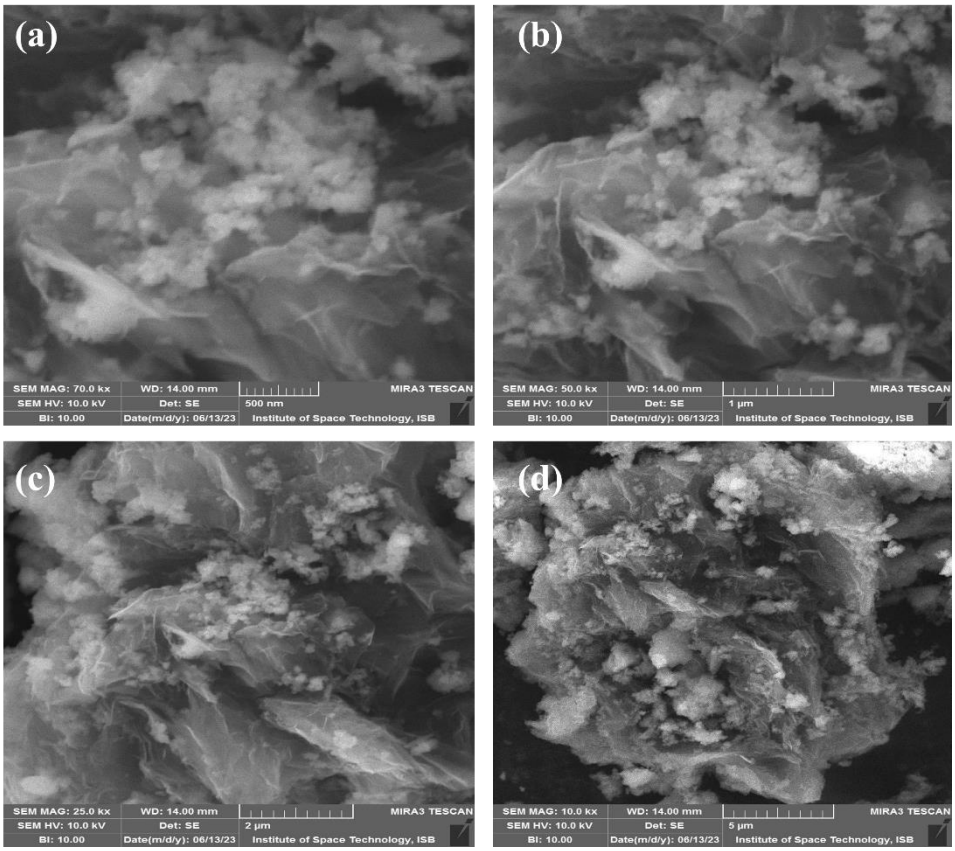

Figure 26:SEM analysis of 5 wt% rGO FeCo-MOF

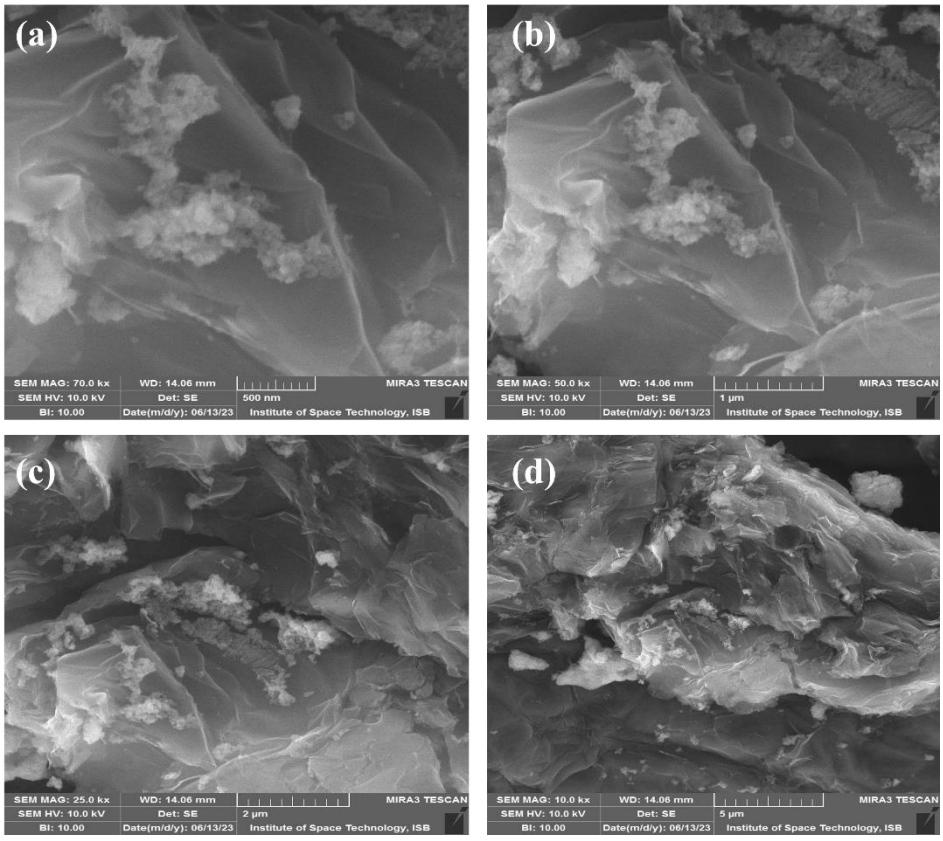

Figure 27:SEM analysis of 5 wt% rGO MnFeCo-MOF

4.1.5 EDX Analysis

The presence of elements in as synthesized FeCo-MOF, MnFeCo-MOF and its composites with rGO i.e. (1, 3, 5 wt%), were studied by (EDS). Figure (28 & 29) illustrate the presence of Fe, CO, Mn, C and O without any impurity. This analysis may also confirm the synthesis of FeCo-MOF and their composites.

Elements	FeCo-MOF	1wt% rGO FeCo-MOF	3wt% rGO FeCo-MOF	5wt% rGO FeCo-MOF
C	34.7	37.5	40.1	42.1
O	22.2	19.4	18.2	16.5
Fe	20.1	20.4	21.4	19.9
Co	23.0	22.7	20.3	21.5

Figure 28:EDX analysis of 1, 3, 5 wt% rGO FeCo-MOF

Elements	MnFeCo-MOF	1wt% rGO MnFeCo-MOF	3wt% rGO MnFeCo-MOF	5wt% rGO MnFeCo-MOF
C	22.2	23.5	26.1	28.6
O	20.0	17.6	15.5	14.7
Fe	19	19.8	18.0	17.1
Co	20.1	18.4	20.1	20.3
Mn	18.7	20.7	21.2	19.3

Figure 29:EDX analysis of 1, 3, 5 wt% rGO MnFeCo-MOF

4.2 Electrochemical Studies

In a solution of 1M potassium hydroxide, various electrochemical characterization procedures were carried out on MOF and rGO electrodes utilizing techniques like chronoamperometry, electrochemical impedance spectroscopy, and cyclic voltammetry. When it comes to metal-air batteries, the type of electrolyte that is used has a significant impact on both the performance and the stability of the electrodes. Acidic electrolytes like H_2SO_4 can boost the activity of oxygen reduction reaction (ORR) or oxygen evolution reaction (OER), but with time, they can also cause the material of the electrode to deteriorate. On the other hand, electrolytes that are less complex, such as sodium hydroxide, might be more stable, but their ORR and OER activities would be lower. Because of this, the choice of an appropriate electrolyte is contingent not only on the electrode materials but also the level of efficiency that is sought. KOH, which is better suited for a wider range of materials due to its higher conductivity, is excellent for cathodes that are based on a variety of elements, including nickel and lithium. When compared to NaOH, it exhibits superior power output and charge/discharge rates and produces far less corrosion in battery components. Both potassium hydroxide (KOH) and sodium hydroxide (NaOH) have their perks and drawbacks, and selecting one over the other is contingent on the specifications of the battery system. The electrochemical tests were carried out with the assistance of a configuration that included three electrodes that were linked to the Gamry setup software version 7.06. Working electrode was represented by the glassy carbon electrode (GCE), counter electrode was represented by platinum wire, and reference electrode was represented by Ag/AgCl. For the manufacture of the ink and the modified electrode, ethanol was used as the solvent, and a solution of Nafion containing 5 weight percent was utilized as the binding agent.

4.2.1 Preparation of electrodes

A three-step technique was utilised to construct the MOF electrode on top of a Ni foam substrate. First, the nickel foam was sonicated with a solution of 1 M HCl, and then it was rinsed with ethanol and DI water for a total of 30 minutes each. After that, it was dried in a vacuum oven at a temperature of 70 degrees Celsius for three hours. In the second phase, an ink was made by combining 4-5 mg of FeCo-MOF catalyst, 80 ul of ethanol, and 20 ul of Nafion as a binder. The ink was then formed by mixing these ingredients together. To achieve an even dispersion of the ingredients, the mixture was

sonicated for a full six hours. In the third phase, the ink was coated onto the prepared Ni foam substrate, and then it was dried in a vacuum oven at a temperature of 80 ^{o}C for one full day. Because of this process, a FeCo-MOF electrode was produced at the end of the experiment. It was determined that the fabrication of the MnFeCo-MOF electrode and the fabrication of electrodes incorporating various weight percentages of rGO in FeCo-MOF and MnFeCo-MOF composites could be accomplished by repeating the same technique but with different weight percentages of rGO.

4.2.2 Cyclic Voltammetry:

The setup used for conducting the electrochemical studies was of GAMRY in potentiostatic mode. The electrochemical analysis started with a scan of bare GCE in 3 electrode system filled with 3M Ethanol and 1M KOH. This results in the response of KOH which acts as supporting electrode. The role of supporting electrode is quite significant. Normally a supporting electrode is a bulky group which helps controlling the population of charged ions, protons in this case, at electrode. As a result, the system counts a cluster of charged species per second giving off a reliable value of current density at a point of scan.

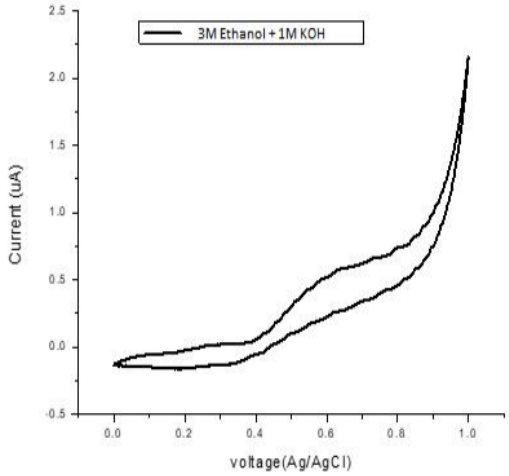

Figure 30:CV of bare electrode

4.2.2.1 Effect of Scan Rate Study

To investigate the impact of scan rate (mVs-1) on the material, analysis was conducted on samples weighing 4mg at various scan rates: 25 mV/s, 50 mVs-1, 75 mV/s, and 100 mV/s. This study included pure FeCo-MOF, MnFeCo-MOF, as well as composites of FeCo-MOF with (1%, 3%, and 5%) weight percentages of rGO, and composites of MnFeCo-MOF with (1%, 3%, and 5%) weight percentages of rGO.

Current has a direct relation with the square root of scan rate. The reasoning is as follows: current is dependent on concentration of Ethanol on the electrode which in turn relies on the concentration gradient. The greater the concentration gradient, the lesser is the availability of Ethanol on the surface and lesser will be the current. What scan rate minimizes the diffusion layer, thus reducing the concentration gradient and enhancing the current.

Another reason for increasing the current density value with increase in scan rate is that at higher scan rates, only those species get oxidized or reduced that are electroactive. Thus, only those species make their way to the electrode surface that can produce electrons [103].

The reason why we have not gone above the scan rate of 100mV/s is because it leaves little time for the reaction to occur. There must be sufficient time for electroactive species to first diffuse from bulk solution to the electrode surface and then react at the electrode surface to get oxidized into products which in the case are carbon dioxide, electrons and protons at the anode.

Therefore, there was no peak of Ethanol oxidation in voltammograms above scan rate of 100mV/s.

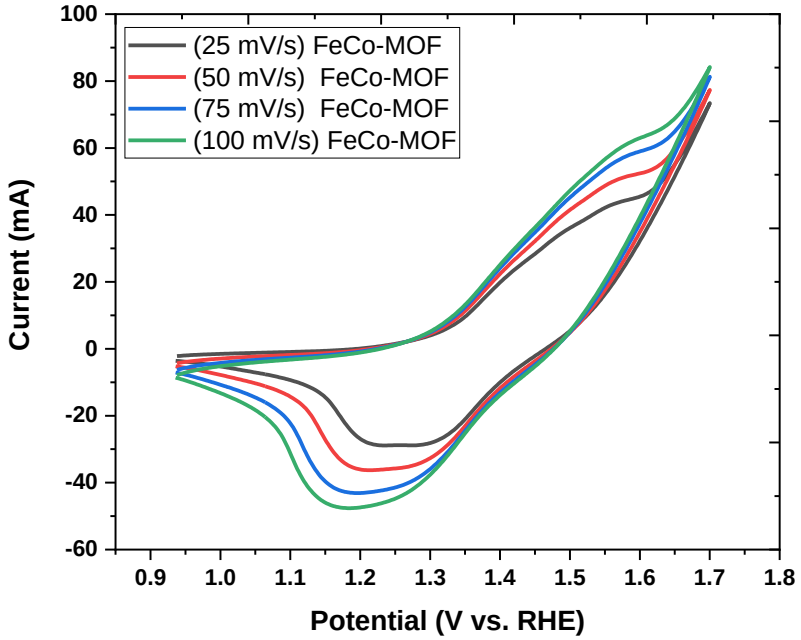

Figure 31:CV of FeCo – MOF at (25, 50, 75, 100 mV/s) scan rates

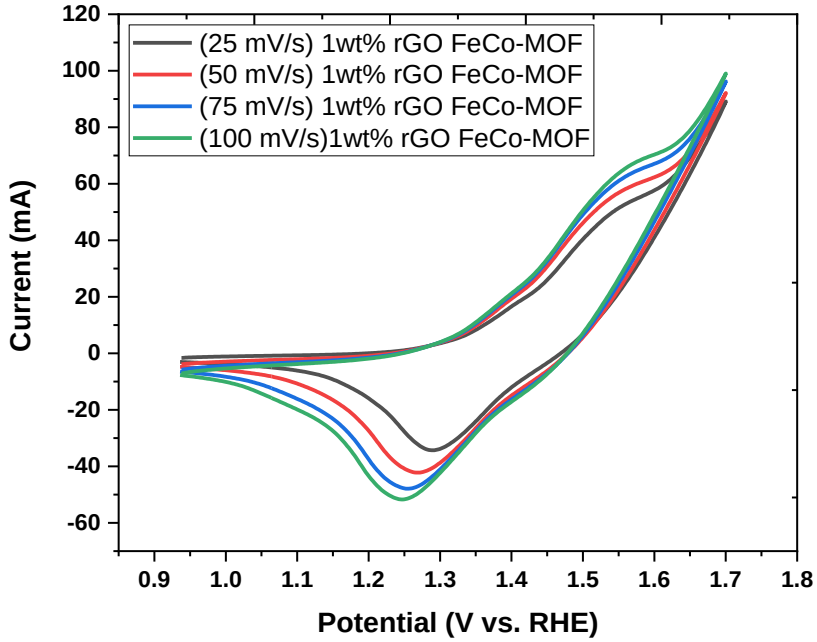

Figure 32:CV of 1 wt% rGO FeCo – MOF at (25, 50, 75, 100 mV/s) scan rates

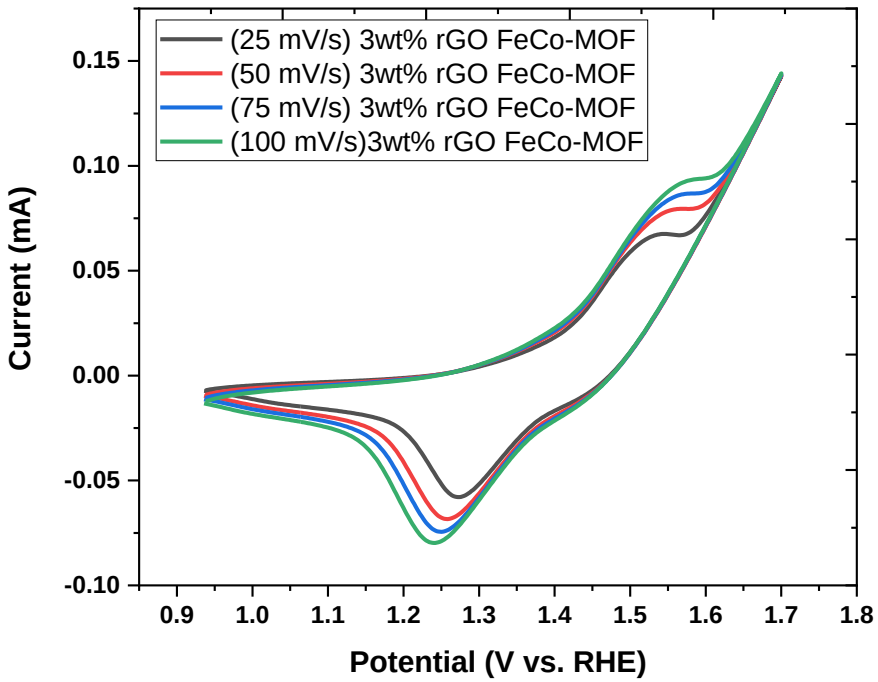

Figure 33:(c) CV of 3 wt% rGO FeCo – MOF at (25, 50, 75, 100 mV/s) scan rates

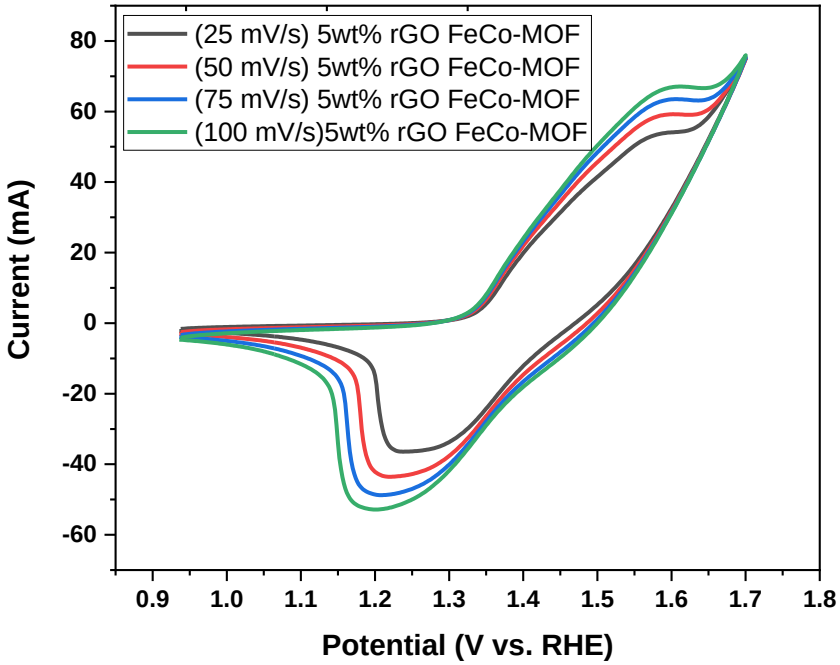

Figure 34:CV of 5 wt% rGO FeCo – MOF at (25, 50, 75, 100 mV/s) scan rates

As the scan rate is increased from 25 mV/s to 100mV/s, the current gradually enhances from 66.56 mA to 92.87 mA, indicating the obeying of Randles-Sevick principle. Increased scan rate leads to depleted diffusion layer around the electrode which helps enhance the electrocatalytic activity by abetting the proton conduction across the electrolyte.

The impact of scan rate on current is quite obvious. As the scan is increased from 25mV/s to 100mV/s, the current has drastically hiked up with the same pace from 66.56 mA/cm2 to 92.87mA signifying the importance of scan rate. This is in complete accordance with Randles Sevick equation which state that current density is directly proportional to square rate of scan rate. This is due to the reason that Increased scan rate leads to depleted.

Diffusion layer around the electrode which helps enhance the electrocatalytic activity by abetting the proton conduction across the electrolyte. The variation of scan rate has a pretty blatant influence on cyclic voltametric calculations.

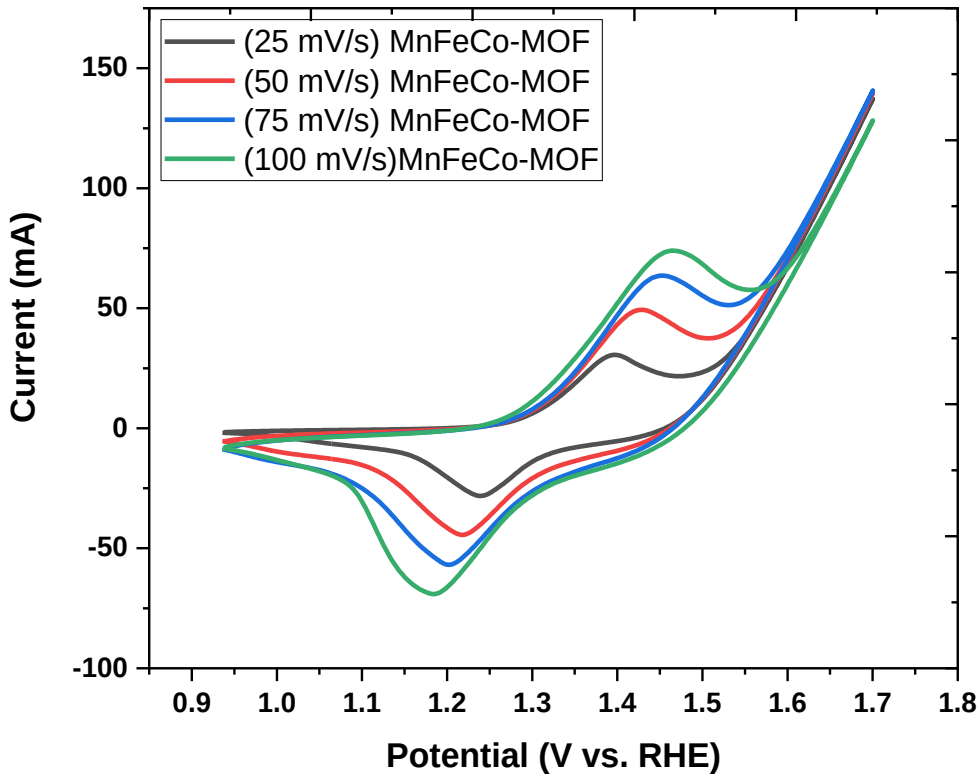

Figure 35:CV of MnFeCo – MOF at (25, 50, 75, 100 mV/s) scan rates

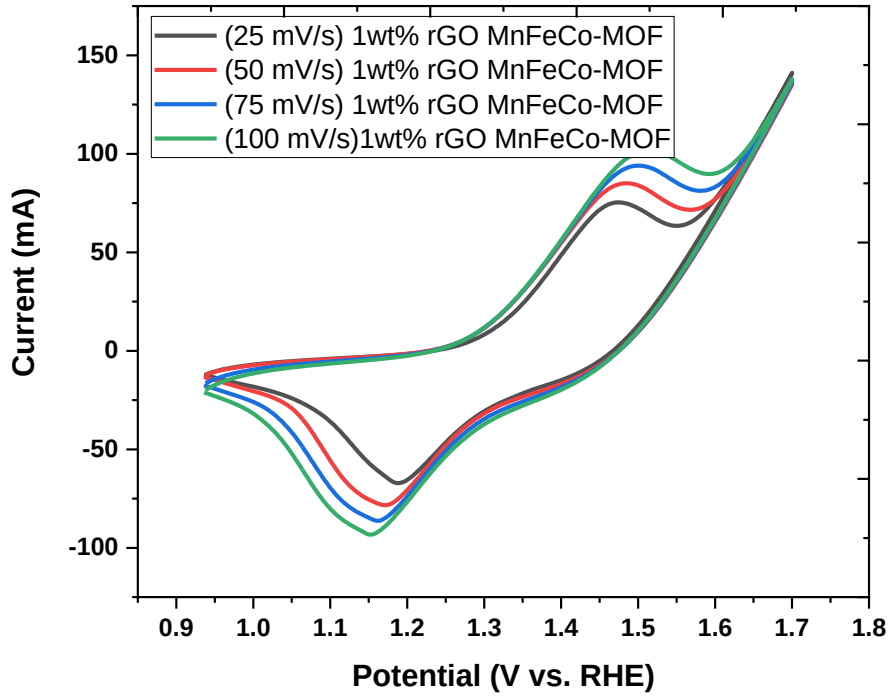

Figure 36:CV of 1 wt% rGO MnFeCo – MOF at (25, 50, 75, 100 mV/s) scan rates

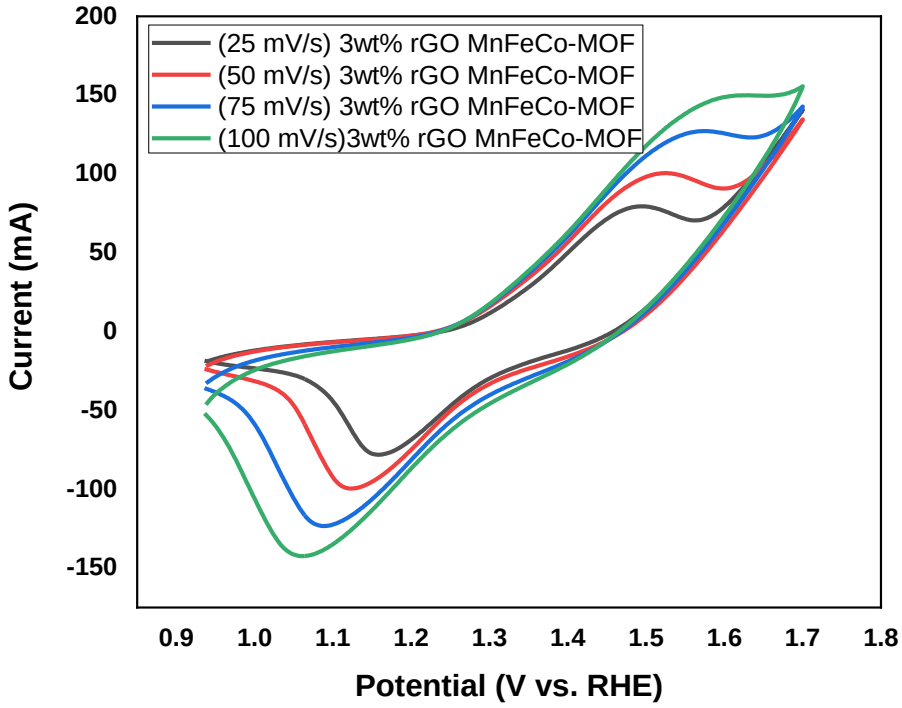

Figure 37:CV of 3 wt% rGO MnFeCo – MOF at (25, 50, 75, 100 mV/s) scan rates

Increasing the scan rate from 50mV/s till 100mV/s, the current has shot up accordingly from 78.45 mA to 92.87 mA. Indicating the following Randles-Sevick equation. Which states the current density is directly linked to square root of scan rate. This is due to the reason that Increased scan rate leads to depleted diffusion layer around the electrode which helps enhance the electrocatalytic activity by abetting the proton conduction across the electrolyte.

The impact of scan rate on cyclic voltametric graphs has been known for a long time. The above diagram depicts that when the scan rate is enhanced from 50mV/s till 100mV/s, the current has gone up from 78.45 mA to 92.87mA indicating the following of Randles-Sevick equation which states the current density is directly linked to square root of scan rate.

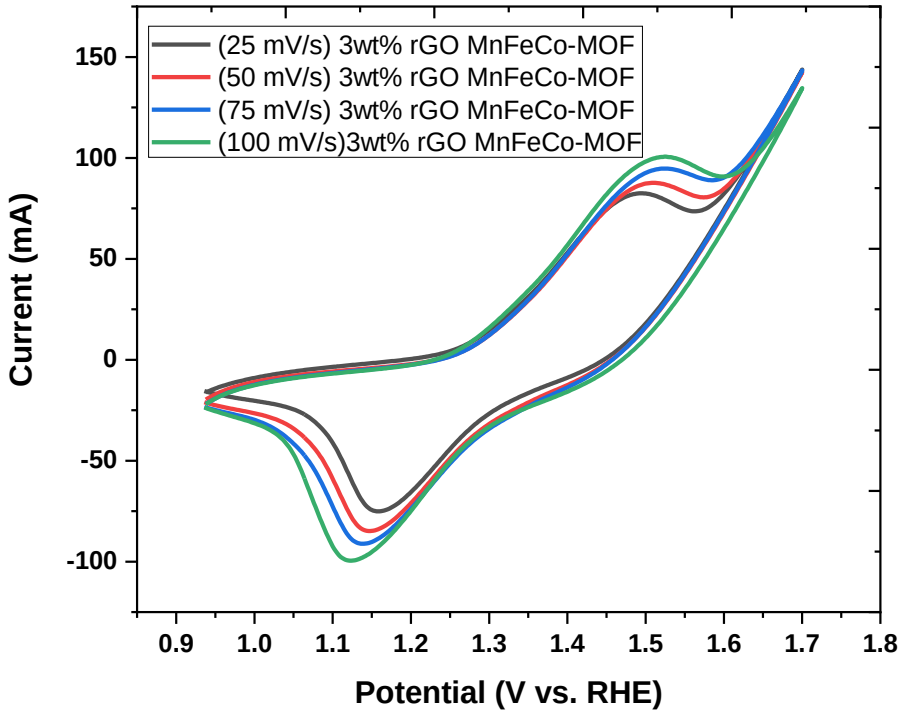

Figure 38:CV of 5 wt% rGO MnFeCo – MOF at (25, 50, 75, 100 mV/s) scan rates

This is due to the reason that increased scan rate leads to depleted concentration gradient around the electrode which helps enhance the electrocatalytic activity by abetting the proton conduction across the electrolyte. The elevated concentration gradient arises from the rapid diffusion of electroactive components from the methanol solution's bulk towards the electrode surface. At the electrode surface, these

components undergo oxidation or reduction processes, resulting in the generation of carbon dioxide, electrons that traverse the external circuit towards the cathode, and protons that diffuse through the electrolyte towards the cathode.

The impact of scan rate on cyclic voltametric graphs has been known since long. The above diagram depicts that when the scan rate is enhanced from 25 mV/s till 100mV/s, the current density has gone up from 53.46 mA to 66.8 mA indicating the following of Randles-Sevick equation which states the current density is directly linked to square root of scan rate. This is due to the reason that increased scan rate leads to depleted diffusion layer around the electrode which helps enhance the electrocatalytic activity by abetting the proton conduction across the electrolyte.

The increased concentration gradient is due to the high diffusion rates of electroactive species from the bulk solution of methanol to the electrode surface where they get oxidized or reduced to give carbon dioxide, electrons that travel through external circuit to reach cathode and protons that diffuse through electrolyte to reach cathode.

4.2.2.2 Effect of rGO concentration

As reduced graphene oxide (rGO) bears unusual properties like high conductivity, high surface area, high hydrophilicity, high electron dispersibility which make it a good material to form a hybrid with catalyst to produce synergistic effect which overall reinforce the efficiency and performance of the material and make it more promising for applications [104].

I also tested my materials with increasing concentration of rGO to study the effect of rGO upon OER. For this purpose the synthesized composites with different weight percentages of rGO are taken over glassy carbon electrode which then modified by FeCo-MOF and MnFeCo-MOF composite materials with 1wt% rGO FeCo-MOF, 3wt% rGO FeCo-MOF, 5wt% rGO FeCo-MOF, 1wt% rGO MnFeCo-MOF, 3wt% rGO MnFeCo-MOF, and 5wt% rGO MnFeCo-MOF by applying a thin layer of the prepared inks and the results were compared with FeCo-MOF and MnFeCo-MOF as shown in Figure. All catalysts under observation were taken in concentration of 3-4mg at scan rate 25 mV/s.

Comparative scans of all the catalysts were taken by running Potentiostatic scan with three electrode system in 1M KOH to observe the gradual change in response of catalysts by increasing the concentration of rGO.

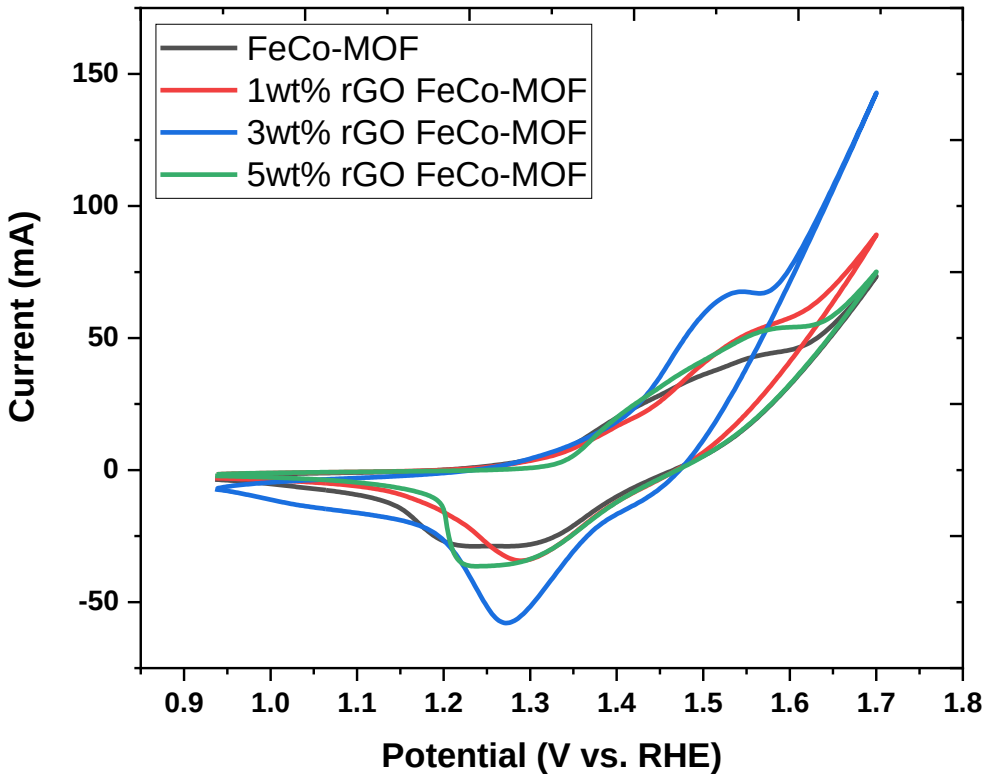

Figure 39:CV of FeCo – MOF & (1,3, 5 wt%) rGO FeCo-MOF

Results clearly demonstrate the participation of rGO in enhancing catalyst conductivity and efficiency by increasing the surface area. High concentration of rGO enhanced the electro catalytic activity for OER. Among all the prepared samples, 3wt% rGO MnFeCo-MOF shows highest current value of 147.2 mA in comparison to all the synthesized catalyst composites i.e. 52 mA, 66.56 mA, and 53.46 mA for 1wt%, 3wt%, and 5wt% respectively at 25 mV/s. Obtained results support the fact that FeCo-MOF and MnFeCo-MOF particles deposited on rGO are more favourable towards oxygen evolution reaction and it lowers the activation energy for oxidation reaction and this is all due to conductive properties of rGO due to its large surface area, large hydrophilicity, restored conjugated network and fewer oxygen functionalities as compared to graphene oxide (GO). So it emerges out as a promising nanomaterial because of its unique combinations and also being not only thinnest but the strongest material as well. Electron mobility of rGO is 100X more than that of silicon. So, rGO

enhances the overall efficiency of the catalyst by producing a synergistic effect and 3wt% rGO MnFeCo-MOF gives the best activity [105].

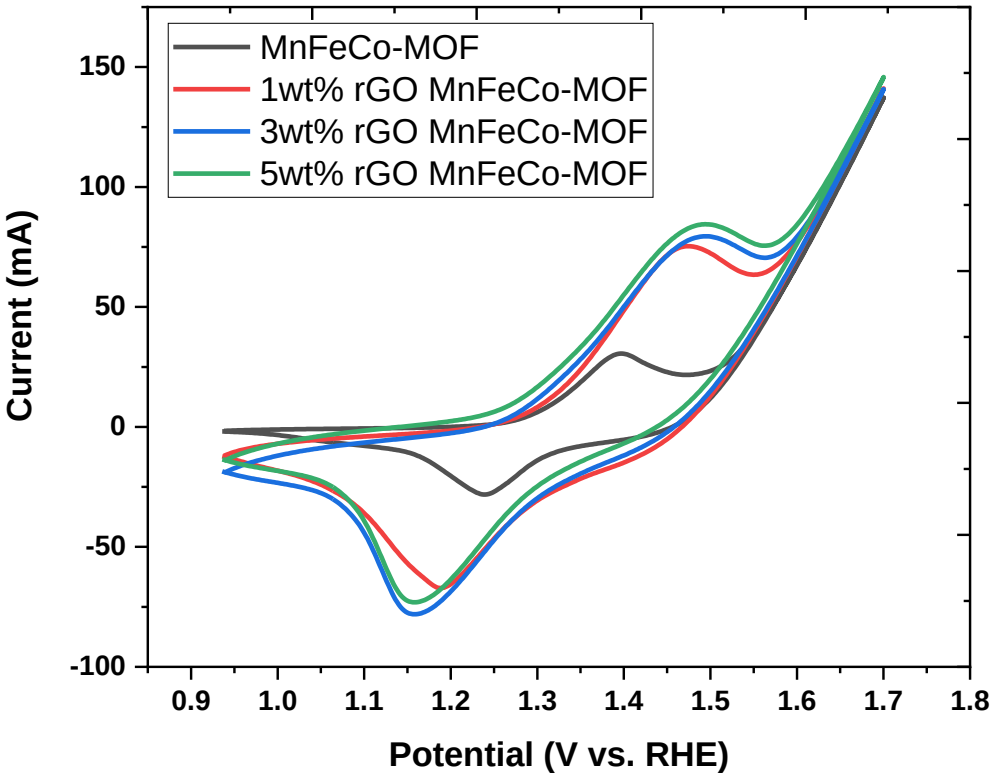

Figure 40:CV of MnFeCo – MOF & (1,3, 5 wt%) rGO MnFeCo-MOF

3wt% rGO MnFeCo-MOF gives peak current value 147 mA which is not satisfactory and expected according to the observation that increasing rGO concentration also increases conductivity. The one possible reason behind this anomalous behaviour of this composite is that rGO clustering may cause blockage of active sites of MOF and secondly charges may accumulate on large surface of rGO.

4.2.3 Electrochemical impedance spectroscopy

Electrochemical impedance spectroscopy (EIS) is a precise technique for evaluating the performance of a catalyzed electrode. EIS measures impedance by employing the potentiostatic mode within the same three-electrode system in the presence of 1M KOH and 3M ethanol, using both the un-deposited and modified GCE. EIS results are typically visualized through Nyquist or Bode plots. The Nyquist plot consists of two axes, with the imaginary component represented on the y-axis and the real parameter on the x-axis. This is because the calculation of charge transfer resistance involves one coordinate with an imaginary value and the other coordinate with a real value.

The impedance of the solution to charge transfer plays a crucial role in electrochemical investigations. It is essential to consider the resistance between the reference and catalyzed working electrode when calculating the electrochemical impedance of a circuit. By comparing the outcomes, it becomes evident that higher concentrations of rGO result in reduced charge impedance. The plot illustrating the relationship between real and imaginary impedance exhibits curves at lower frequencies for the modified GCE, whereas the bare GCE shows a linear trend. With an increase in MOF concentration, there was a corresponding decrease in impedance, resulting in enhanced conductivity and easier passage of charges with minimal resistance. This observation suggests that higher catalyst concentrations lead to a reduction in the distance between the catalyst layer and the electrode surface. As a result, charge transfer becomes smoother, with reduced hindrance to diffusion. In essence, increasing the catalyst concentration promotes more efficient and effective charge transfer processes [106].

Impedance investigations were conducted on composites of FeCo-MOF and MnFeCo-MOF, examining the influence of rGO concentration on the system's overall impedance. The comparative findings reveal a significant reduction in the overall impedance, indicating that graphene has facilitated an easier diffusion-controlled charge transfer mechanism. Based on this observation, it can be inferred that the conductivity property of rGO has played a significant role in enhancing the overall conductivity of the catalyst.

The resistance of the solution is a significant factor in the diffusion of species from the bulk solution to the electrode surface and should not be overlooked when determining

the overall resistance. Typically, the charge transfer resistance is determined by analyzing the radius of the incomplete semi-circle observed in the Nyquist plot.

As depicted in the provided image, an increase in the concentration of rGO results in a corresponding decrease in the charge transfer resistance.

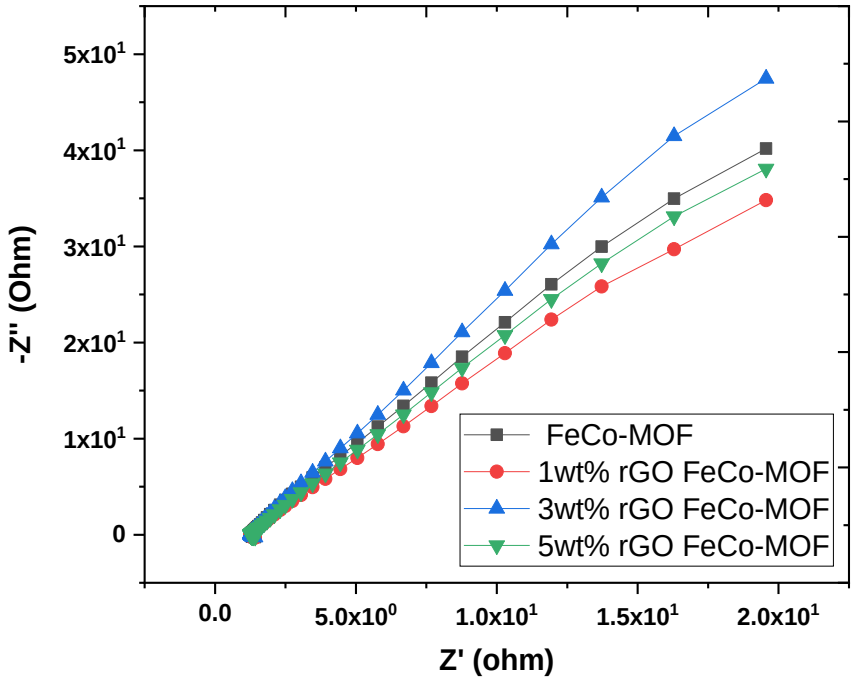

Figure 41:EIS graph of FeCo – MOF & (1,3, 5 wt%) rGO FeCo-MOF

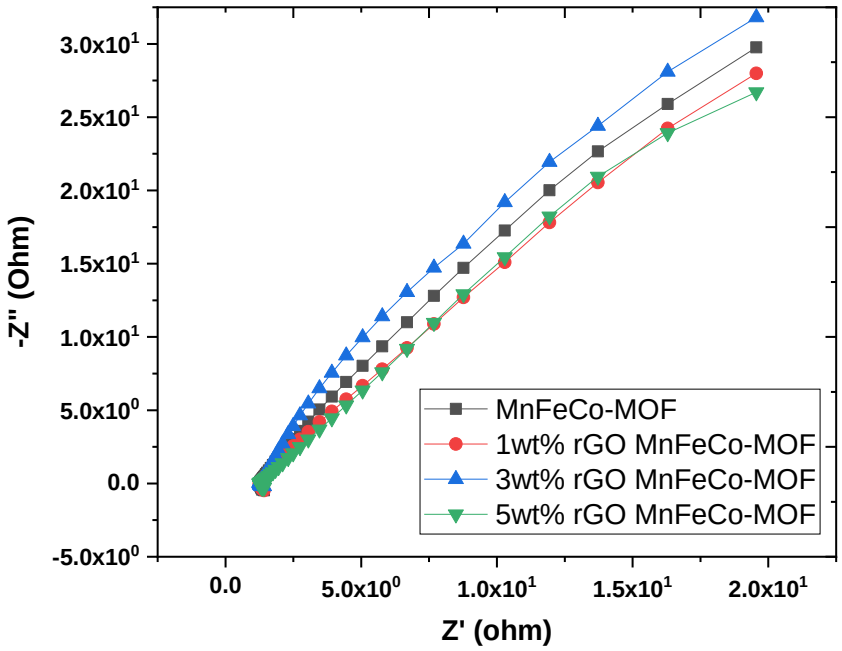

Figure 42:EIS graphs of MnFeCo – MOF & (1,3, 5 wt%) rGO MnFeCo-MOF

The explanation for this phenomenon is that the higher concentration of rGO leads to an increased surface area and enhanced conductivity for the electroactive species. As a result, they gain improved accessibility to the catalytically active sites, which are essential for the catalytic process and involve Copper atoms. The comparative findings clearly demonstrate a significant reduction in the overall impedance, indicating that rGO has facilitated a diffusion-controlled mechanism for easier charge transfer.

The Nyquist plot for varying concentration of catalyst shows that as the increased catalyst concentration, the charge transfer resistance for Ethanol oxidation reaction has decreased correspondingly. This effect goes to show that higher catalyst concentration provides greater catalytic area and easy access to catalytic active sites for electroactive species because the more the amount of catalyst, the greater will be the catalytic active sites and greater will be the surface area and conductivity of the material.

In this catalyst, Fe, Co, Mn atoms, which are the coordination centres, act as catalyst for Ethanol oxidation reaction while the ligand of the MOF, which is Benzene bicarboxylate and rGO play the role of catalyst support to provide enhanced surface area and better conductivity.

4.2.4 Tafel Studies

It is a polarization technique used for potentiostatic measurements, including cyclic polarization and linear polarization resistance. This method is widely employed to assess corrosion rates and offers a faster experimental approach compared to traditional weight-loss estimation. The corrosion reactions can be effectively described using Tafel slopes, which allow for the representation of mixed potential theory based on electrochemical kinetics. This theory takes into account both the kinetics and thermodynamics of all the reactions happening on the electrode surface to predict the corrosion rate and potential. Tafel kinetics generally provide an accurate explanation of corrosion kinetics. Figure depicts the Tafel plots for the prepared catalysts, demonstrating the electrochemical kinetics through the comparison of overpotential and current density. In the oxygen evolution reaction, commercially available Pt exhibits these curves at a voltage as low as 0.0 V.

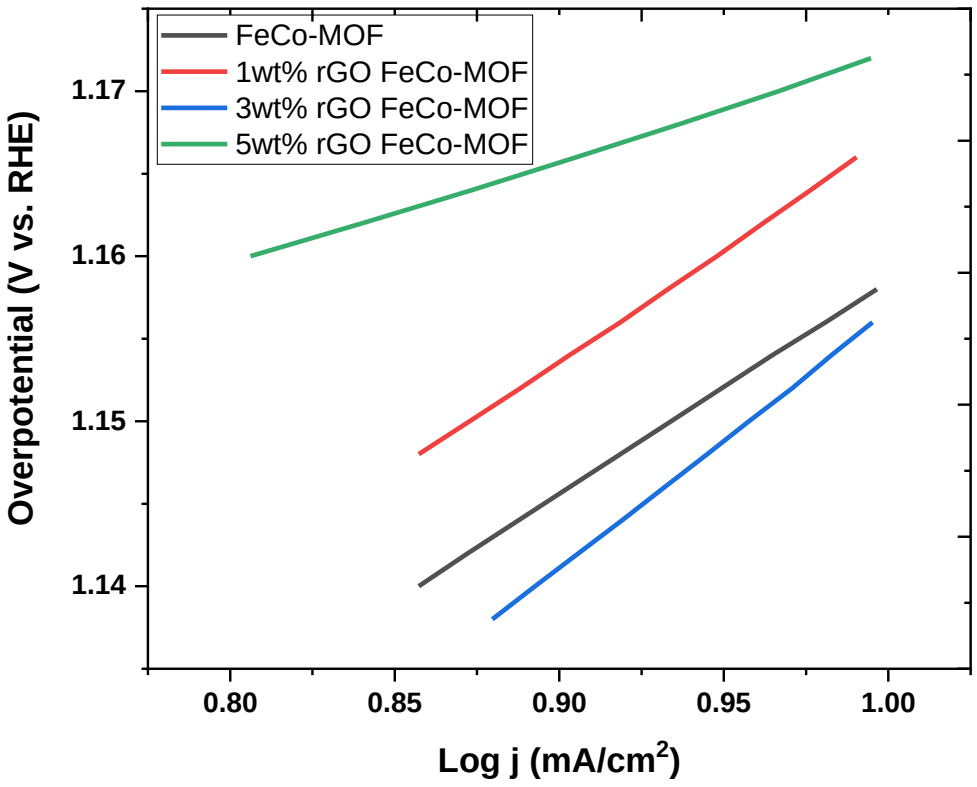

Figure 43:Tafel slopes of FeCo – MOF & (1,3, 5 wt%) rGO FeCo-MOF

In contrast, all the prepared FeCo-MOF and MnFeCo-MOF composites show lower potentials, indicating that the incorporation of rGO into to MOF increases the surface area and enhances the accessibility of reactants to the electrode. Consequently, it captures more ions and exhibits higher reaction activity for oxygen evolution reaction.

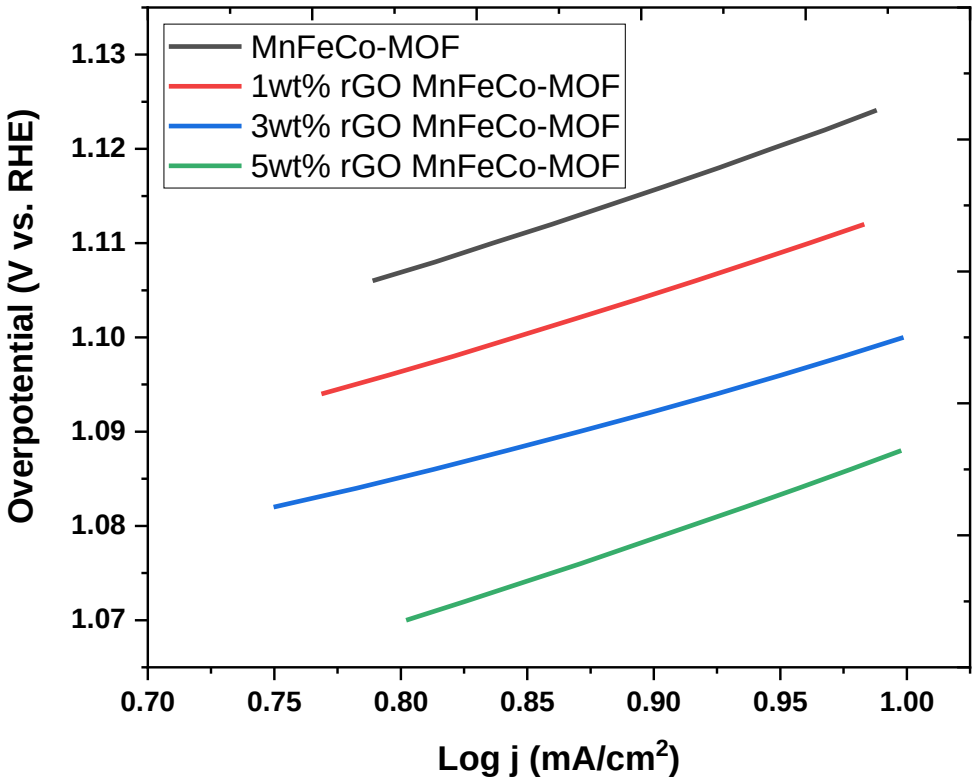

Figure 44: Tafel slopes of MnFeCo – MOF & (1,3, 5 wt%) rGO MnFeCo-MOF

4.2.5 Chronopotentiometry

The stability of the synthesized samples was assessed using the identical three-electrode electrochemical setup. The working electrode consisted of a glassy carbon electrode (GCE), while the counter electrode was a Pt wire. The reference electrode utilized was Ag/AgCl. The experiments were conducted in a 1M KOH solution. The stability assessment was performed using chronopotentiometry at a fixed potential of 0.6V. This technique involved applying a constant current and monitoring the resulting potential over time to evaluate the stability of the synthesized samples. Figure illustrate the chronoamperometric curves of all prepared samples of electro catalysts. All these curves show comparison among FeCo-MOF and MnFeCo-MOF and its composites

with rGO with different proportions of rGO i.e. 1wt%, 3wt%, and 5wt% show stability over a period of time 3600s.

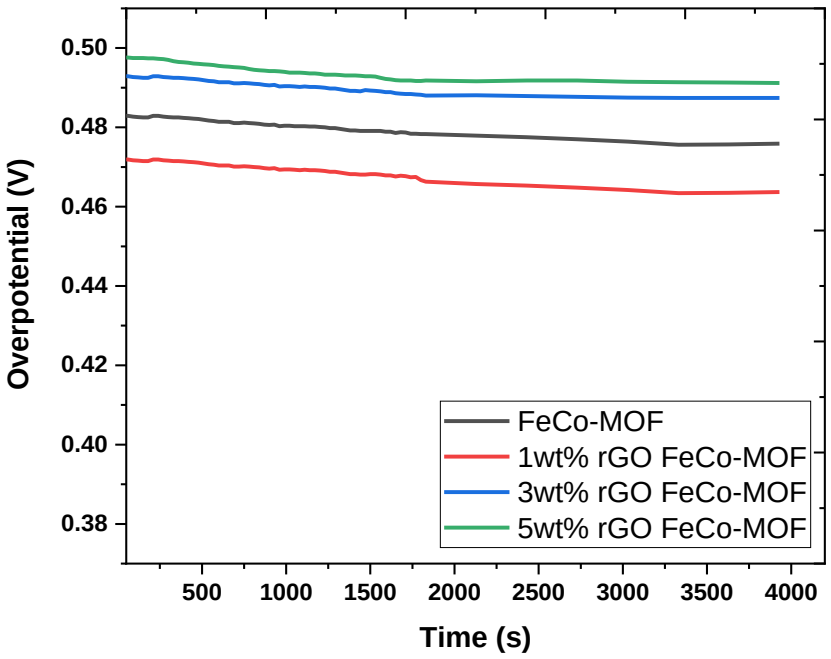

Figure 45:Chronopotentiometry of FeCo – MOF & (1,3, 5 wt%) rGO FeCo-MOF

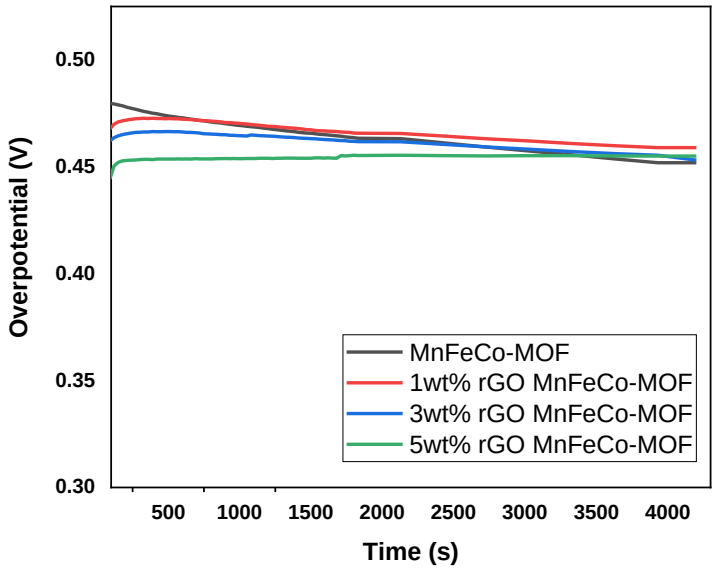

Figure 46:Chronopotentiometry of MnFeCo – MOF & (1,3, 5 wt%) rGO MnFeCo-MOF

4.3 Oxygen Reduction Reaction (ORR)

The ORR involves the reduction of oxygen molecules (O_2) to hydroxide ions (OH^-) according to the following overall reaction:

$O_2 + 2H_2O + 4e^- \rightarrow 4OH^-$

In metal-air batteries, the cathode is typically composed of a porous, high surface area material that provides active sites for ORR. The efficiency of the ORR at the cathode directly influences the overall performance of the battery, including its energy conversion efficiency, power output, and cycle life.

One of the main challenges in MABs is ORR sluggish kinetics, leading to high overpotentials and reduced overall energy efficiency. Therefore, developing efficient ORR catalysts is crucial to develop.

Recent advances in MOFs composites techniques have also shown promise in enhancing the ORR kinetics by providing high surface area, exposed active sites, and enhanced mass transport of reactants.

In conclusion, the efficient reduction of oxygen at the cathode is a critical aspect of metal-air batteries' performance. Developing cost-effective, efficient, and stable ORR catalysts is essential for the widespread commercialization and practical application of metal-air batteries as a clean and sustainable energy storage solution.

Continued research and innovation in ORR catalysts are expected to drive the advancement of metal-air battery technology in the future.

4.3.1 Linear Sweep Voltammetry (LSV) for ORR

The resulting current-potential curve provides valuable information about the ORR kinetics, onset potential, and overall electrocatalytic activity of the cathode material.

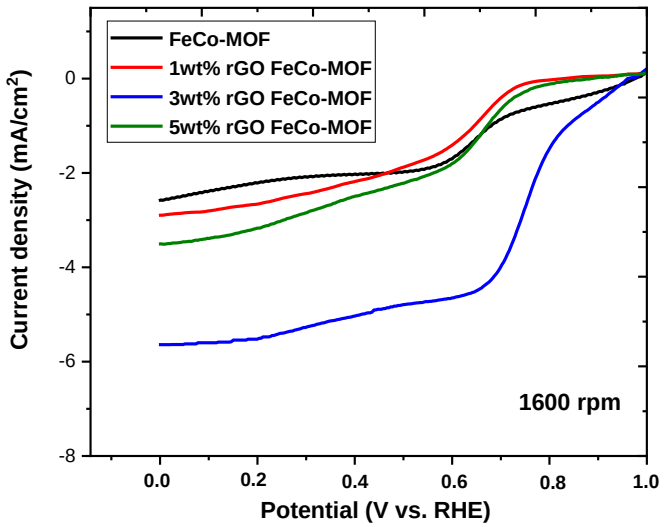

Figure 47 FeCo-MOF & its Composites

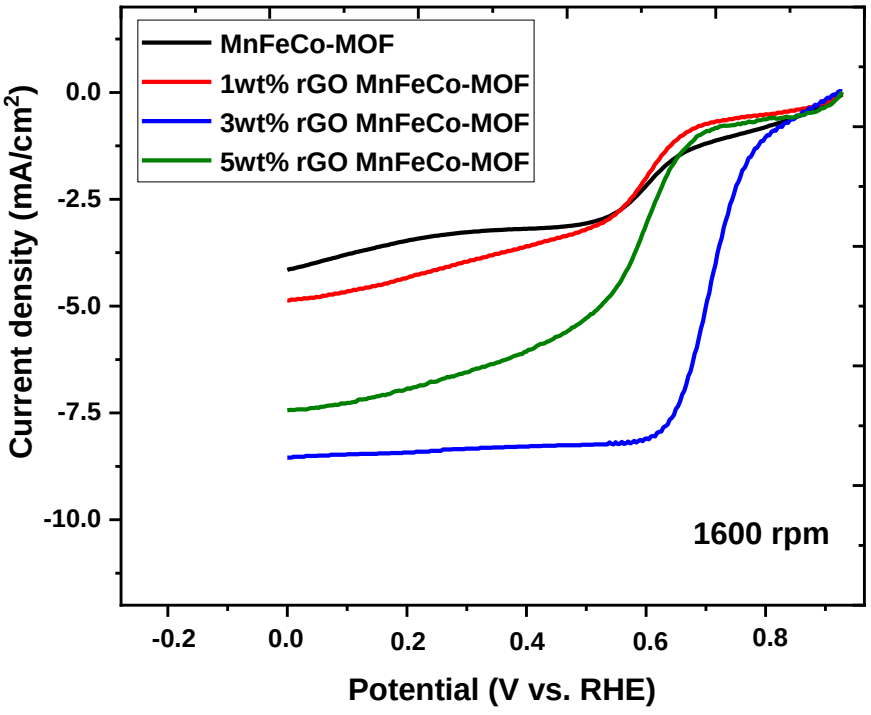

Figure 48 MnFeCo – MOF & its Composites

4.3.2 Effect of RPM on ORR LSV

The effect of RPM on the Linear Sweep Voltammetry (LSV) experiment for ORR is an important consideration in electrochemical studies. RPM refers to the rotation speed of the rotating disk electrode (RDE) used in the LSV experiment.

In ORR LSV experiments, the RPM can significantly influence the kinetics and mass transport processes at the electrode surface, leading to changes in the observed electrochemical behavior.

Overall, understanding the effect of RPM on ORR LSV experiments is crucial for obtaining reliable and meaningful data on the electrocatalytic performance of materials used.

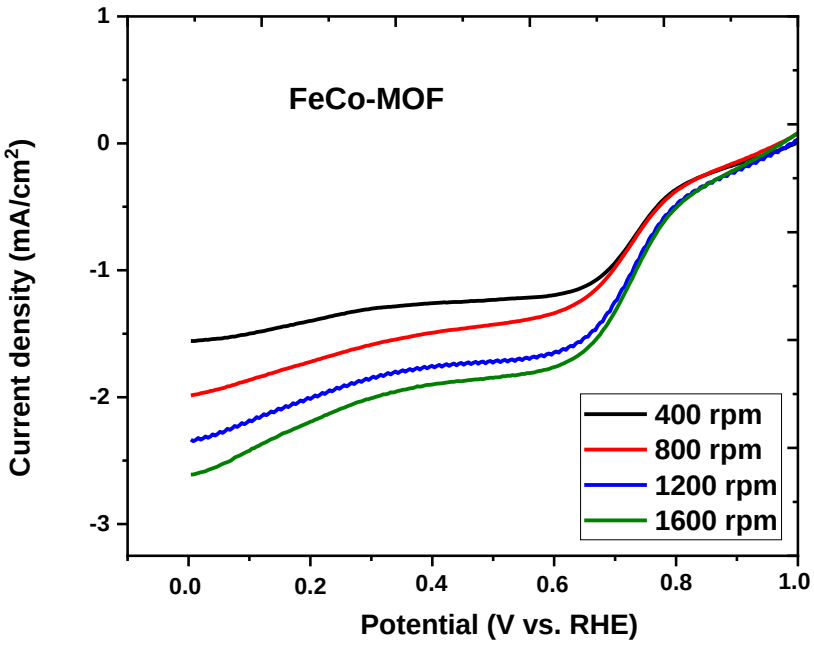

Figure 49 Effect of RPM for FeCo-MOF

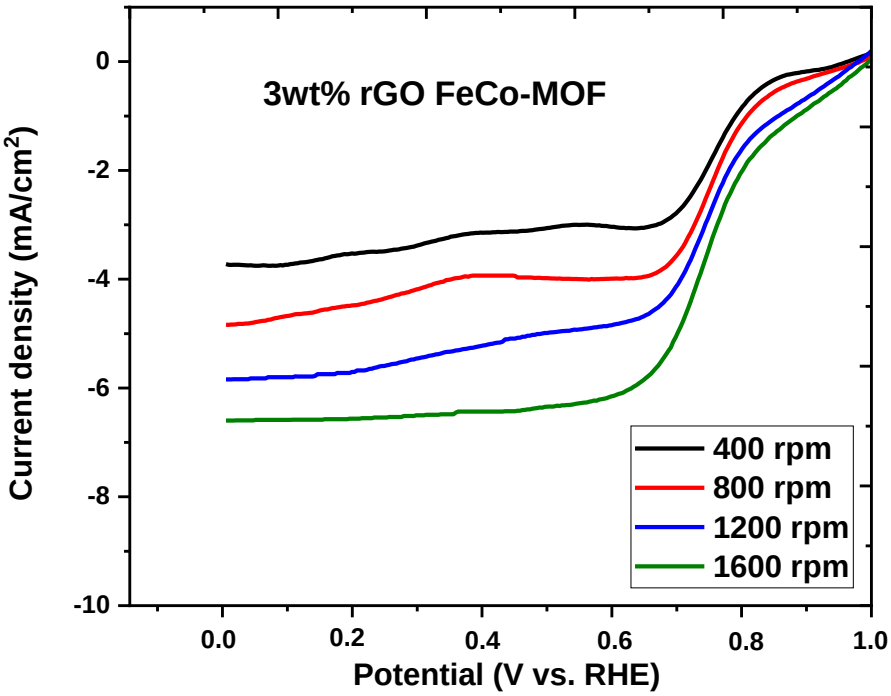

Figure 50 Effect of RPM for FeCo-MOF Composite

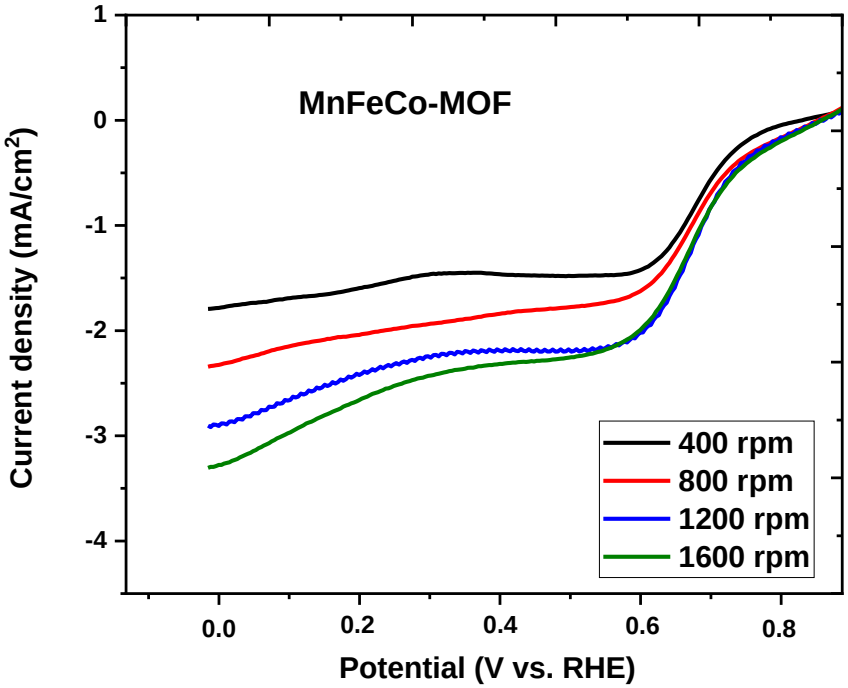

Figure 51 Effect of RPM for MnFeCo-MOF

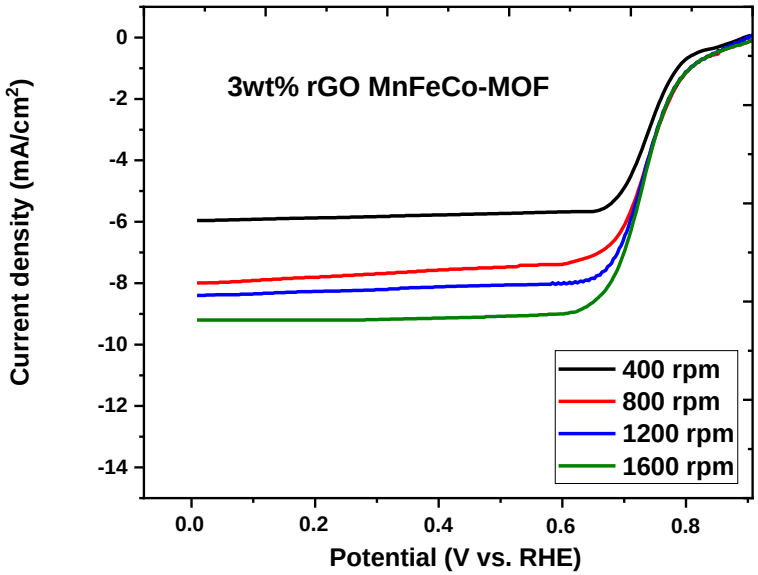

Figure 52 Effect of RPM for MnFeCo-MOF Composite

4.3.3 Halfwave Potential Analysis

Halfwave potential analysis is a valuable electrochemical technique used to characterize the kinetics of redox reactions. In the case of ORR, the halfwave potential is the potential at which half of the oxygen molecules are reduced to form reactive oxygen species on the electrode surface. Similarly, for OER, it is the potential at which half of the reactive oxygen species are oxidized back to oxygen molecules. This potential is crucial in understanding the efficiency and kinetics of the oxygen-related reactions.

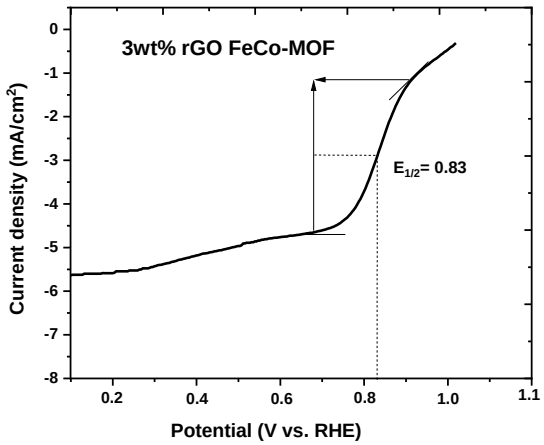

Figure 53 Halfwave Potential for 3 wt% rGO FeCo-MOF

The halfwave potential analysis provides valuable insights into the catalytic activity and performance of electrocatalysts in metal-air batteries. A lower halfwave potential indicates a faster and more efficient reaction, suggesting better electrocatalytic activity. On the other hand, a higher halfwave potential may indicate slower kinetics or poor electrocatalytic performance. By comparing the halfwave potentials of different catalysts or materials MABs performance can be identified.

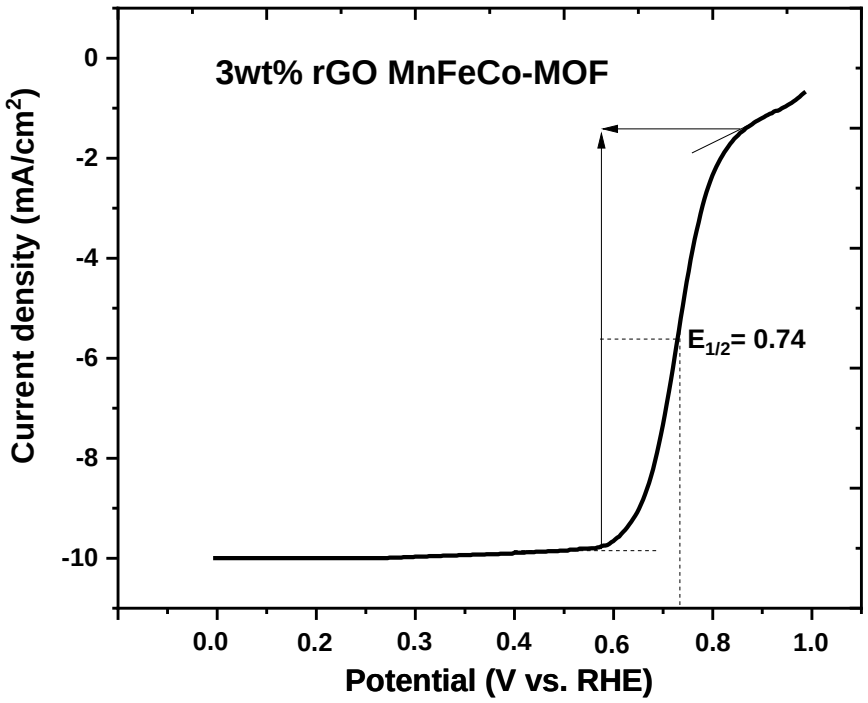

Figure 54 Halfwave Potential for 3 wt% rGO MnFeCo-MOF

4.3.4 Koutecky-Levich (K-L) Plots

Koutecky-Levich (K-L) plots are a widely used technique in electrochemistry to analyze the kinetics of electrochemical reactions, particularly in the context of electrode processes which is typically varied in a rotating disk electrode (RDE) experiment. The resulting curve exhibits a linear relationship, and the slope of this line is used to extract valuable information about the electrocatalytic activity and reaction mechanism.

In K-L plots, the slope of the linear region, known as the Koutecky-Levich slope, is related to the kinetic parameters of the electrochemical reaction. The K-L slope provides insights into the rate of electron transfer and the diffusion of reactants to the electrode surface. By analyzing the K-L slope, researchers can determine the number of electrons transferred in the redox reaction, which is essential for understanding the underlying mechanism. Moreover, the K-L plots can be used to study the effects of different experimental parameters, such as electrode rotation speed and reactant concentration, on the electrochemical kinetics. Overall, Koutecky-Levich plots offer a powerful and widely used tool for characterizing the performance and catalytic efficiency of electrocatalysts in metal-air batteries and other electrochemical systems.

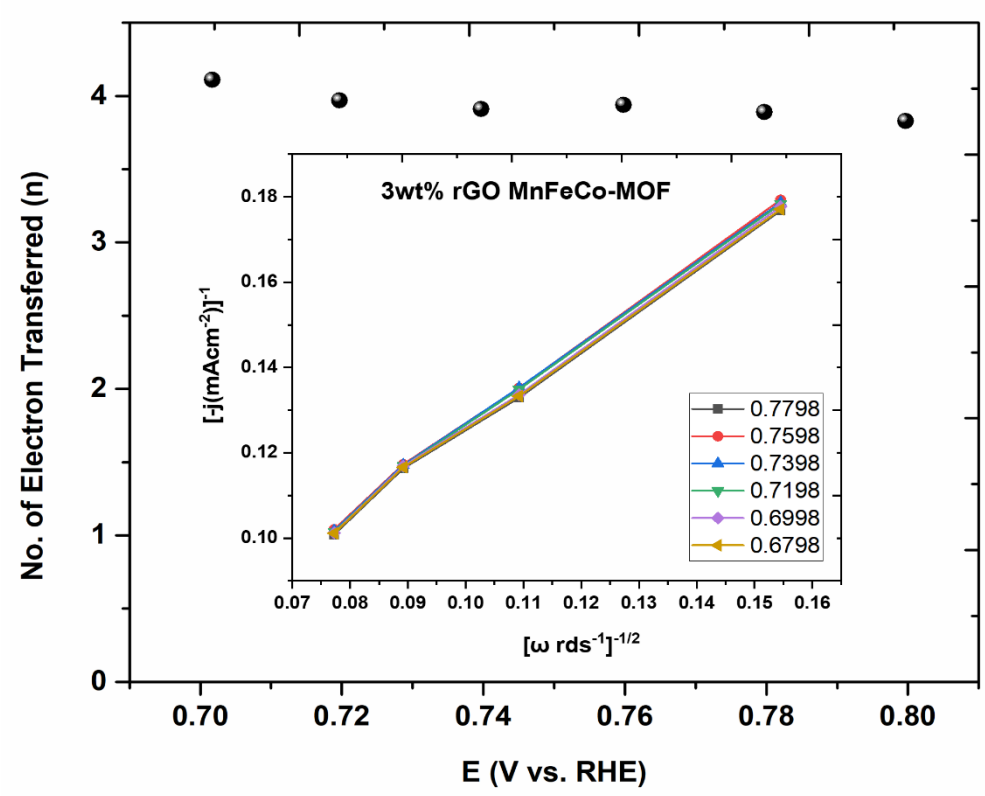

Figure 55 Koutecky–Levich (K–L) Plot of 3 wt% rGO MnFeCo-MOF

4.3.5 CV Profile for OER/ORR

The combined CV profile provides valuable information about the material's ability to facilitate the conversion of oxygen to water during OER and the reverse process of water to oxygen during ORR. This technique is crucial in evaluating the overall efficiency and stability of electrocatalysts, helping to design and optimize advanced metal-air batteries for sustainable energy storage applications.

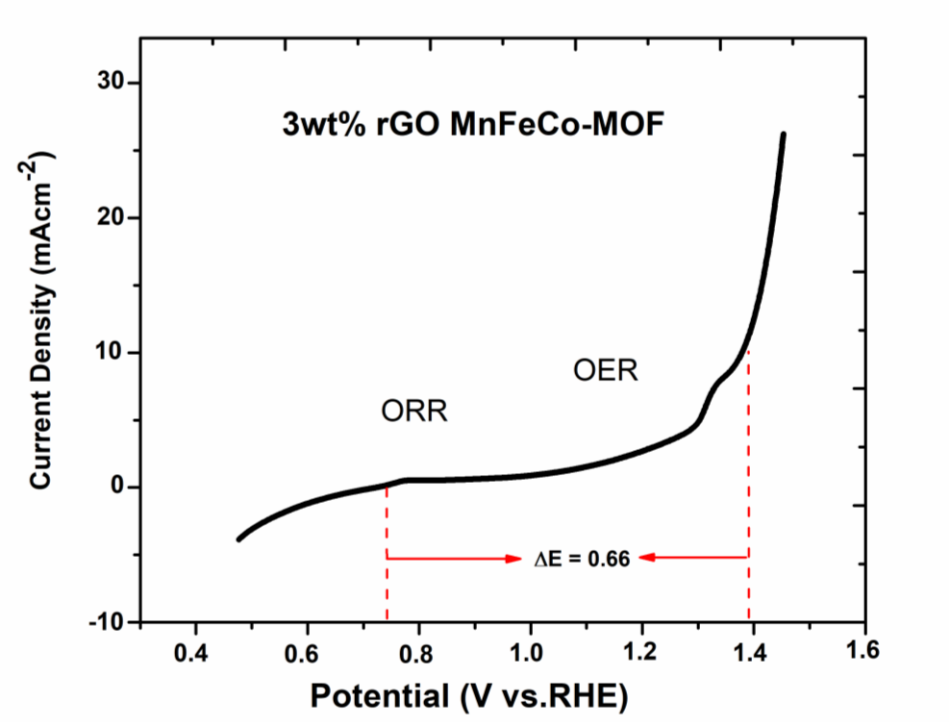

Figure 56 CV Profile for OER/ORR of 3 wt% rGO MnFeCo-MOF

Conclusions

Summary

The synthesis and characterization of MOFs and rGO composites have been investigated for their potential as electrocatalysts. FeCo-MOF and MnFeCo-MOF were successfully synthesized, and their properties were analyzed using XRD, SEM, RAMAN, and FTIR. The addition of 3wt% rGO to MnFeCo-MOF resulted in a remarkable improvement in performance due to a unique synergistic effect between the two materials.

The enhanced performance of the 3wt% rGO MnFeCo-MOF composite can be attributed to the presence of numerous active sites that facilitate the movement of charges and electrons, leading to improved electrocatalytic activity. Notably, this composite exhibited the lowest Tafel slope, measuring at 63.4 mV/dec, signifying its efficiency in catalyzing the OER. For OER at a current density of 10mA/cm^2, an overpotential of 178 mV was required. Moreover, the halfwave potential for the oxygen reduction reaction (ORR) was measured at 0.74 V, highlighting its capability to facilitate the ORR process.

Furthermore, the composite catalyst demonstrated excellent stability when subjected to chronopotentiometry testing. This result indicates that the 3wt% rGO MnFeCo-MOF composite is a promising candidate for long-term and stable electrocatalytic applications. The synergistic effect between rGO and MnFeCo-MOF provides advantages such as enhanced electrocatalytic activity, increased active sites, and reduced charge transfer resistance, making it an attractive option for various electrochemical applications.

Overall, the successful synthesis and thorough characterization of the 3wt% rGO MnFeCo-MOF composite have shed light on its potential as an efficient electrocatalyst for both OER and ORR. These findings contribute to the development of advanced materials for energy storage and conversion technologies, bringing us closer to sustainable and environmentally friendly solutions for various applications in the field of electrochemistry.

Future Recommendations

- The long-term stability of the FeCo and MnFeCo MOFs @ rGO composites under realistic operating conditions can be done to assess their practical applicability in metal-air batteries.
- Explore the effect of different weight ratios of rGO in the composites to optimize the electrocatalytic performance for OER.
- Conducting further characterization techniques such as XPS, TEM, and X-ray absorption spectroscopy to gain deeper insights into the structural and electronic properties of the composites.
- Exploring the potential of other metal dopants in the MOFs to further enhance electrocatalytic activity and stability.
- Studying the performance of the FeCo and MnFeCo MOFs @ rGO composites as bifunctional catalysts for the oxygen reduction reaction (ORR) to evaluate their overall electrochemical performance in metal-air batteries.
- Investigating the influence of different electrolyte compositions and pH values on the electrocatalytic activity of the composites to understand their performance in various operating conditions.
- Explore scalable and cost-effective synthesis methods for the FeCo and MnFeCo MOFs @ rGO composites to facilitate their large-scale production and commercialization for practical applications in metal-air batteries.

References

[1] J.-T. Han, Y.-H. Huang, and J. B. Goodenough, "New anode framework for rechargeable lithium batteries," *Chemistry of Materials,* vol. 23, no. 8, pp. 2027-2029, 2011.

[2] C. J. Zhang *et al.*, "Highly flexible and transparent solid-state supercapacitors based on RuO2/PEDOT: PSS conductive ultrathin films," *Nano Energy,* vol. 28, pp. 495-505, 2016.

[3] C. Zhang *et al.*, "Synthesis and charge storage properties of hierarchical niobium pentoxide/carbon/niobium carbide (MXene) hybrid materials," *Chemistry of Materials,* vol. 28, no. 11, pp. 3937-3943, 2016.

[4] X. Xiao *et al.*, "Intercalation of cations into partially reduced molybdenum oxide for high-rate pseudocapacitors," *Energy Storage Materials,* vol. 1, pp. 1-8, 2015.

[5] H. Gwon, J. Hong, H. Kim, D.-H. Seo, S. Jeon, and K. Kang, "Recent progress on flexible lithium rechargeable batteries," *Energy & Environmental Science,* vol. 7, no. 2, pp. 538-551, 2014.

[6] C. N. S. C. Z. F. Sa, "Ji X. Sun YK Amine K. Yushin G. Nazar LF Cho J. Bruce PG Angew," *Chem., Int. Ed,* vol. 51, pp. 9994-10024, 2012.

[7] W. Lee, J. Kim, S. Yun, W. Choi, H. Kim, and W.-S. Yoon, "Multiscale factors in designing alkali-ion (Li, Na, and K) transition metal inorganic compounds for next-generation rechargeable batteries," *Energy & Environmental Science,* vol. 13, no. 12, pp. 4406-4449, 2020.

[8] J. B. Goodenough and K.-S. Park, "The Li-ion rechargeable battery: a perspective," *Journal of the American Chemical Society,* vol. 135, no. 4, pp. 1167-1176, 2013.

[9] Z. Cui, C. Zu, W. Zhou, A. Manthiram, and J. B. Goodenough, "Mesoporous titanium nitride-enabled highly stable lithium-sulfur batteries," *Advanced materials,* vol. 28, no. 32, pp. 6926-6931, 2016.

[10] Z. W. Seh, Y. Sun, Q. Zhang, and Y. Cui, "Designing high-energy lithium–sulfur batteries," *Chemical society reviews,* vol. 45, no. 20, pp. 5605-5634, 2016.

[11] N. Mahne *et al.*, "Singlet oxygen generation as a major cause for parasitic reactions during cycling of aprotic lithium–oxygen batteries," *Nature Energy,* vol. 2, no. 5, pp. 1-9, 2017.

[12] Y. G. Gogotsi and E. Pomerantseva, "Two-dimensional heterostructures for energy storage," *Nature Energy,* vol. 2, no. 7, 2017.

[13] Y. Liang, H. Dong, D. Aurbach, and Y. Yao, "Current status and future directions of multivalent metal-ion batteries," *Nature Energy,* vol. 5, no. 9, pp. 646-656, 2020.

[14] J. Xiao *et al.*, "Understanding and applying coulombic efficiency in lithium metal batteries," *Nature Energy,* vol. 5, no. 8, pp. 561-568, 2020.

[15] Q. Xu *et al.*, "Surface engineering of LiNi0. 8Mn0. 1Co0. 1O2 towards boosting lithium storage: Bimetallic oxides versus monometallic oxides," *Nano Energy,* vol. 77, p. 105034, 2020.

[16] X. Wang, G. Tan, Y. Bai, F. Wu, and C. Wu, "Multi-electron reaction materials for high-energy-density secondary batteries: current status and prospective," *Electrochemical Energy Reviews,* vol. 4, pp. 35-66, 2021.

[17] J. Fu *et al.*, "Recent progress in electrically rechargeable zinc–air batteries," *Advanced Materials,* vol. 31, no. 31, p. 1805230, 2019.

[18] R. Gomes and A. J. Bhattacharyya, "Carbon nanotube-templated covalent organic framework nanosheets as an efficient sulfur host for room-temperature metal–sulfur batteries," *ACS Sustainable Chemistry & Engineering,* vol. 8, no. 15, pp. 5946-5953, 2020.

[19] H. Yang, B. Zhang, Y. X. Wang, K. Konstantinov, H. K. Liu, and S. X. Dou, "Alkali-Metal Sulfide as Cathodes toward Safe and High-Capacity Metal (M= Li, Na, K) Sulfur Batteries," *Advanced Energy Materials,* vol. 10, no. 37, p. 2001764, 2020.

[20] S. H. Chung and A. Manthiram, "Current status and future prospects of metal–sulfur batteries," *Advanced Materials,* vol. 31, no. 27, p. 1901125, 2019.

[21] Y.-J. Wang *et al.*, "A review of carbon-composited materials as air-electrode bifunctional electrocatalysts for metal–air batteries," *Electrochemical Energy Reviews,* vol. 1, pp. 1-34, 2018.

[22] X. Chen *et al.*, "A review on recent advancement of nano-structured-fiber-based metal-air batteries and future perspective," *Renewable and Sustainable Energy Reviews,* vol. 134, p. 110085, 2020.

[23] Y.-L. Zhang *et al.*, "Advanced non-noble materials in bifunctional catalysts for ORR and OER toward aqueous metal–air batteries," *Nanoscale,* vol. 12, no. 42, pp. 21534-21559, 2020.

[24] S. Ibraheem *et al.*, "Three-dimensional Fe, N-decorated carbon-supported NiFeP nanoparticles as an efficient bifunctional catalyst for rechargeable zinc–O2 batteries," *ACS applied materials & interfaces,* vol. 11, no. 1, pp. 699-705, 2018.

[25] S. W. Kim *et al.*, "Highly active bifunctional electrocatalysts for oxygen evolution and reduction in Zn–air batteries," *ChemSusChem,* vol. 11, no. 24, pp. 4203-4208, 2018.

[26] N. Xu, Y. Zhang, T. Zhang, Y. Liu, and J. Qiao, "Efficient quantum dots anchored nanocomposite for highly active ORR/OER electrocatalyst of advanced metal-air batteries," *Nano Energy,* vol. 57, pp. 176-185, 2019.

[27] D. Yan, Y. Li, J. Huo, R. Chen, L. Dai, and S. Wang, "Defect chemistry of nonprecious-metal electrocatalysts for oxygen reactions," *Advanced materials,* vol. 29, no. 48, p. 1606459, 2017.

[28] J. Sun *et al.*, "Sandwich-like reduced graphene oxide/carbon black/amorphous cobalt borate nanocomposites as bifunctional cathode electrocatalyst in rechargeable zinc-air batteries," *Advanced Energy Materials,* vol. 8, no. 27, p. 1801495, 2018.

[29] A. R. Zeradjanin, "Is a major breakthrough in the oxygen electrocatalysis possible?," *Current Opinion in Electrochemistry,* vol. 9, pp. 214-223, 2018.

[30] X. Peng *et al.*, "Hierarchically porous carbon plates derived from wood as bifunctional ORR/OER electrodes," *Advanced Materials,* vol. 31, no. 16, p. 1900341, 2019.

[31] H. Maleki Kheimeh Sari and X. Li, "Controllable cathode–electrolyte interface of Li [Ni0. 8Co0. 1Mn0. 1] O2 for lithium ion batteries: a review," *Advanced Energy Materials,* vol. 9, no. 39, p. 1901597, 2019.

[32] C. Li *et al.*, "Highly compact CsPbBr3 perovskite thin films decorated by ZnO nanoparticles for enhanced random lasing," *Nano Energy,* vol. 40, pp. 195-202, 2017.

[33] M. P. Browne, Z. Sofer, and M. Pumera, "Layered and two dimensional metal oxides for electrochemical energy conversion," *Energy & Environmental Science,* vol. 12, no. 1, pp. 41-58, 2019.

[34] D. Wu *et al.*, "Metal–organic frameworks as cathode materials for Li–O2 batteries," *Advanced Materials*, vol. 26, no. 20, pp. 3258-3262, 2014.

[35] K. M. Choi, H. M. Jeong, J. H. Park, Y.-B. Zhang, J. K. Kang, and O. M. Yaghi, "Supercapacitors of nanocrystalline metal–organic frameworks," *ACS nano*, vol. 8, no. 7, pp. 7451-7457, 2014.

[36] W. Xia, A. Mahmood, R. Zou, and Q. Xu, "Metal–organic frameworks and their derived nanostructures for electrochemical energy storage and conversion," *Energy & Environmental Science*, vol. 8, no. 7, pp. 1837-1866, 2015.

[37] R. Bendi, V. Kumar, V. Bhavanasi, K. Parida, and P. S. Lee, "Metal organic framework-derived metal phosphates as electrode materials for supercapacitors," *Advanced Energy Materials*, vol. 6, no. 3, p. 1501833, 2016.

[38] L. Wang *et al.*, "Flexible solid-state supercapacitor based on a metal–organic framework interwoven by electrochemically-deposited PANI," *Journal of the American Chemical Society*, vol. 137, no. 15, pp. 4920-4923, 2015.

[39] Z. Liang, R. Zhao, T. Qiu, R. Zou, and Q. Xu, "Metal-organic framework-derived materials for electrochemical energy applications," *EnergyChem*, vol. 1, no. 1, p. 100001, 2019.

[40] S. Dang, Q.-L. Zhu, and Q. Xu, "Nanomaterials derived from metal–organic frameworks," *Nature Reviews Materials*, vol. 3, no. 1, pp. 1-14, 2017.

[41] L. Jiang *et al.*, "Building aqueous K-ion batteries for energy storage," *Nature Energy*, vol. 4, no. 6, pp. 495-503, 2019.

[42] G. Crabtree, E. Kócs, and L. Trahey, "The energy-storage frontier: Lithium-ion batteries and beyond," *Mrs Bulletin*, vol. 40, no. 12, pp. 1067-1078, 2015.

[43] J.-Q. Shen *et al.*, "Modular and stepwise synthesis of a hybrid metal–organic framework for efficient electrocatalytic oxygen evolution," *Journal of the American Chemical Society*, vol. 139, no. 5, pp. 1778-1781, 2017.

[44] X. L. Wang *et al.*, "Exploring the performance improvement of the oxygen evolution reaction in a stable bimetal–organic framework system," *Angewandte Chemie International Edition*, vol. 57, no. 31, pp. 9660-9664, 2018.

[45] N. Stock and S. Biswas, "Synthesis of metal-organic frameworks (MOFs): routes to various MOF topologies, morphologies, and composites," *Chemical reviews*, vol. 112, no. 2, pp. 933-969, 2012.

[46] C. Gucuyener, J. van den Bergh, J. Gascon, and F. Kapteijn, "Ethane/ethene separation turned on its head: selective ethane adsorption on the metal− organic framework ZIF-7 through a gate-opening mechanism," *Journal of the American Chemical Society*, vol. 132, no. 50, pp. 17704-17706, 2010.

[47] Y. Hou, T. Huang, Z. Wen, S. Mao, S. Cui, and J. Chen, "Metal− organic framework-derived nitrogen-doped core-shell-structured porous Fe/Fe3C@ C nanoboxes supported on graphene sheets for efficient oxygen reduction reactions," *Advanced Energy Materials*, vol. 4, no. 11, p. 1400337, 2014.

[48] K. Shen, X. Chen, J. Chen, and Y. Li, "Development of MOF-derived carbon-based nanomaterials for efficient catalysis," *Acs Catalysis*, vol. 6, no. 9, pp. 5887-5903, 2016.

[49] Y. Li and J. J. A. E. L. Lu, "Metal–air batteries: will they be the future electrochemical energy storage device of choice?," vol. 2, no. 6, pp. 1370-1377, 2017.

[50] J. S. Lee *et al.*, "Metal–air batteries with high energy density: Li–air versus Zn–air," vol. 1, no. 1, pp. 34-50, 2011.

[51] C. Wang *et al.*, "Recent progress of metal–air batteries—a mini review," vol. 9, no. 14, p. 2787, 2019.

[52] L. Grande *et al.*, "The Lithium/Air Battery: Still an Emerging System or a Practical Reality?," vol. 27, no. 5, pp. 784-800, 2015.

[53] J. Lu, L. Li, J.-B. Park, Y.-K. Sun, F. Wu, and K. J. C. r. Amine, "Aprotic and aqueous Li–O2 batteries," vol. 114, no. 11, pp. 5611-5640, 2014.

[54] J. Hassoun, F. Croce, M. Armand, and B. J. A. C. Scrosati, "Investigation of the O2 electrochemistry in a polymer electrolyte solid-state cell," vol. 123, no. 13, pp. 3055-3058, 2011.

[55] L. Johnson *et al.*, "The role of LiO2 solubility in O2 reduction in aprotic solvents and its consequences for Li–O2 batteries," vol. 6, no. 12, pp. 1091-1099, 2014.

[56] C. O. Laoire, S. Mukerjee, K. Abraham, E. J. Plichta, and M. A. J. T. J. o. P. C. C. Hendrickson, "Elucidating the mechanism of oxygen reduction for lithium-air battery applications," vol. 113, no. 46, pp. 20127-20134, 2009.

[57] X. Ren and Y. J. J. o. t. A. C. S. Wu, "A low-overpotential potassium–oxygen battery based on potassium superoxide," vol. 135, no. 8, pp. 2923-2926, 2013.

[58] J. Zhang, W. Xu, X. Li, and W. J. J. o. T. E. S. Liu, "Air dehydration membranes for nonaqueous lithium–air batteries," vol. 157, no. 8, p. A940, 2010.

[59] J. Xiao *et al.*, "Hierarchically porous graphene as a lithium–air battery electrode," vol. 11, no. 11, pp. 5071-5078, 2011.

[60] K. Abraham, Z. Jiang, and B. J. C. o. m. Carroll, "Highly conductive PEO-like polymer electrolytes," vol. 9, no. 9, pp. 1978-1988, 1997.

[61] T. Ogasawara, A. Débart, M. Holzapfel, P. Novák, and P. G. J. J. o. t. A. C. S. Bruce, "Rechargeable Li2O2 electrode for lithium batteries," vol. 128, no. 4, pp. 1390-1393, 2006.

[62] Y.-C. Lu, H. A. Gasteiger, M. C. Parent, V. Chiloyan, Y. J. E. Shao-Horn, and S.-S. Letters, "The influence of catalysts on discharge and charge voltages of rechargeable Li–oxygen batteries," vol. 13, no. 6, p. A69, 2010.

[63] C. O. Laoire, S. Mukerjee, K. Abraham, E. J. Plichta, and M. A. J. T. J. o. P. C. C. Hendrickson, "Influence of nonaqueous solvents on the electrochemistry of oxygen in the rechargeable lithium− air battery," vol. 114, no. 19, pp. 9178-9186, 2010.

[64] Y. Wang and H. J. C. c. Zhou, "A lithium–air fuel cell using copper to catalyze oxygen-reduction based on copper-corrosion mechanism," vol. 46, no. 34, pp. 6305-6307, 2010.

[65] B. Kumar, J. Kumar, R. Leese, J. P. Fellner, S. J. Rodrigues, and K. J. J. o. T. E. S. Abraham, "A solid-state, rechargeable, long cycle life lithium–air battery," vol. 157, no. 1, p. A50, 2009.

[66] W. Zhu, B. Poole, D. Cahela, and B. J. J. o. a. e. Tatarchuk, "New structures of thin air cathodes for zinc–air batteries," vol. 33, no. 1, pp. 29-36, 2003.

[67] T. Dirkse and D. J. J. o. A. E. Kroon, "Effect of ionic strength on the passivation of zinc electrodes in KOH solutions," vol. 1, no. 4, pp. 293-296, 1971.

[68] P. Sapkota, H. J. J. o. I. Kim, and E. Chemistry, "Zinc–air fuel cell, a potential candidate for alternative energy," vol. 15, no. 4, pp. 445-450, 2009.

[69] H.-C. Zhou, J. R. Long, and O. M. Yaghi, "Introduction to metal–organic frameworks," vol. 112, ed: ACS Publications, 2012, pp. 673-674.

[70] B. Liu, H. Shioyama, T. Akita, and Q. Xu, "Metal-organic framework as a template for porous carbon synthesis," *Journal of the American Chemical Society*, vol. 130, no. 16, pp. 5390-5391, 2008.

[71] H. Li, M. Eddaoudi, M. O'Keeffe, and O. M. Yaghi, "Design and synthesis of an exceptionally stable and highly porous metal-organic framework," *nature*, vol. 402, no. 6759, pp. 276-279, 1999.

[72] C.-C. Wang and J. Y. Ying, "Sol− gel synthesis and hydrothermal processing of anatase and rutile titania nanocrystals," *Chemistry of materials*, vol. 11, no. 11, pp. 3113-3120, 1999.

[73] A. Martinez Joaristi, J. Juan-Alcañiz, P. Serra-Crespo, F. Kapteijn, and J. Gascon, "Electrochemical synthesis of some archetypical Zn2+, Cu2+, and Al3+ metal organic frameworks," *Crystal Growth & Design*, vol. 12, no. 7, pp. 3489-3498, 2012.

[74] N. Arul Dhas and A. Gedanken, "A sonochemical approach to the surface synthesis of cadmium sulfide nanoparticles on submicron silica," *Applied physics letters*, vol. 72, no. 20, pp. 2514-2516, 1998.

[75] A. Lagashetty, V. Havanoor, S. Basavaraja, S. D. Balaji, and A. Venkataraman, "Microwave-assisted route for synthesis of nanosized metal oxides," *Science and Technology of Advanced Materials*, vol. 8, no. 6, p. 484, 2007.

[76] S. L. James *et al.*, "Mechanochemistry: opportunities for new and cleaner synthesis," *Chemical Society Reviews*, vol. 41, no. 1, pp. 413-447, 2012.

[77] C. Dey, T. Kundu, B. P. Biswal, A. Mallick, and R. Banerjee, "Crystalline metal-organic frameworks (MOFs): synthesis, structure and function," *Acta Crystallographica Section B: Structural Science, Crystal Engineering and Materials*, vol. 70, no. 1, pp. 3-10, 2014.

[78] Q. Wang and D. Astruc, "State of the art and prospects in metal–organic framework (MOF)-based and MOF-derived nanocatalysis," *Chemical reviews*, vol. 120, no. 2, pp. 1438-1511, 2019.

[79] T. Mehtab *et al.*, "Metal-organic frameworks for energy storage devices: batteries and supercapacitors," *Journal of Energy Storage*, vol. 21, pp. 632-646, 2019.

[80] D. Farrusseng, *Metal-organic frameworks: applications from catalysis to gas storage*. John Wiley & Sons, 2011.

[81] Y. Li, Y. Wang, W. Fan, and D. Sun, "Flexible metal–organic frameworks for gas storage and separation," *Dalton Transactions*, vol. 51, no. 12, pp. 4608-4618, 2022.

[82] J. Caro, "Are MOF membranes better in gas separation than those made of zeolites?," *Current Opinion in Chemical Engineering*, vol. 1, no. 1, pp. 77-83, 2011.

[83] Z. Chen, K. Adil, Ł. J. Weseliński, Y. Belmabkhout, and M. Eddaoudi, "A supermolecular building layer approach for gas separation and storage applications: the eea and rtl MOF platforms for CO 2 capture and hydrocarbon separation," *Journal of Materials Chemistry A*, vol. 3, no. 12, pp. 6276-6281, 2015.

[84] R. C. Huxford, J. Della Rocca, and W. Lin, "Metal–organic frameworks as potential drug carriers," *Current opinion in chemical biology*, vol. 14, no. 2, pp. 262-268, 2010.

[85] P. Kumar, A. Deep, and K.-H. Kim, "Metal organic frameworks for sensing applications," *TrAC Trends in Analytical Chemistry*, vol. 73, pp. 39-53, 2015.

[86] D. L. Bish and J. E. Post, *Modern powder diffraction*. Walter de Gruyter GmbH & Co KG, 2018.

[87] R. Morent, N. De Geyter, C. Leys, L. Gengembre, and E. Payen, "Comparison between XPS-and FTIR-analysis of plasma-treated polypropylene film surfaces," *Surface and Interface Analysis: An International Journal devoted to the development and application of techniques for the analysis of surfaces, interfaces and thin films*, vol. 40, no. 3-4, pp. 597-600, 2008.

[88] J. I. Goldstein, D. E. Newbury, J. R. Michael, N. W. M. Ritchie, J. H. J. Scott, and D. C. Joy, *Scanning electron microscopy and X-ray microanalysis*. Springer, 2017.

[89] L. Reimer, *Transmission electron microscopy: physics of image formation and microanalysis*. Springer, 2013.

[90] J. J. Van Benschoten, J. Y. Lewis, W. R. Heineman, D. A. Roston, and P. T. Kissinger, "Cyclic voltammetry experiment," *Journal of Chemical Education*, vol. 60, no. 9, p. 772, 1983.

[91] M. E. Orazem and B. Tribollet, "Electrochemical impedance spectroscopy," *New Jersey*, vol. 1, pp. 383-389, 2008.

[92] K. Ge *et al.*, "Facile synthesis of two-dimensional iron/cobalt metal–organic framework for efficient oxygen evolution electrocatalysis," *Angewandte Chemie International Edition,* vol. 60, no. 21, pp. 12097-12102, 2021.

[93] J. Li, Q. He, Y. Lin, L. Han, and K. Tao, "MOF-Derived Iron–Cobalt Bimetallic Selenides for Water Electrolysis with High-Efficiency Oxygen Evolution Reaction," *Inorganic Chemistry,* vol. 61, no. 47, pp. 19031-19038, 2022.

[94] W. Fang *et al.*, "Metal-organic framework derived Fe-Co-CN/reduced graphene oxide for efficient HER and OER," *Electrochimica Acta,* vol. 365, p. 137384, 2021.

[95] B. Ghasemidehkordi *et al.*, "Concentration of lead and mercury in collected vegetables and herbs from Markazi province, Iran: a non-carcinogenic risk assessment," *Food and chemical toxicology,* vol. 113, pp. 204-210, 2018.

[96] M. Li *et al.*, "Defect-rich hierarchical porous UiO-66 (Zr) for tunable phosphate removal," *Environmental Science & Technology,* vol. 55, no. 19, pp. 13209-13218, 2021.

[97] G. Yusibova *et al.*, "Bimetallic Metal-Organic-Framework-Derived Porous Cobalt Manganese Oxide Bifunctional Oxygen Electrocatalyst," *Journal of Electroanalytical Chemistry,* p. 117161, 2023.

[98] S. N. Alam, N. Sharma, and L. Kumar, "Synthesis of graphene oxide (GO) by modified hummers method and its thermal reduction to obtain reduced graphene oxide (rGO)," *Graphene,* vol. 6, no. 1, pp. 1-18, 2017.

[99] S. Zheng *et al.*, "Transition-metal (Fe, Co, Ni) based metal-organic frameworks for electrochemical energy storage," *Advanced Energy Materials,* vol. 7, no. 18, p. 1602733, 2017.

[100] J. Chen, B. Yao, C. Li, and G. Shi, "An improved Hummers method for eco-friendly synthesis of graphene oxide," *Carbon,* vol. 64, pp. 225-229, 2013.

[101] M. Anbia, V. Hoseini, and S. Sheykhi, "Sorption of methane, hydrogen and carbon dioxide on metal-organic framework, iron terephthalate (MOF-235)," *Journal of Industrial and Engineering Chemistry,* vol. 18, no. 3, pp. 1149-1152, 2012.

[102] J. Liu *et al.*, "Fe-MOF-derived highly active catalysts for carbon dioxide hydrogenation to valuable hydrocarbons," *Journal of CO2 Utilization,* vol. 21, pp. 100-107, 2017.

[103] X. L. Zhang, Z. H. Jiang, Z. P. Yao, Y. Song, and Z. D. Wu, "Effects of scan rate on the potentiodynamic polarization curve obtained to determine the Tafel slopes and corrosion current density," *Corrosion science,* vol. 51, no. 3, pp. 581-587, 2009.

[104] N. Cao and Y. Zhang, "Study of reduced graphene oxide preparation by Hummers' method and related characterization," *Journal of Nanomaterials,* vol. 2015, pp. 2-2, 2015.

[105] Y. Zhu *et al.*, "Graphene and graphene oxide: synthesis, properties, and applications," *Advanced materials,* vol. 22, no. 35, pp. 3906-3924, 2010.

[106] C. A. Cordeiro, M. G. De Vries, T. Cremers, and B. H. C. Westerink, "The role of surface availability in membrane-induced selectivity for amperometric enzyme-based biosensors," *Sensors and Actuators B: Chemical,* vol. 223, pp. 679-688, 2016.